

Special Issue: Integrating ZooMS and Zooarchaeology: Methodological Challenges and Interpretive Potentials

Comparing Neanderthal and Modern Human Subsistence at Riparo Bombrini: An Integrated Archaeozoological, Multivariate Taphonomic, and ZooMS Analysis

GENEVIÈVE POTHIER-BOUCHARD*

Département des sciences historiques, Pavillon Charles-De Koninck, Université Laval, 1030 avenue des Sciences-Humaines, G1V 0A6, Québec; and, Département d'anthropologie, Pavillon Lionel-Groulx, Université de Montréal, 3150 Jean-Brillant, H3T 1N8, Montréal, CANADA; genevieve.pothier-bouchard.1@ulaval.ca

ARIANE BURKE

Département d'anthropologie, Pavillon Lionel-Groulx, Université de Montréal, 3150 Jean-Brillant, H3T 1N8, Montréal, CANADA; a.burke@umontreal.ca

MICHAEL BUCKLEY

Manchester Institute of Biotechnology, School of Natural Sciences, University of Manchester, 131 Princess Street, M1 7DN, Manchester, UNITED KINGDOM; M.Buckley@manchester.ac.uk

FABIO NEGRINO

Dipartimento di Antichità, Filosofia, Storia, Università degli Studi di Genova, Via Balbi, 2, 16126, Genova, ITALY; fabio.negrino@unige.it

AMÉLIE VALLERAND

Département d'anthropologie, Pavillon Lionel-Groulx, Université de Montréal, 3150 Jean-Brillant, H3T 1N8, Montréal, CANADA; amelie.vallerand@umontreal.ca

ANA B. MARÍN-ARROYO

Departamento Ciencias Históricas, Universidad de Cantabria, Avda. de los Castros 52, 39005, Santander, SPAIN; anabelen.marin@unican.es

JULIEN RIEL-SALVATORE

Département d'anthropologie, Pavillon Lionel-Groulx, Université de Montréal, 3150 Jean-Brillant, H3T 1N8, Montréal, CANADA; julien.riel-salvatore@umontreal.ca

*corresponding author: Geneviève Pothier-Bouchard; genevieve.pothier-bouchard.1@ulaval.ca

submitted: 19 December 2023; revised: 14 August 2024; revised: 13 September 2024; accepted: 13 September 2024

Guest Editors: Geoff M. Smith (School of Anthropology and Conservation, University of Kent, and Department of Archaeology, University of Reading), Karen Ruebens (Department of Archaeology, University of Reading, and Chaire de Paléanthropologie, CIRB, Collège de France), Virginie Sinet-Mathiot (PACEA and Bordeaux Proteome-CBMN, Université de Bordeaux), and Frido Welker (Globe Institute, University of Copenhagen)

Handling Editor in Chief: Erella Hovers

ABSTRACT

The Liguro-Provençal arc yields unique deposits documenting the Middle-Upper Paleolithic transition. However, interpreting shifts in subsistence strategies in this region has been challenging, mainly due to taphonomic processes and the scarcity of archaeological assemblages excavated with modern techniques. For instance, faunal assemblages from the Balzi Rossi Paleolithic site complex, dated to 43–36 ky cal BP, are notoriously fragmented, impeding morphology-based taxonomic identification and limiting the application of most conventional archaeozoological methods. Additionally, poor collagen preservation often hinders identification through proteomic techniques such as ZooMS. This study examines three assemblages documenting the transition at one of Balzi Rossi's sites, Riparo Bombrini, using an integrated approach that combines archaeozoological methods, multivariate taphonomic analysis, stable isotopic data, and FTIR-aided ZooMS.

Despite the low frequency of identifiable faunal remains and readable bone surfaces, the results suggest that the Proto-Aurignacian faunal assemblages were primarily accumulated by anatomically modern human foragers, whereas the final Mousterian was accumulated as a result of brief, alternating site visits by Neanderthals and carnivores. A continuous exploitation of prime-aged cervids hunted near the site is observed through the final Mousterian and the Proto-Aurignacian levels. However, the faunal assemblages also suggest changes in the taxonomic richness, mortality profiles, carcass treatment, site function, and land-use, starting in the Proto-Aurignacian. These changes include prolonged occupations of the site, increased carcass curation for bone fuel, decreased carnivore activities on the site, and the diversification of bone tool types and raw materials to produce symbolic objects. In addition, the results align with previous hypotheses suggesting a hyperlocal adaptation of the very last Neanderthals to have occupied the site, followed by dense occupations of the site and shifting mobility strategies within a large territory associated with the overlying Proto-Aurignacian assemblages lasting through climatic instability. In spite of the challenging taphonomic context at Riparo Bombrini, this study provides the first detailed insight into human subsistence during the transition in this region and establishes testable hypotheses regarding the changing nature of hominin behavioral ecology during this period.

INTRODUCTION

Recent regional overviews of the subsistence patterns in the faunal record of western France and the Italian Peninsula highlight differences in adaptive behavior between Neanderthals and anatomically modern humans (hereafter modern humans) during the Middle-Upper Paleolithic transition (Rendu et al. 2019; Romandini et al. 2020; 2023; Marín-Arroyo et al. 2023). Changes in human-environmental interactions, including hunting technology, human-carnivore interactions, carcass processing, and the diversity of exploited animal prey and raw materials, may have provided modern humans with a significant adaptive advantage (Vidal-Cordasco et al. 2023). However, the lack of comprehensive archaeozoological data in the Liguro-Provençal arc has limited our ability to examine patterns of subsistence continuity and change in this region, which serves as a crucial link between the Italian Peninsula and other parts of Western Europe during the transition.

This study explores subsistence adaptations in the Liguro-Provençal arc, presenting the first detailed diachronic archaeozoological and taphonomic analysis of the transitional sequence at Riparo Bombrini (i.e., Levels A1, A2, and MS). Our main goal is to reconstruct and compare the hunting strategies and patterns of animal exploitation of the final Neanderthal occupation of the site (MS) and the first occupations by modern humans (A1, A2). The comparatively poor state of preservation of the faunal remains provides an excellent opportunity to apply and test the limits of a multivariate taphonomic approach (e.g., Bar-Oz and Dayan 2003; Bar-Oz and Munro 2004) in a challenging context and to implement a large-scale ZooMS technique to complement this approach effectively. The archaeozoological data are combined with environmental, chronological, and technological information to discuss hunting strategies, site function, subsistence, land-use, and mobility through time at Riparo Bombrini and at the scale of the Liguro-Provençal arc. Finally, this study discusses the chosen methodological approach to highlight the advantages and the interpretive limitations posed by the challenging preservation of faunal remains at Riparo Bombrini.

SUBSISTENCE BEHAVIORS DURING THE MIDDLE-UPPER PALEOLITHIC TRANSITION

The study of faunal assemblages associated with the Middle-Upper Paleolithic transition has contributed significantly to our knowledge of behavioral continuities and discontinuities during this process, marked by the disappearance of Neanderthals and other local hominin populations from the fossil record and the first dispersals of modern humans into western Eurasia between 50 to 30 thousand calibrated years before present (ky cal. BP). Neanderthals are now recognized as skillful hunters (e.g., Grayson and Delpech 2002; Marean 1998; Mellars 1996; Speth and Tchernov 2001; Stiner 1994; Thieme 1997) and their position at the top of the food chain is supported by stable isotopic studies (Bocherens, 2009; Richards and Trinkaus, 2009; Wißing et al., 2019). Archaeozoological studies have documented the range and regional variability of Neanderthal subsistence practices. Middle Paleolithic assemblages document the selection of prime-aged adults (e.g., Gaudzinski and Roebroeks 2000), the use of flexible hunting strategies, including drive tactics and the communal hunting of migrating species (e.g., Burke 2000; Gaudzinski 2006; Niven 2006), logistical exploitation, *sensu* Binford, of the landscape (e.g., Costamagno et al. 2015), and the potential storage of meat surpluses (Rendu et al. 2012). Additionally, they exploited a broad range of regionally available resources, including aquatic resources (e.g., Cortés-Sánchez et al. 2011; Guillaud et al. 2021; Hardy and Moncel 2011; Stiner 2001; Zilhão et al. 2020) and small game (e.g., Blasco and Fernández Peris 2012; Finlayson et al. 2012; Morin et al. 2019).

Furthermore, increased interdisciplinary efforts to reconstruct subsistence strategies have provided much evidence of diet continuities across the Middle-Upper Paleolithic transition. Methodological developments in stable isotopic analysis highlight a higher intake of plant-based foods than previously estimated for both Neanderthals and modern humans (Drucker et al. 2017; Naito et al. 2016). The considerable vegetal component of Neanderthal diets is also visible through studies of dental calculus, tooth microwear, fecal biomarkers, and plant residue analyses (Fio-

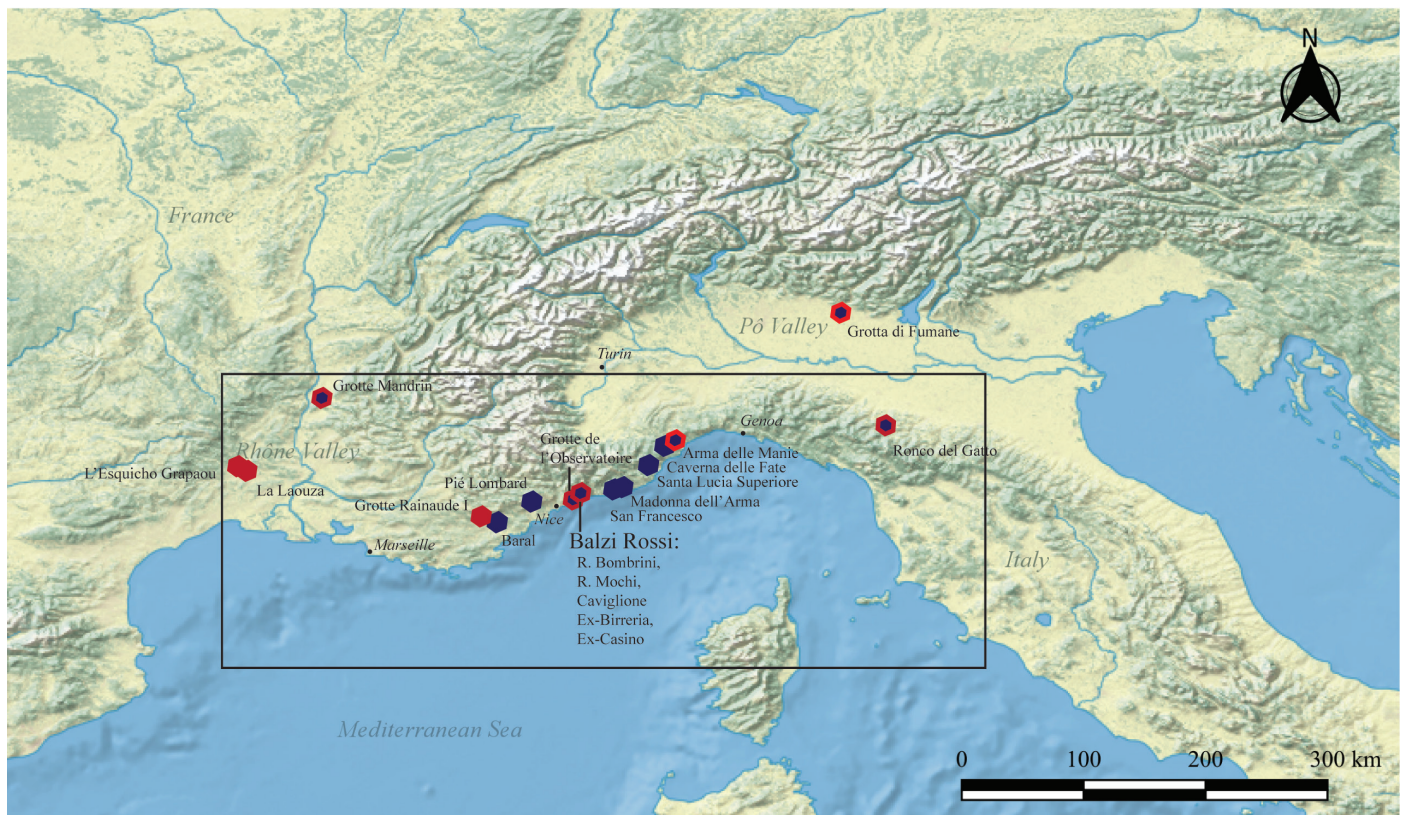


Figure 1. Map of the Liguro-Provençal arc (highlighted within the rectangle) displaying key sites documenting Proto-Aurignacian (marked in red) and late Mousterian (marked in blue) levels (basemap produced in QGIS with Natural Earth data).

renza et al., 2015; Henry et al. 2011; Mariotti Lippi et al. 2023; Power et al. 2018; Rampelli et al. 2021; Sistiaga et al. 2014). Inter-assemblage continuities in taxonomic composition and skeletal representation have also been observed in numerous western Eurasian sites with long transitional sequences (e.g., Adler et al. 2006; Discamps et al. 2011; Münzel and Conard 2004; Yravedra et al. 2016).

Despite the continuities often indicated by the presence or absence of certain behaviors, many scholars have highlighted contrasting regional trends in early Upper Paleolithic contexts across Europe. These trends could reflect pronounced adaptability, changes in social organization, and human-environment interactions (Pederzani et al. 2024; Rendu et al. 2019; Romandini et al. 2020; Smith et al. 2021; Soulier 2013). In this study, we examine and discuss three such trends related to animal exploitation within the context of the Liguro-Provençal arc: 1) the technological change toward long-range weapons, 2) the increased human exploitation of carnivores, and 3) the exploitation of an increasingly broader range of animal raw materials for symbolic and technological purposes.

REGIONAL PERSPECTIVE ON THE LIGURO-PROVENÇAL ARC

The Liguro-Provençal arc is a biogeographic corridor constrained by the pre-alps to the north and the Mediterranean Sea to the south, linking peninsular Italy, which is thought to have formed a temperate refugium during the Last Gla-

cial (Carvalho and Bicho 2022; Finlayson et al. 2006; Valensi 2009), to the western European mainland. It extends approximately 400km from the Rhône Valley to the Po valley in northeastern Italy (Figure 1). Its topography would have constrained human and animal mobility on an east-west axis along the littoral, with limited north-south movement between the shore and the mountains (Negrino and Riel-Salvatore 2018).

Recent studies of raw material sourcing have shown how the geophysical context and the availability of lithic raw material shaped the resource management strategies adopted by human populations in this region, while also highlighting contrasts in raw material procurement between the Mousterian and Proto-Aurignacian (Grimaldi and Santaniello 2014; Grimaldi et al. 2014; Porraz and Negrino 2008; Porraz et al. 2010; Rossoni-Notter and Simon 2016; Rossoni-Notter et al. 2017; Tomasso and Porraz 2016). Interpretations of land-use patterns depict Neanderthal groups as having locally focused mobility strategies (i.e., less than 30km), while still extending their social networks from eastern Liguria to western Provence (Riel-Salvatore and Negrino 2009). In contrast, early modern human groups appear to have been more selective regarding raw material quality, sourcing exotic raw materials from 50km to 200km away within regions of generally poor-quality local raw material. This suggests more extensive social networks and long-distance mobility between the Po and the Rhône valleys (Porraz and Negrino 2008; Porraz et al. 2010;

TABLE 1. RECOVERY METHODS FOR EACH EXCAVATION PHASE AND PUBLISHED DATA ON FAUNA AT RIPARO BOMBRINI.

Excavation year	Levels	Recovery methods	Published archaeozoological data	Published ZooMS data
1976	A1–2	1m ² excavation units/ 5cm spits; piece-plotted diagnostic artifacts and bones >10cm; sediments water-sieved.	n/a	n/a
1976	MS; M1–5	1m ² excavation units/ 5–10cm spits; piece-plotted diagnostic artifacts and bones; sieved sediments not yet available.	n/a	n/a
2002–2005	A1; A2; MS; M1–7	1m ² excavation units/ 5cm spits; piece-plotted diagnostic artifacts and bones >5cm; sediments water-sieved.	Part of piece-plotted fauna in Holt et al. (2019); Part of PA levels in Pothier-Bouchard et al. (2019)	Part of PA levels in Pothier-Bouchard et al. (2020)
2015	A1	1m ² excavation units/ 5cm spits; piece-plotted diagnostic artifacts and bones >5cm; sediments water-sieved; recovery of the small fraction (<1cm) of coprolites in square-meter unit EE3.	Part of PA levels in Pothier-Bouchard et al. (2020)	<i>idem</i>
2016–2021	A1; A2; MS	50cm ² excavation subunits/ 5cm spits; piece-plotted diagnostic artifacts and bones >2cm; sediments water-sieved; recovery of small fraction (<1cm) of coprolites from the sieve.	<i>idem</i>	<i>idem</i>

Riel-Salvatore and Negrino 2009).

Interpreting the subsistence strategies of both human populations has been challenging due to a lack of sites excavated with modern methods, limiting the availability of high-resolution and well-dated faunal collections (see the list of sites with Mousterian and Proto-Aurignacian faunal collections in Supplemental Information (SI) Table 1). The rich Mousterian record, dated between MIS 5–3, that documents Neanderthal subsistence strategies in the Liguro-Provençal arc, mostly comes from sites excavated before the introduction of modern excavation methods during the second half of the 20th century. These sites include Madonna dell'Arma, Caverna delle Fate, Arma delle Manie, Santa Lucia Superiore, and Via San Francesco (Psathi 2003; Valensi 2009; Valensi et al, 2001). Nevertheless, the synthesis by Valensi and Psathi (2004) highlights the dominance of red deer in all assemblages, indicating the persistence of rich forested environments. The authors also suggest that hunting strategies were likely influenced by the exploitation of readily available game, determined by topography and climate.

The Proto-Aurignacian record is particularly challenging, with only three sites: Riparo Bombrini, Riparo Mochi, and Grotte de l'Observatoire. The latter suffers from recovery biases that prevent secure chronostratigraphic association of the faunal remains (Brugal et al. 2017; Romandini 2017). Nevertheless, the collections from Riparo Bombrini and Riparo Mochi both document a long stratigraphic sequence spanning the Mousterian and the Proto-

Aurignacian and have both benefited from careful archaeological analyses (Alhaique 2000; Holt et al. 2019; Pothier Bouchard et al. 2020, 2023; Perez et al. 2022; Stiner 1999). These analyses show that modern humans continuously exploited taxa living near the site, primarily red deer, followed by ibex, bovines, horses, and wild boars.

MATERIAL AND METHODS

SAMPLING STRATEGY FOR THE ARCHAEOZOOLOGICAL ANALYSIS

Prior observations of excavation methods and the state of preservation of the faunal remains at Riparo Bombrini were crucial in designing our sampling strategy for the levels in our study (i.e., Levels A1, A2, and MS), which aimed to meet three objectives: 1) maximize morphological and taxonomic identifications, 2) adequately represent the different parts of the site where the three levels are undisturbed and excavated, and 3) achieve a high taphonomic resolution. The three phases of excavation on the site (1976, 2002–2005, and 2015–2019) employed different recovery standards, which affected the taphonomic resolution of the faunal assemblages (Table 1; SI text on the faunal assemblages of Riparo Bombrini).

A total of 19,804 faunal remains from different areas of the site were analyzed in this study. To meet the first objective, we focused on the area outside the rockshelter. This area is defined as all the square-meter units located to the south and west of the rockshelter's dripline, corre-

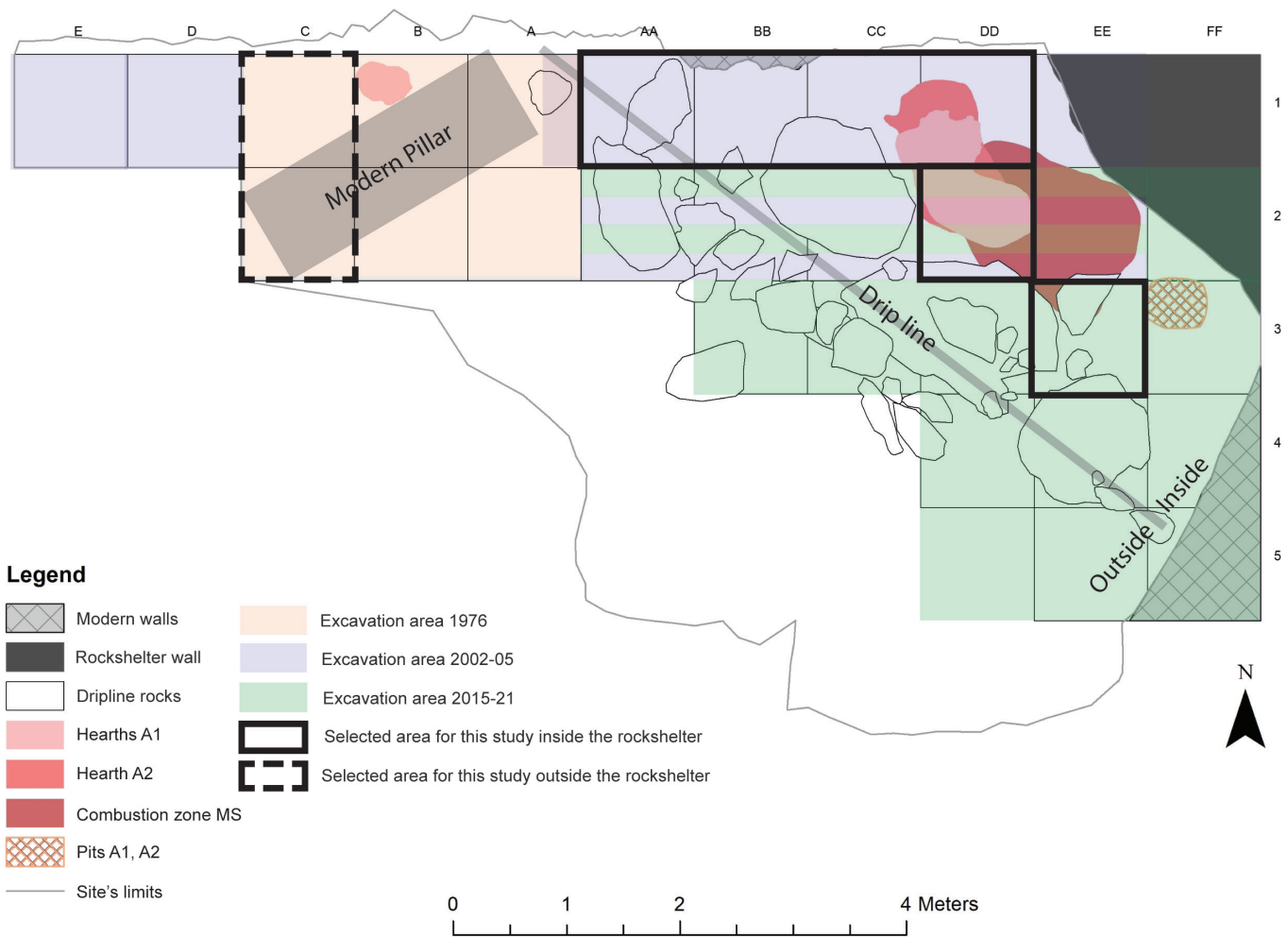


Figure 2. Map of Riparo Bombrini showing the three excavation phases, the overlapping features documented in Levels A1, A2, and MS, and the square-meter units selected for our analysis.

sponding to a line of fallen blocks from what used to be the limit of the rockshelter's roof (Figure 2). Our previous archaeozoological and ZooMS analyses of the Proto-Aurignacian assemblages revealed that the skeletal remains in this area were better preserved for both morphological and proteomic identification (Pothier Bouchard et al. 2020). However, only the area excavated in 1976 documents distinct and *in situ* Levels A1, A2, and MS, thus lacking the desired taphonomic resolution, especially in Level MS where the sieved archaeological material is not yet available. In this area, we selected square-meter units C1 and C2 for systematic ZooMS sampling during the archaeozoological analysis of the entire faunal assemblages available in those square-meter units (Table 2; see Figure 2).

Unit C1 documents the bulk of the fauna recovered in 1976, especially for the MS levels, and is located immediately next to a small combustion area in Level A1. C2 does not document the Proto-Aurignacian levels. However, adding this square-meter unit helped enrich Level MS, which is poorly documented in the area outside the rockshelter. In this better-preserved area, isotope samples were also select-

ed from sixteen bone samples that had rendered positive ZooMS identifications. These samples come from the two Proto-Aurignacian Levels A1 and A2, and the Final Mousterian Levels M3 to M5 underlying Level MS. This choice was made due to the inadequate preservation of the MS skeletal remains for isotope analysis.

Inside the rockshelter, we selected square-meter units AA1, BB1, CC1, DD1, DD2, and EE3. The first four square-meter units involve partly published data from the Proto-Aurignacian levels (Pothier Bouchard et al. 2020) and newly studied data from the three Levels A1, A2, and MS. Units DD1 and DD2 document the bulk of the faunal remains and artifacts of the area, concentrated within superimposed hearth features close to the rockshelter wall (see Figure 2; Figure 5 below). Finally, Unit EE3 is the only square-meter unit excavated exclusively during the most recent campaigns, which included the recovery of the smallest fraction of coprolites within the three stratigraphic levels. In total, this sample corresponds to over 50% of the undisturbed excavated areas on the site (see Table 2).

TABLE 2. NUMBER OF BONE SPECIMENS SAMPLED FOR THE FAUNAL ANALYSIS, FTIR SCREENING, ZOOMS, AND ISOTOPES.*

Levels	Square-units	Archaeozoology and taphonomy	FTIR	ZooMS				Isotopes	Excavation year
				Acid-soluble	Acid-insoluble	RPC Acid-soluble	RPC Acid-insoluble		
A1	<i>C1</i>	832	165	98	15	45	6	8	1976
	<i>C2</i>	<i>n/a</i>	<i>n/a</i>	<i>n/a</i>	<i>n/a</i>	<i>n/a</i>	<i>n/a</i>	<i>n/a</i>	<i>n/a</i>
	AA1	212	35	12	<i>n/a</i>	<i>n/a</i>	<i>n/a</i>	<i>n/a</i>	2002
	BB1	408	39	6	<i>n/a</i>	1	<i>n/a</i>	<i>n/a</i>	2002
	CC1	270	23	6	<i>n/a</i>	1	<i>n/a</i>	<i>n/a</i>	2002
	DD1	1316	100	43	<i>n/a</i>	4	<i>n/a</i>	<i>n/a</i>	2002–05
	DD2	453	3	<i>n/a</i>	<i>n/a</i>	<i>n/a</i>	<i>n/a</i>	<i>n/a</i>	2002–04
	EE3	997	22	22	<i>n/a</i>	<i>n/a</i>	<i>n/a</i>	<i>n/a</i>	2015–16
Total Level A1		4488	387	187	15	51	6	8	
A2	<i>C1</i>	1422	177	77	12	27	7	3	1976
	<i>C2</i>	<i>n/a</i>	<i>n/a</i>	<i>n/a</i>	<i>n/a</i>	<i>n/a</i>	<i>n/a</i>	<i>n/a</i>	<i>n/a</i>
	AA1	20	5	2	<i>n/a</i>	<i>n/a</i>	<i>n/a</i>	<i>n/a</i>	2002
	BB1	80	13	4	<i>n/a</i>	<i>n/a</i>	<i>n/a</i>	<i>n/a</i>	2002
	CC1	622	37	10	<i>n/a</i>	1	<i>n/a</i>	<i>n/a</i>	2002
	DD1	6400	291	81	<i>n/a</i>	1	<i>n/a</i>	<i>n/a</i>	2002–05
	DD2	459	15	14	2	<i>n/a</i>	<i>n/a</i>	<i>n/a</i>	2003–04; 2016–17
	EE3	1420	40	36	<i>n/a</i>	3	<i>n/a</i>	<i>n/a</i>	2016–17
Total Level A2		10,423	578	224	14	32	7	3	
MS	<i>C1</i>	38	21	13	8	4	3	<i>n/a</i>	1976
	<i>C2</i>	3	3	1	<i>n/a</i>	1	<i>n/a</i>	<i>n/a</i>	1976
	AA1	66	11	1	<i>n/a</i>	1	<i>n/a</i>	<i>n/a</i>	2002–05
	BB1	45	3	<i>n/a</i>	<i>n/a</i>	<i>n/a</i>	<i>n/a</i>	<i>n/a</i>	2002
	CC1	111	7	<i>n/a</i>	<i>n/a</i>	<i>n/a</i>	<i>n/a</i>	<i>n/a</i>	2002–05
	DD1	1520	46	2	2	<i>n/a</i>	1	<i>n/a</i>	2005
	DD2	2881	123	9	7	2	<i>n/a</i>	<i>n/a</i>	2005; 2017–19
	EE3	229	34	1	1	<i>n/a</i>	<i>n/a</i>	<i>n/a</i>	2017
Total Level MS		4893	248	27	18	8	4	<i>n/a</i>	
M3-5	<i>C1</i>	<i>n/a</i>	<i>n/a</i>	<i>n/a</i>	<i>n/a</i>	<i>n/a</i>	<i>n/a</i>	1	1976
	<i>C2</i>	<i>n/a</i>	<i>n/a</i>	<i>n/a</i>	<i>n/a</i>	<i>n/a</i>	<i>n/a</i>	4	1976
Total Levels M3–5		0	<i>n/a</i>	<i>n/a</i>	<i>n/a</i>	<i>n/a</i>	<i>n/a</i>	5	

*The data in italics corresponds to the site area outside the rockshelter dripline. RPC= reverse phase chromatography.

Morphological Taxonomic Identification

We identified teeth by consulting the reference collection of herbivore and carnivore skulls curated by the Museo Civico di Storia Naturale di Genova. We identified skeletal remains using osteological atlases (Barone 1975; Pales and Garcia 1981; Schmid 1972) and three open-source virtual collections—the 3D models provided by the Max-Planck-Gesellschaft Department of Human Evolution (<https://www.eva.mpg.de/evolution/downloads.html>), the 3D

models of the Laetoli project (<https://laetoli-production.fr>), and the photographic osteological collection of the Archéo-Zoothèque (<https://www.archeozoo.org/archeozootheque>). When skeletal remains of ungulates could not be identified to a species, they were assigned to size categories adapted from Brain (1981) and Bunn (1986)—smaller ungulates size 1: <50kg (e.g., *Rupicapra rupicapra*, *Capreolus capreolus*) and size 2: 50–100kg (e.g., *Capra ibex*, *Sus scrofa*, *Dama dama*); larger ungulates size 3: 100–300kg (e.g., *Rangifer tarandus*,

Cervus elaphus) and size 4: 300–1000kg (e.g., *Bos/Bison* sp., *Equus* sp.); megafauna size 5: >1000kg (e.g., *Mammuthus* sp., *Coelodonta* sp.). Intermediate categories such as Cervidae size 1/2 or artiodactyl size 3/4 were often more appropriate at Riparo Bombrini, given the high level of bone fragmentation. Carnivores are classified within three size classes—size 1: small carnivores (e.g., *Vulpes vulpes*), size 2: medium carnivores (e.g., *Canis lupus*, *Crocuta crocuta*), and size 3: large carnivores (e.g., *Ursus* sp.).

FTIR Screening and ZooMS Identification

Because collagen preservation is compromised at Riparo Bombrini, we applied a screening method using a portable FTIR developed and tested elsewhere (Pothier Bouchard et al. 2019) while conducting the faunal analysis at the University of Genoa (Italy). We tested bone samples for collagen preservation distributed within the three stratigraphic levels (see Table 2) using a sampling strategy based on three criteria, prioritizing (by order of importance): 1) bones morphologically identified to a skeletal element and a broad taxonomic category (e.g., ungulate size 3/4, artiodactyl size 1/2), 2) taxonomically unidentifiable bones of juvenile and fetal remains that maximize age and seasonal data acquisition, 3) and bones with surface alterations such as anthropic action (e.g., percussion marks, cut marks, splinters) and carnivore action (e.g., gnawing, tooth punctures, gastric digestion) to assess taphonomic attrition biases. Finally, we conducted a random selection of bones of variable size and cortical thickness from the indeterminate fraction of the collection to improve the NISP tally and assess faunal diversity and post-depositional attrition. It is important to note that the attribution of animal size categories according to cortical thickness classes was shown to be highly variable in other ZooMS analyses (Sinet-Mathiot et al. 2019).

Approximately 1mg of bone powder was extracted using a scientific mortar and pestle. We processed each sample using an Agilent 4500a portable FTIR instrument equipped with a single-bounce diamond ATR and internal battery following the method detailed in Pothier Bouchard et al. (2020). The screening threshold of 0.06 was selected, meaning a sample was rejected for ZooMS analysis when its CO/P ratio scored less than 0.06. When a bone specimen was selected for ZooMS, another 25mg to 50mg of bone powder was extracted in the same manner and placed in a 1.5mL Eppendorf tube, which was then brought to the ZooMS laboratory at the University of Manchester (UK).

We followed the ZooMS protocols previously applied at Riparo Bombrini (Pothier Bouchard et al. 2019; 2020). The bone samples (N=438; see Table 2) were first processed with low through-put acid-soluble ZooMS analysis following the method adapted from Buckley et al. (2009). We carried out MALDI-MS on a Bruker Ultraflex II instrument, with a m/z window of 700–3,700 mass units and up to 2,000 laser acquisitions per spot. We analyzed the obtained collagen fingerprints with mMass software (v5.5.0), and we identified animal species using previously published collagen peptide markers from reference spectra following

Buckley et al. (2009; 2017) (see SI Table 2 for the list of peptide markers used in this analysis). The resulting spectra exhibiting lower collagen preservation (i.e., missing peptide markers) were selected for further analysis (see Table 2). We first applied the same ZooMS protocol on the acid-insoluble residue on the 47 samples identified to a wide taxonomic category (e.g., ungulate) following Buckley et al. (2009). Next, we purified and fractionated 102 samples using reverse phase chromatography (RPC) with C18 solid phase extraction (SPE) pipette tips, following the manufacturer's protocol (Varian, UK). This method helped clarify some of our cervid identifications by improving the signal intensity of the A2T67(G) biomarker, essential to distinguish between *Cervus* (m/z value of 3033) and *Capreolus* (m/z value of 3059.4), and between *Rupicapra* (m/z value of 3033) and *Capra* (m/z value of 3093.4) (see Buckley et al. 2010 for discussion on the isolation of collagen-peptide markers). However, it is worth noting that red deer (*Cervus elaphus*) and fallow deer (*Dama dama*) are too closely related to be distinguished with ZooMS (Buckley and Kansa 2011). It is thus possible that some of our *Cervus* ZooMS identification also includes anecdotal *Dama* specimens (see Pothier Bouchard et al. 2020).

Stable Isotopic Analysis

To help previous paleoenvironmental reconstructions on the site (see Holt et al. 2019), we selected a total of 16 bone specimens previously identified taxonomically with ZooMS (n=1 *Capra*; n=1 *Bos/Bison* sp.; n=2 *Sus*; n=6 *Cervus*; n=4 *Cervus/Capreolus*; n=2 *Capra/Rupicapra*) to measure $\delta^{13}\text{C}$, $\delta^{15}\text{N}$, and $\delta^{34}\text{S}$ values in bone collagen (see Table 2; SI Table 3). When possible, bones with evidence of anthropic modification, such as butchering marks or fresh fractures, were selected at each level to ensure that the paleoenvironmental evidence was directly linked to periods of human presence. Approximately 1g of bone was extracted using a low-vibration micromotor with a diamond-edge cutting wheel for each bone specimen. The selected specimens were sampled at the EvoAdapta laboratory of the University of Cantabria, Spain, where collagen extraction was carried out following the Longin (1971) method with modifications as suggested by Collins and Galley (1998). The surface of the samples was cleaned for abrasion with a drill head tool. Samples were demineralized in 0.5M HCl at 20°C for between 6 and 15 days. Then, samples were washed three times with de-ionized water and gelatinized in a pH3 solution (distilled water and 0.5M HCl), and sealed into a pre-heated oven set at 75°C for 48 hours. The samples were filtered using 5–8 μm Ezee® mesh filters (Elkay Laboratory Products), frozen for 48 hours at -23°C, and lyophilized at -46°C with a pressure of 0.093mBar for 48 hours. The collagen weight obtained was between 380mg and 764mg. Carbon, nitrogen and sulfur isotope analysis of samples was undertaken by Elemental Analysis - Isotope Ratio Mass Spectrometry (EA-IRMS) at the Iso-Analytical facility (UK). The $\delta^{13}\text{C}$, $\delta^{15}\text{N}$ and $\delta^{34}\text{S}$ values are reported relative to the International V-PDB, AIR, and VCDT standards (see details in the SI). Specimens were analyzed in duplicate every five samples. The aver-

age reproducibility of samples measured in duplicate was 0.2%. The following established bone collagen quality indicators were used: % collagen (>1), %C (30–44%), %N (11–16%), %S (0.15–0.35%), C:N (2.9–3.6), C:S (600±300) and N:S (200±100) (Ambrose 1990; DeNiro 1985; Nehlich and Richards 2009; van Klinken 1999).

Quantification Methods

We applied standard quantification methods, including measures of taxonomic abundance (total number of specimens – NSP, Number of identified specimens – NISP, Minimum number of individuals – MNI) and the calculation of skeletal part frequencies (minimum number of elements – MNE, minimum animal units – MAU), and the food utility index (FUI) (Grayson 1984; Lyman 2008; Metcalfe and Jones 1988) to the extent possible given the highly fragmentary nature of the assemblages. Statistical tests were done in Excel and Past 3.14 software.

Our tallies are affected by the usual problems related to measuring taxonomic abundance, such as intertaxonomic variability, differential preservation, the interdependence of skeletal remains, and differential recovery (Grayson 1984; Lyman 2008). The high degree of fragmentation at Riparo Bombrini hinders the MNI count to the point of reducing most MNI tallies to either one or two individuals per taxon. For this reason, NISP is preferred over MNI and MNI-derived measures (e.g., biomass measures, meat weight) when discussing taxonomic abundance and taxonomic structure and composition on the site.

Owing to the degree of fragmentation, skeletal-part frequencies are presented on the nominal scale using NISP counts of the skeletal elements (NISPe), a simple count of all skeletal elements (right, left, and indeterminate sides) for each taxon. The NISPe tallies of all skeletal elements are then grouped by skeletal region following Stiner (2002b) adding two indeterminate categories (indeterminate limb and indeterminate) because several ZooMS identifications were obtained from morphologically unidentifiable skeletal elements. We summarized NISPe values by grouping taxonomic categories at the family and sub-family levels (Cervidae size 1/2 = *Capreolus* + *Dama dama* + cervid size 1/2; Cervidae size 2/3 = *Cervus elaphus* + *Cervus sp* + cervid size 2/3; Caprinae size 1/2 = *Capra sp* + caprine size 2/3 + bovid size 2/3; bovine = *Bos/Bison sp.* + bovid size 3/4; suidae = *Sus sp.*; ungulate size 1/2 = Artiodactyle size 1/2+ ungulate size 1/2; ungulate size 3/4 = Artiodactyle size 3/4, ungulate size 3/4) and two broader size categories (ungulate size 1/2 and ungulate size 3/4) and normalize using the most abundant taxa in order to be in a position to cautiously discuss carcass treatment and transport for these taxonomic categories. Where possible, we calculated MNE according to three criteria: 1) the overlap of skeletal elements and diagnostic anatomical landmarks as proposed in Morin et al. (2017), 2) the age and sex of the skeletal remains, and 3) the size of the specimens. Unfortunately, the high level of fragmentation precluded us from statistically testing density-mediated attrition and carcass transport strategies with MNE-derived

quantitative values (MNE<10).

Finally, we calculated four measures of taxonomic structure and composition based on the NISP of ungulate taxa at the genus level (Grayson 1984; Lyman 2008): 1) the taxonomic Richness *S* or NTAXA calculated as the number of taxonomic categories (on the family and sub-family level) present in the assemblages, 2) the taxonomic heterogeneity *H* calculated with the Shannon index ($H = -\sum P_i(\ln P_i)$, where P_i is the proportion P of the taxon i in the assemblage, 3) the taxonomic evenness index e derived from H and the log of NTAXA using the formula $e=H/\ln S$, and 4) the reciprocal of Simpson's index $1/D$ with the formula $1/\sum P_i^2$. Finally, we tested the correlation between taxonomic richness (NTAXA) and sample size ($\sum NISP$) by calculating the Pearson linear correlation of the different faunal assemblages (Grayson and Delpech 1998).

Age and Sex

We recorded data related to age, sex, and seasonality where possible. Age assessments for teeth were based on wear patterns and eruption stages across various species—Cervinae and Capreolinae (Brown and Chapman 1991; Carter 2006; d'Errico and Vanhaeren 2002), Caprinae (Payne 1987), Bovinae (Grant 1982), Suidae (Grant 1982; Magnell 2006), Equidae (Bignon 2006; Levine 1982), Ursidae (Stiner 1998), and Canidae (Gipson et al. 2000). We also measured the crown heights of Cervidae and Equidae, applying the quadratic crown height method (QCHM) using the formula by Klein et al. (1983) and incorporating potential ecological longevity data for *Cervus elaphus* and *Equus przewalskii* (Klein and Cruz-Urbe 1984: 49–50). Additionally, epiphyseal stages were calculated for Cervinae (Carden and Hayden 2006; Reitz and Wing 2008), Bovinae (Koch 1932 in Julien 2011), and Caprinae (Zeder 2006).

Due to the poor preservation of the occlusal surfaces of ungulate teeth, which precluded the use of species-specific wear patterns and crown height measurements, we adapted the age classification systems from Discamp and Costamagno (2015) for the main ungulate taxa—for Caprinae, juvenile (J: 0–1.5 years), adult (A: 1.5–8 years), and old (O: >8 years); for Cervinae, J: 0–2 years, A: 2–12 years, O: >12 years; for Bovinae, J: 0–3 years, A: 3–12 years, O: >12 years; and for Equidae, J: 0–2 years, A: 2–15 years, O: >15 years. The limited sample size for age determinations also prevented us from drawing mortality profiles using MNI tallies. Therefore, age determinations will be expressed qualitatively using NISP tallies.

Sex identification was based on the presence or absence of canines for Equidae and Cervinae (typically present in males and absent or vestigial in females) and the presence of antlers for Cervidae (males), excluding reindeer. The presence of unshed antlers and juvenile prey informed discussions about the seasonality of site occupations. Microwear analysis was not feasible for these collections, as most teeth had either damaged occlusal surfaces or were embedded in concretion.

TABLE 3. DESCRIPTION OF THE BONE BURNING CATEGORIES SELECTED IN THIS STUDY.

	Color description	Color categories (Stiner 1995)	Stage of combustion (Marques et al. 2018)
Unburned	No visible burning coloration	0	Intact or dehydration (0 to 250°C)
Carbonized	All black or traces of black	1, 2, and 3	Decomposition of the organic component (400 to 600°C)
Calcined	Transition from black to white/blue/greyish or completely white/grey	4, 5, and 6	Inversion and fusion (600 to 1000°C)

TAPHONOMIC METHODS

We utilized taphonomic indices to reconstruct depositional and post-depositional processes affecting the preservation of the archaeozoological assemblages. This analysis included plotted finds, complete and partial elements, and every bone shaft fragment larger than 2 centimeters. We documented bone surface alterations using a three-stage intensity scale (i.e., stage 1: <50% covered, stage 2: >50% covered, and stage 3: entirely covered), which encompassed anthropic alterations (Blumenschine 1995; Blumenschine et al. 1996; Domínguez-Rodrigo 2009; Fisher Jr. 1995; Lyman 1994). We also recorded burning levels according to a simplified set of color classes (unburned, carbonized, and calcined) adapted from Stiner et al. (1995) and Marques et al. (2018) (Table 3).

Fracture freshness angles were recorded for long bone shafts (Villa and Mahieu 1991), and the mean Fracture Freshness Index (FFI) calculated according to Outram (2001). All surface modifications were identified using a Dino-Lite Edge Digital Microscope 20X–220X with enhanced DOF, operated with DinoCapture 2.0 software.

At Riparo Bombrini, the unidentifiable fraction constitutes the majority of the faunal remains, ranging from 95% to 99% of the total number of specimens (NSP). Given this, it was crucial to rapidly and efficiently gather a maximum of taphonomic information from the entire assemblage. We conducted a detailed taphonomic study of this fraction by sorting each bulk bag into eight size classes based on maximum length (0–20mm, 20–30mm, 30–40mm, 40–50mm, 50–60mm, 60–80mm, 80–100mm, >100mm). These classes were further categorized by burning level (unburned, carbonized, and calcined) and bone type (appendicular cancellous, axial cancellous, indeterminate cancellous, appendicular cortical, flat bones, teeth, cranial, and indeterminate) (Pothier Bouchard et al. 2020). Each subdivision was quantified and weighed with a Tangent KP-103 scale (Max 120.0g, d=0.1g).

INTRA-SITE MULTIVARIATE TAPHONOMIC ANALYSIS

We conducted a detailed intra-site multivariate taphonomic analysis of three faunal assemblages, starting with a general description of the taphonomic variables impacting each assemblage. These variables were categorized into four groups (detailed in SI Table 4): 1) general assemblage data, (2) bone preservation, 3) natural taphonomic processes affecting long bones, and 4) anthropic processes affecting long bone damage. The hierarchical analysis then proceeded as follows: 1) bone completeness and fragmentation documenting density-mediated attrition, post-depositional *in situ* attrition, and pre-depositional fragmentation (variables detailed in SI Table 5), 2) agents of bone accumulation, documenting carnivore and human action (variables detailed in SI Table 6), and 3) on-site carcass treatment, documenting marrow extraction, grease rendering, and bone as fuel (variables detailed in SI Table 7).

We displayed the taphonomic variables in tables and illustrated them with line graphs to aid inter-assemblage comparisons. The variables were primarily quantified as percentages of NSP (total number of specimens) to illustrate how variables affect the entire assemblages, and NSP.lb (total number of specimens of long bone shaft fragments) to observe specific taphonomic alterations on long bone shafts. Additionally, comparisons were made between small game (ungulate taxa corresponding to body sizes 1 and 2) and large game (ungulate taxa corresponding to body sizes 3 and 4). These comparisons involved expressing taphonomic variables as percentages of NISP (number of identified specimens) and NISP.lb (number of identified specimens of long bone shaft fragments) tallies for these broad taxonomic groups to explore how variables interact with body size.

TABLE 4. RELATIVE ABUNDANCE OF TAXA.*

Taxa	Bombrini A1				Bombrini A2				Bombrini MS			
	NISP	%NISP	%NSP	MNI	NISP	%NISP	%NSP	MNI	NISP	%NISP	%NSP	MNI
Herbivores												
<i>Bos/Bison</i> sp.	14	8.0	0.3	1	25	11.8	0.2	1	n/a	n/a	n/a	n/a
<i>Capra ibex</i>	23	13.1	0.5	1	21	9.9	0.2	1	3	4.1	0.1	1
<i>Capreolus</i> sp.	6	3.4	0.1	1	2	0.9	0.0	1	n/a	n/a	n/a	n/a
<i>Cervus elaphus</i>	3	1.7	0.1	1	n/a	n/a	n/a	n/a	1	1.4	0.0	1
<i>Cervus</i> sp.	60	34.3	1.3	1	36	17.0	0.3	1	11	14.9	0.2	1
<i>Dama dama</i>	1	0.6	0.0	1	n/a	n/a	n/a	n/a	n/a	n/a	n/a	n/a
<i>Equus</i> sp.	2	1.1	0.0	1	11	5.2	0.1	2	1	1.4	0.0	1
<i>Sus scrofa</i>	2	1.1	0.0	1	6	2.8	0.1	1	3	4.1	0.1	1
Bovidae size 1/2	1	0.6	0.0	1	n/a	n/a	n/a	n/a	2	2.7	0.0	1
Caprinae size 1/2	5	2.9	0.1	1	n/a	n/a	n/a	n/a	n/a	n/a	n/a	n/a
Cervidae size 1/2	n/a	n/a	n/a	n/a	n/a	n/a	n/a	n/a	1	1.4	0.0	1
Cervidae size 2/3	5	2.9	0.1	1	3	1.4	0.0	1	4	5.4	0.1	1
Cervidae indeterminate size	2	1.1%	0.0	1	8	3.8	0.1	1	3	4.1	0.1	1
Artiodactyla size 1/2	n/a	n/a	n/a	n/a	3	1.4	0.0	1	6	8.1	0.1	2
Artiodactyla size 3/4	14	8.0%	0.3	1	35	16.5	0.3	3	12	16.2	0.2	1
Artiodactyla indeterminate size	n/a	n/a	n/a	n/a	3	1.4	0.0	1	7	9.5	0.1	1
Ungulate size 1/2	4	2.3	0.1	1	1	0.5	0.0	1	n/a	n/a	n/a	n/a
Ungulate size 3/4	14	8.0	0.3	1	40	18.9	0.4	1	12	16.2	0.2	1
Ungulate indeterminate size	17	9.7	0.4	1	15	7.1	0.1	1	1	1.4	0.0	1
Carnivores												
<i>Ursus</i> sp.	n/a	n/a	n/a	n/a	1	0.5	0.0	1	1	1.4	0.0	1
Carnivore size 1/2	n/a	n/a	n/a	n/a	n/a	n/a	n/a	n/a	1	1.4	0.0	1
Carnivore size 2/3	2	1.1	0.0	1	2	0.9	0.0	1	5	6.8	0.1	1
Total NISP	175	100	3.9		212	100	2.0		74	100	1.5	
Indeterminate	4313		96.1		10,211		98.0		4819		98.5	
Total NSP	4488		100		10,423		100		4893		100	

*Number of identified specimens (NISP), total number of specimens (NSP), and minimum number of individuals (MNI).

RESULTS

SUMMARY OF THE ARCHAEOZOOLOGICAL DATA

Relative Abundance of Taxa

The three assemblages exhibit low rates of identifiable skeletal remains—4%NSP in Level A1, 2%NSP in Level A2, and 2%NSP in Level MS. Notably, a higher proportion of the identifiable specimens is located outside the rockshelter's dripline across the three levels, influenced by various taphonomic factors to be detailed in the multivariate taphonomic analysis.

Despite this differential preservation, discernible trends in the relative abundance of taxa across the archaeological levels are apparent. The faunal spectra are predominantly composed of large Cervidae, likely red deer and some fallow deer (Table 4). In the Proto-Aurignacian Level A1, large Cervidae constitute 40% of NISP, decreasing to 18% in Level A2 and 9% in Level MS. Roe deer frequencies are slightly higher in Level A1 at 3% NISP, compared to 1% in Level A2 and nonexistent in Level MS. Ibex are consistently present but more prevalent in the Proto-Aurignacian (13%NISP in A1 and 10%NISP in A2) than in the Mousterian level (4%NISP). Bovinae, corresponding to either bison or auroch, appear solely in the Proto-Aurignacian levels, com-

TABLE 5. TAXONOMIC COMPOSITION OF UNGULATES AT RIPARO BOMBRINI.*

Faunal assemblages	ΣNISP	NTAXA	H	e	1/D
Level A1	111	7	1.254	0.644	2.600
Level A2	101	6	1.527	0.595	4.043
Level MS	19	4	1.028	0.742	2.215
Level A1 - inside	21	5	0.882	0.548	2.921
Level A1 - outside	90	7	1.157	0.595	2.360
Level A2 - inside	26	6	1.277	0.713	4.630
Level A2 - outside	75	6	1.068	0.596	3.718
Level MS - inside	5	3	0.688	0.627	2.778
Level MS - outside	14	4	0.655	0.472	1.849

*Richness (NTAXA), heterogeneity with Shannon index (H), evenness index (e), and reciprocal of Simpson's index (1/D).

prising the second most abundant taxon in Level A2 with 12%NISP and the third most abundant in Level A1 with 8%NISP. Suidae and Equidae, though widespread, remain less frequent. Finally, carnivore remains are scarce in the Proto-Aurignacian (~1%NISP) and slightly more abundant in Level MS (8%NISP), primarily consisting of unidentifiable medium-sized carnivores. The presence of a few Ursidae teeth in Levels A2 and MS is also notable (see Table 4).

The relationship between the sample size (ΣNISP) and the number of taxa (NTAXA within the sub-assemblages (divided between site areas) shows a statistically significant correlation ($r=0.94$, $p=0.0048$) (SI Figure 3). This correlation suggests that variations in sample size influence taxonomic richness across the areas of the site. Level A1 (ΣNISP=111) is richer but less evenly distributed than A2 (ΣNISP=101) (Table 5). Level MS displays the least evenly distributed and least rich assemblage. However, it also has the smallest sample size, which is more susceptible to bias (ΣNISP=19).

Skeletal Frequencies

Skeletal frequencies across all three assemblages (NISPe) exhibit patterns dominated by head (primarily fragmented teeth) and limb elements, with notable qualitative trends evident at the family and sub-family levels, as well as within the broader ungulate size 3/4 taxonomic category (Figure 3; SI Table 8). While MNE tallies are too low (MNE<10) to illustrate skeletal frequencies and to statistically assess bone survivorship (%MAU) against bone mineral density (BMD) and food utility indices, MNE tallies for the most abundant taxa (i.e., *Cervus* sp., *Capra ibex*, and *Bos/Bison* sp.) are detailed in SI Tables 11 to 19.

In Level A1, the less abundant taxa, Cervidae size 1/2, and Bovinae predominantly include indeterminate limbs and skeletal elements, the latter mainly consisting of small cortical bone fragments (<2cm) identified using ZooMS. Similarly, Caprinae display a predominance of indetermi-

nate limbs and skeletal elements, along with some axial skeleton and head elements. Cervinae and ungulates size 3/4 are primarily represented by limbs, phalanges, and head elements, while medium carnivore remains are represented by head and axial elements.

In Level A2, Cervinae and Caprinae are characterized by head, indeterminate limbs, and indeterminate skeletal elements with a minimal representation of other skeletal portions. In contrast, Bovinae and Equidae exhibit patterns primarily represented by lower limb and toe elements with a few head elements (see Figure 3). The ungulates size 3/4 display a prevalence of head elements, accounting for 60% of total NISPe, along with axial, limb, and toe elements. The scarce medium carnivore and Ursidae elements correspond to indeterminate limb fragments (see SI Table 8).

Level MS is distinguished by the dominance of head elements across almost all taxa, including medium carnivores and Ursidae (see Figure 3). Exceptions include Cervinae and ungulates size 3/4, which show a predominance of axial post-cranial skeletal elements—mostly ribs—and a few limb and head elements. Finally, Cervidae size 1/2 and ungulates size 1/2, though less abundant, display some lower limb and toe elements, but are mainly head-dominated (see SI Table 8).

Age, Sex, and Seasonality Indices

Prime-age adult ungulates dominate the three assemblages (SI Table 9). In Level A1, all ageable remains are adult ungulates (NISP=3 *Cervus elaphus*, NISP=1 *Dama dama*, and NISP=1 *Capra ibex*) with a single exception of one older wild boar. Level A2 presents a slightly broader range of ages among larger ungulates, predominantly prime-age adults (NISP=1 *Cervus* sp., NISP=2 Cervidae size 2/3, NISP=2 *Bos/Bison* sp., and NISP=1 Artiodactyla size 3/4), followed by juveniles (NISP=2 *Equus* sp., and NISP=1 Artiodactyla size 3/4), and a single element corresponding to an older *Equus*

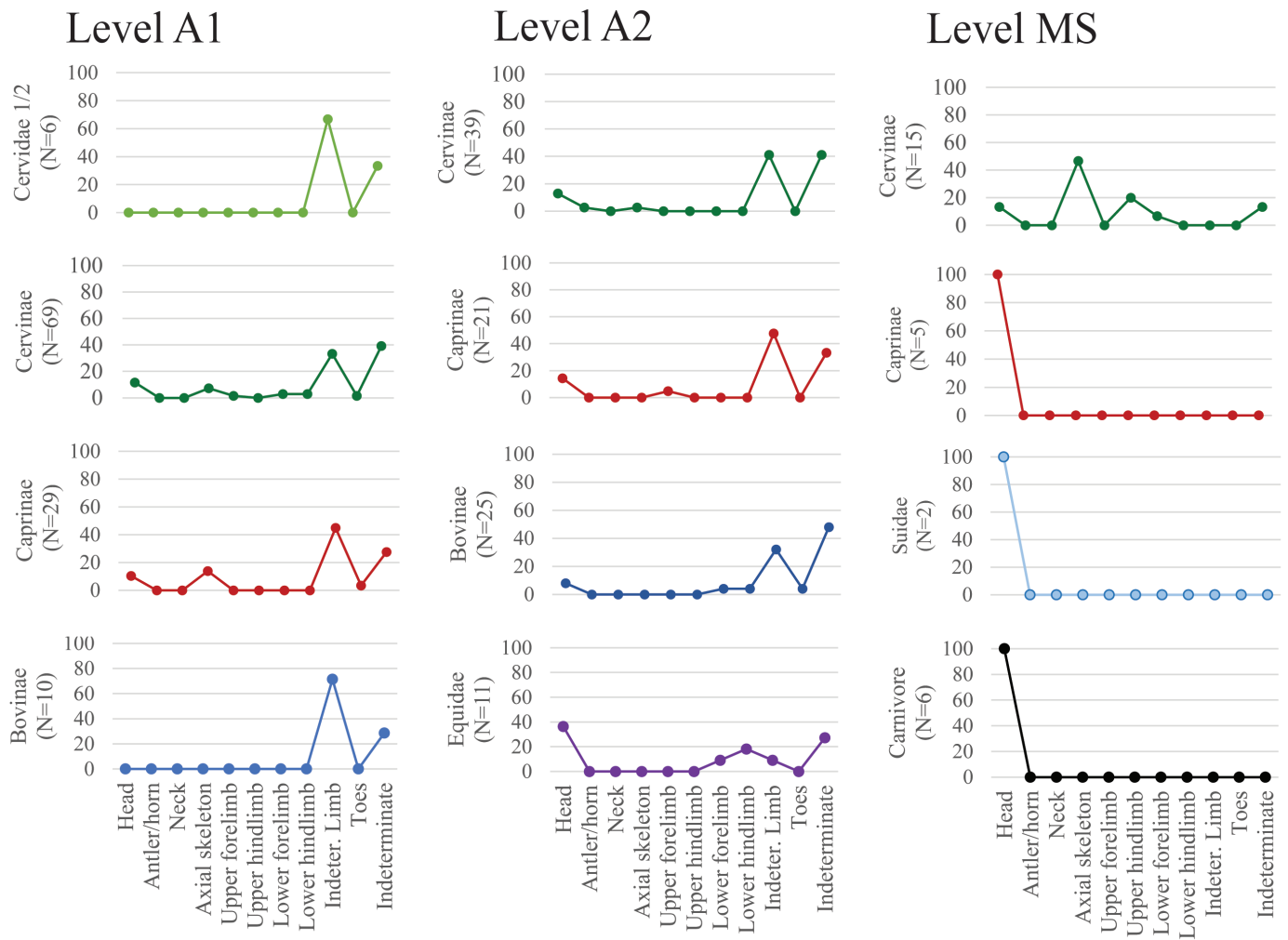


Figure 3. Skeletal frequencies using the number of identified specimens of skeletal elements (NISPe) for the most abundant taxa in Level A1 (left), A2 (middle), and MS (right).

sp. Additionally, post-cranial elements include an indeterminate fetal animal.

In Level MS, all ungulate teeth correspond to prime-age adults (NISP=1 *Cervus elaphus*, NISP=3 *Cervus* sp., NISP=2 Cervinae size 2/3, NISP=2 *Capra ibex*, and NISP=1 *Equus* sp.), with the exception of one older ibex and one juvenile Artiodactyla size 1/2. In contrast, carnivore teeth from this level all correspond to juvenile animals (NISP=1 *Ursus* sp., and NISP=2 carnivores size 3).

Two skeletal elements are associated with male ungulates on the site (see SI Table 9): a Cervidae antler fragment recovered in Level A2, and the canine of a prime-age (~2–4 years) *Cervus elaphus* recovered in Level MS. Although the antler was too altered to be aged, the fragment survived the heavy taphonomic alterations on the site, which suggests that it was fully mineralized. This could indicate the hunting of a male deer near the end of its antler cycle (fall or winter) or the collecting of shed antlers. The presence of a fetal bone in Level A2, if it belongs to an ungulate, indicates the likely presence of a gestating female brought on the site during winter or spring.

MULTIVARIATE INTRA-SITE TAPHONOMIC ANALYSIS

General Taphonomic Observations

The largest faunal assemblage, as indicated by the total number of specimens is found in Level A2 (NSP=10,423), with Levels MS (NSP=4,893) and A1 (NSP=4,488) following (see Table 4; Table 6). In each of the three stratigraphic levels, the faunal assemblages located outside the rockshelter are smaller than those inside. This is because the area outside the dripline encompasses one to two square meters, whereas it spans six square meters inside.

The quarry data in Table 6 clarifies the absolute tallies of skeletal remains for each assemblage, still positioning the largest assemblage in Level A2 (NSP/m³=14,896), based on the volumetric density of skeletal remains. This is followed by Level A1 (NSP/m³=8,614) and Level MS (NSP/m³=4,697). The disparity between site areas remains apparent with a notable wider gap in Level A1, where the volumetric density of piece-plotted fauna outside the dripline is comparable to that in Level MS. Additionally, the data

TABLE 6. GENERAL TAPHONOMIC OBSERVATIONS.*

	Level A1		Level A2		Level MS	
	inside	outside	inside	outside	inside	outside
General assemblage data						
NSP	3656	832	9001	1422	4852	41
NISP	59	114	95	116	50	24
NSP.lb	130	95	148	103	59	1
N ZooMS samples	98	89	77	147	13	14
Quarry data						
Size of studied area (m ²)	6	1	6	1	6	2
Deposit volume (m ³)	0.60	0.33	0.99	0.25	1.81	0.19
Density of piece-plotted artifacts (n/m ³)**	340 (n=204)	170 (n=67)	319 (n=316)	652 (n=163)	110 (n=199)	58 (n=11)
Density of piece-plotted fauna (n/m ³)**	32 (n=19)	33 (n=11)	46 (n=46)	116 (n=29)	81 (n=147)	132 (n=25)
Density of bone fragments (NSP/m ³)**	6093	2521	9092	5688	2681	216
Spatial distribution of fauna – patchiness	Patchy	Slightly patchy	Highly patchy	Even	Slightly patchy	Slightly patchy
Bone state of preservation						
%identifiable before ZooMS (NSP)	1.0	4.4	0.8	3.8	0.9	56
%bone fragments <2cm (NSP)	93	76	96	84	96	37
%ZooMS success (n ZooMS samples)	27	99	39	50	46	100
Long bone damage of natural processes (NSP.lb)						
%Abrasion stage 2 <	18	31	36	36	61	0
%Abrasion and polish	7	8	5	0	27	0
%Concretion stage 2 <	20	23	34	25	66	0
%Manganese coloration stage 2 <	18	35	15	55	20	0
%Trampling	1	2	2	1	0	0
%Etching stage 2 <	2	5	7	6	0	0
%Carnivore gnawing	2	0	1	4	10	0
%Weathering stage 2 <	2	13	5	9	0	0
%Modern fractures	15	20	23	33	69	100
Mean FFI score	5.48	4.12	4.97	4.02	4.92	n/a
Long bone damage of anthropic processes (NSP.lb)						
%Fresh fracture angles	13	54	28	48	31	100
%Burned (carbonized + calcined)	32	21	22	25	7	n/a
%Anthropic percussion	3.1	6.3	0	4.9	0	n/a
%Cut marks	0	0	0	1.9	0	n/a
N Percussion flakes	3	15	13	3	0	n/a
N Bone manufacture	2	0	2	0	0	n/a

*See SI Table 4 for detailed information on the taphonomic variables.

**The measures of density correspond to the theoretical concentration of remains per cubic meters.

illustrate variable concentrations of piece-plotted artifacts relative to the volume of excavated deposit across site areas and archaeological levels. The Proto-Aurignacian levels generally exhibit higher artifact densities than the Mousterian level. While Level MS has similar artifact densities inside and outside the rockshelter, Level A1 is denser in artifacts inside the rockshelter, and Level A2 shows a much higher density of artifacts outside the dripline.

The spatial distribution of the piece-plotted faunal remains suggests potential clustering patterns (Figure 4). In Level A1, bones cluster around the small combustion feature in square-meter unit B1, whereas they are more uniformly distributed in Level A2 (Vallerand et al. 2024). Inside the rockshelter, the distribution of piece-plotted skeletal remains is relatively even except in unit FF3, where a high concentration of bones fills a discard pit adjacent to a disturbed area. This pattern is consistent in Level A2. In Level MS, bones are primarily concentrated within the combustion area and its vicinity. The collapse events of the rockshelter roof during the deposition of Level MS account for the recovery of some skeletal remains beneath the large blocks.

All three faunal assemblages located inside the rockshelter exhibit a low rate ($\leq 1\%$ NSP) of identifiable skeletal remains before ZooMS analysis. In contrast, the area outside the dripline shows higher identifiability—4.4%NSP in Level A1, 3.8%NSP in Level A2, and 56%NSP in Level MS. This discrepancy is primarily due to the degree of fragmentation as shown by the frequency of bone fragments smaller than 2cm, and the readability of bone surfaces obscured by concretion (see Table 6). In Level MS, the percentage of identifiable remains outside the rockshelter is also overestimated due to a comparatively small sample size (NSP=41), partly explained by the recovery methods in the Mousterian levels on the site (see Table 1). However, the area's better morphological preservation is evidenced by a few near-complete skeletal elements in anatomical connection, such as the three aligned ribs with intact bone surfaces recorded in square-meter unit C1, which we identified as red deer with ZooMS (see Figure 9 below). In addition to the better morphological integrity outside the rockshelter, collagen preservation is notably better in this area as well as across the three archaeological levels, as evidenced by the ZooMS success rates (after FTIR screening)—99% in Level A1, 50% in Level A2, and 100% in Level MS. This contrasts with the rates inside the rockshelter—27% in Level A1, 39% in Level A2, and 46% in Level MS (see Table 6).

Aside from fragmentation, the primary taphonomic processes influencing our three faunal assemblages include abrasion and concretion. These processes impact over 60% of long bone shaft fragments in Level MS—inside, 25 to 35% in Level A2, and 15 to 25% in Level A1 (Figure 5). Additionally, a high number of modern fractures are associated with the presence of concretions; this is because the excavation of heavily concreted skeletal remains frequently requires the use of hammers and chisels.

The intensity of manganese coloration is similar across the three assemblages but varies spatially within each, be-

ing higher outside the rockshelter in Levels A1 (35%NSP.lb) and A2 (55%NSP.lb). Unfortunately, further taphonomic analysis on long bone shafts outside the rockshelter in Level MS is not possible due to the recovery of only one long bone diaphysis.

Other taphonomic processes generally affect less than 10% of the Proto-Aurignacian long bone shaft assemblages (see Figure 5), although slight variations are noted, such as increased bone weathering outside the rockshelter, especially in Level A1. Abrasion with polish and carnivore alterations, are more prevalent in Level MS, affecting 27% and 10% of the long bone shafts, respectively.

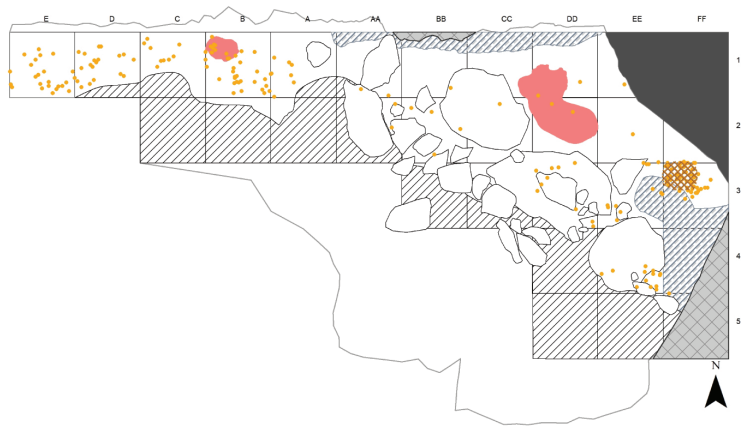
Few anthropic surface alterations were observed on long bone shaft fragments, most likely masked by the heavy concretion and abrasion. Cut marks are completely absent from Levels A1 and MS and are only present on two bone shaft fragments in Level A2—outside. Percussion marks are somewhat more frequent, present on 3% of the long bone shafts in Level A1—inside, 6% in Level A1—outside, and 5% in Level A2—outside. The most notable anthropic alteration observed on long bone shafts at Riparo Bombrini is burning, varying between 20% and 32% in the Proto-Aurignacian levels, compared to 7% in Level MS. Finally, a few bone flakes resulting from direct percussion (n=34), along with four bone fragments with modifications related to tool manufacture were recovered in both Proto-Aurignacian levels (see Table 6).

Bone Completeness and Fragmentation, Agents of Bone Accumulation and Carcass Processing

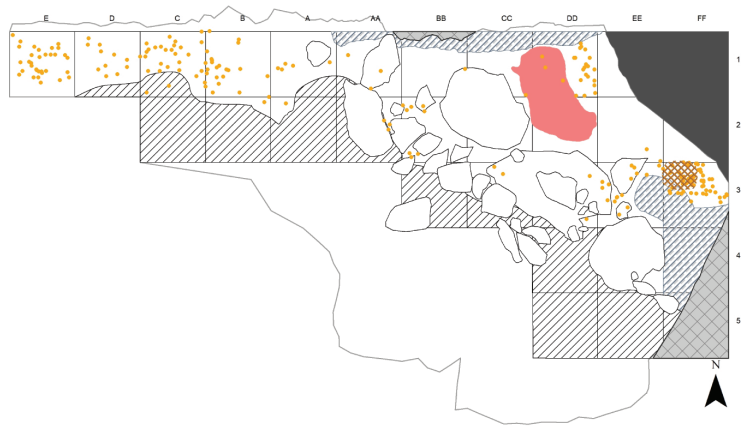
Many of the taphonomic variables concerning bone completeness and fragmentation did not yield notable results due to the low NISP and NISP.lb data for small and large game, particularly inside the rockshelter and in Level MS. Despite this, the data in Table 7 suggest that bone attrition is influenced by bone density. The mean FFI index, potentially indicating pre-depositional attrition, typically shows higher values inside than outside the rockshelter compared to outside for both small and large game, wherever data is available. In addition, the mean FFI values are generally higher for the small game within each level. This suggests that larger animals exhibit higher levels of fresh fractures than small ones across the assemblages.

The taphonomic variables calculated to identify the agents of bone accumulation reveal a higher concentration of carnivore-related alterations in Level MS compared to the two Proto-Aurignacian levels, as shown in Table 8. They also suggest a near-absence of human-related actions, such as percussion marks and burned bones, on taxonomically identified taxa within Level MS.

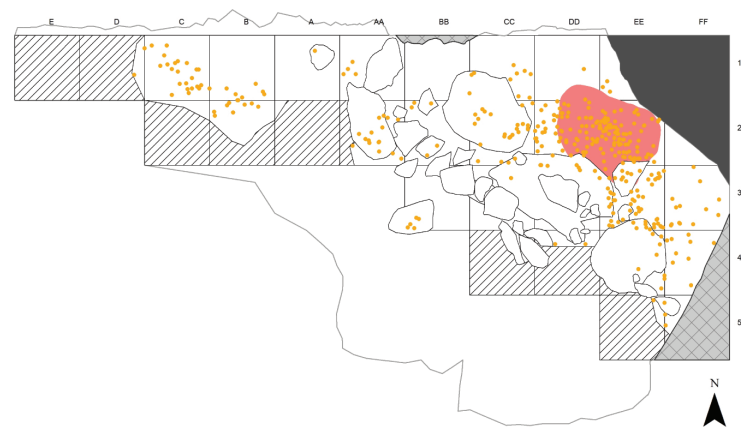
The taphonomic variables focused on carnivore-related action, depicted in Figure 6, underscore higher indices of carnivore accumulation in Level MS. For instance, approximately 45% of the total weight of coprolites recovered within our sample of the site comes from Level MS, compared to 25% and 30% from Levels A2 and A1, respectively. However, the coprolite densities should be approached with caution, as all identified coprolites are of small size (<1cm)



Level A1



Level A2



Level MS

Legend

- Bone
- ▨ Modern walls
- ▩ Shelter wall
- ▤ Pit
- Dripline
- ▨ Aurignacian level not found
- ▤ Disturbed
- Combustion feature
- Site's limits

Figure 4. Spatial distribution of the piece-plotted bones within Level A1 (top), Level A2 (middle), and Level MS (bottom).



Figure 5. Summary of long bone surface damage illustrated from data in Table 6. Frequencies of the total number of specimens of long bone shaft fragments (NISP.lb) in Level A1 (top), Level A2 (middle), and Level MS (bottom).

and were systematically collected only in square-meter unit EE3. The frequency of small and large carnivores accounts for 8%NISP in Level MS, compared to ~1%NISP in both Proto-Aurignacian levels (see Table 4). Notably, all carnivore skeletal remains are located inside the rockshelter in Level MS and Level A1, while the two elements in Level A2 are split between both sides of the dripline.

Finally, the taphonomic variables related to anthropic carcass processing reveal variations in fracture freshness (expressed as mean FFI) and in the distribution of bone flakes and percussion marks across different ungulate taxa and site areas (Table 9). Data indicate a higher frequency of anthropogenic modifications outside the rockshelter in the

Proto-Aurignacian levels, while such alterations are nearly absent in Level MS.

Additionally, the frequency of burning levels between bone type categories illustrates a clear pattern in Level A2 inside the rockshelter, where the relative abundance of burned and calcined cancellous bones is much higher than that of burned bone shaft fragments (Figure 7). This pattern is also present in Level A1, albeit less pronounced than in Level A2. Outside the rockshelter, the frequency of burned bone shaft fragments is comparable to or exceeds that of burned cancellous bones. In Level MS, all categories of bone types are less prevalent compared to the Proto-Aurignacian levels.

TABLE 7. TAPHONOMIC OBSERVATIONS ON BONE COMPLETENESS AND FRAGMENTATION.*

	Level A1		Level A2		Level M5	
	Inside	Outside	Inside	Outside	Inside	Outside
General data						
NISP small game	9	32	10	23	10	4
NISP large game	31	82	65	85	21	20
NISP.lb small game	4	16	0	12	0	0
NISP.lb large game	10	38	9	28	0	1
Density-mediated attrition						
Ratio NISP of small game: NISP of large game	0.29	0.39	0.15	0.27	0.52	0.2
%bone fragments >4cm (NISP of small game)	0	3	10	22	0	75
%bone fragments >4cm (NISP of large game)	6	29	9	32	5	80
Ratio N compact bones: n long bones and axial elements (small game)	0 (n=5)	0.05 (n=22)	1 (n=2)	0.07 (n=15)	1 (n=2)	0.5 (n=3)
Ratio compact bones: long bones and axial elements (large game)	0.25 (n=15)	0.1 (n=53)	0.08 (n=14)	0.4 (n=48)	1 (n=4)	0 (n=16)
Ratio N appendicular cancellous bone: n appendicular cortical bone	0.5 (n=192)	0.03 (n=98)	0.6 (n=236)	0.2 (n=119)	0.05 (n=62)	1 (n=2)
Post-depositional <i>in situ</i> attrition						
%completeness of tarsals and carpals (small game)	n/a	n/a	n/a	n/a	n/a	n/a
%completeness of tarsals and carpals (large game)	n/a	50 (n=2)	n/a	62.5 (N=4)	n/a	n/a
%completeness of phalanx1 and phalanx2 (small game)	n/a	100 (n=1)	100 (n=1)	n/a	n/a	100 (n=1)
%completeness of phalanx1 and phalanx2 (large game)	25 (n=3)	25 (n=1)	25 (n=1)	25 (n=4)	25 (n=2)	0
Ratio N cranial: n tooth fragments	0.07 (n=88)	0.5 (n=24)	0.02 (n=188)	0 (n=38)	0.03 (n=104)	0.4 (n=7)
Ratio MNE cranial: MNE tooth elements (small game)	0 (n=2)	1 (n=2)	0 (n=3)	0 (n=1)	0 (n=8)	1 (n=4)
Ratio MNE cranial: MNE tooth elements (large game)	0 (n=3)	0.8 (n=11)	0 (n=6)	0 (n=8)	0 (n=6)	0 (n=3)
Pre-depositional fragmentation						
Mean FFI (NISP.lb of small game)	5.8	4.3	n/a	3.08	n/a	n/a
Mean FFI (NISP.lb of large game)	5	3.4	6	2.6	n/a	2

*See SI Table 5 for detailed information on the taphonomic variables.

STABLE ISOTOPIC ANALYSIS

The results on the sixteen selected bone samples indicate poor collagen preservation, with only half of the samples with collagen yields higher than 1%. Seven samples exhibited an atomic C:N ratio between 3.2 and 3.5, which was considered sufficient for interpretation despite only a large bovine sample from Level M5 having a %N higher than 11 and a %C higher than 30. We considered the C:N ratio to interpret the values cautiously. Overall, the results show $\delta^{13}\text{C}$, $\delta^{15}\text{N}$, and $\delta^{34}\text{S}$ value ranges that are consistent with animals inhabiting terrestrial ecosystems feeding on C_3 plants as observed in ecosystems during the upper Pleistocene (see SI Table 3) (Jones et al. 2018; Nehlich 2015). Despite the low number of individuals analyzed and the poor collagen

preservation limiting statistical comparisons of intra-individual and temporal variability, some qualitative observations can be drawn. For instance, slightly lower $\delta^{13}\text{C}$ values are observed in *Cervus/Capreolus*, when compared with *Capra/Rupicapra*, *Sus* sp., and *Bos/Bison* sp. This is consistent with cervid species inhabiting more partially forested areas than the three other taxa feeding on more open landscapes (Drucker et al. 2008).

When plotted, $\delta^{13}\text{C}$ and $\delta^{15}\text{N}$ values of all species range between 4‰ and 6‰ except for *Bos/Bison* sp., which exhibited higher $\delta^{15}\text{N}$ and $\delta^{13}\text{C}$ values possibly indicative of its diverging ecological habits involving grass eating in open landscapes (see SI Figure 4). In addition, a small cluster represented by *Capra/Rupicapra* appears when $\delta^{13}\text{C}$ and $\delta^{34}\text{S}$

TABLE 8. TAPHONOMIC OBSERVATIONS ON BONE ACCUMULATION.*

	Level A1		Level A2		Level MS	
	Inside	Outside	Inside	Outside	Inside	Outside
General Data						
NSP	3656	832	9001	1422	4852	41
NISP	59	114	95	116	50	24
NISP small game	9	32	10	23	10	4
NISP large game	31	82	65	85	21	20
NISP.lb small game	4	16	0	12	0	0
NISP.lb large game	10	38	9	28	0	1
NSP.lb	130	95	148	103	59	1
Deposit volume (m ³)	0.60	0.33	0.99	0.25	1.81	0.19
Carnivore action						
% of carnivores (NISP)	3.3	0	1	1.7	14	0
N Coprolites	427	n/a	1141	n/a	4586	n/a
Density of coprolites g/m ³ of sediment	106	n/a	88	n/a	154	n/a
%long bone shafts >1/2 circumference (NSP.lb)	4.6	9.5	11.4	4.9	23.7	100
%long bone shafts >1/2 circumference (NISP.lb of small game)	0	12.5	n/a	16.7	n/a	n/a
%long bone shafts >1/2 circumference (NISP.lb of large game)	0	18.4	22.0	7.1	n/a	100
%gnawed (NSP)	0.08	0	0.04	0.8	2	7.3
%gnawed (NISP of small game)	0	0	0	13	20	50
%gnawed (NISP of large game)	3.2	0	0	7.1	9.5	5
%head (NISP of small game)	22.2	6.3	30.0	4.3	80.0	100.0
%head (NISP of large game)	9.7	13.4	10.8	9.4	28.6	15.0
%head (NSP)	2.4	2.9	2.1	2.7	2.1	17.1
Human action						
%percussion marks (NISP of small game)	0	0	0	4.3	0	0
%percussion marks (NISP of large game)	9.7	3.7	0	4.7	0	0
%burned bones (NISP of small game)	44.4	0	20	0	0	0
%burned bones (NISP of large game)	3.2	4.9	21.5	15.3	0	0

*See SI Table 6 for detailed information on the taphonomic variables.

values are plotted. The higher $\delta^{34}\text{S}$ values of the two caprine bone fragments from the Proto-Aurignacian Level A1 might be related to habitat in higher altitudes (see SI Figure 4). Finally, despite proximity to the Mediterranean shoreline, ungulate species do not exhibit the expected higher $\delta^{34}\text{S}$ values typical of marine ecosystems (Jones et al. 2018). Considering our limited dataset, this aspect would require further investigation of the $\delta^{34}\text{S}$ variability within the Liguro-Provençal region.

DISCUSSION

LEADING CAUSES OF PRESERVATION BIAS AND ATTRITION

Our first line of taphonomic investigation at Riparo Bombrini reveals that the mineral density of the skeletal remains

at Riparo Bombrini strongly influences bone fragmentation and preservation. While a direct statistical correlation between bone mineral density and skeletal survivorship could not be established due to limited data, other taphonomic indicators (e.g., abundance of bones >4cm, mean FFI, ratios of less dense to dense remains) consistently point to a density-mediated attrition pattern (see Tables 6 and 7). This pattern is especially pronounced within the rockshelter and underscores better morphological and molecular preservation outside the dripline. The predominant factors contributing to this attrition include natural post-depositional *in situ* processes, possibly bone-crushing by sediment compaction, and repeated freeze-thaw cycles (Lyman 1994; Marean 1991), as suggested by the low cranial-to-tooth ratios (see Table 7).

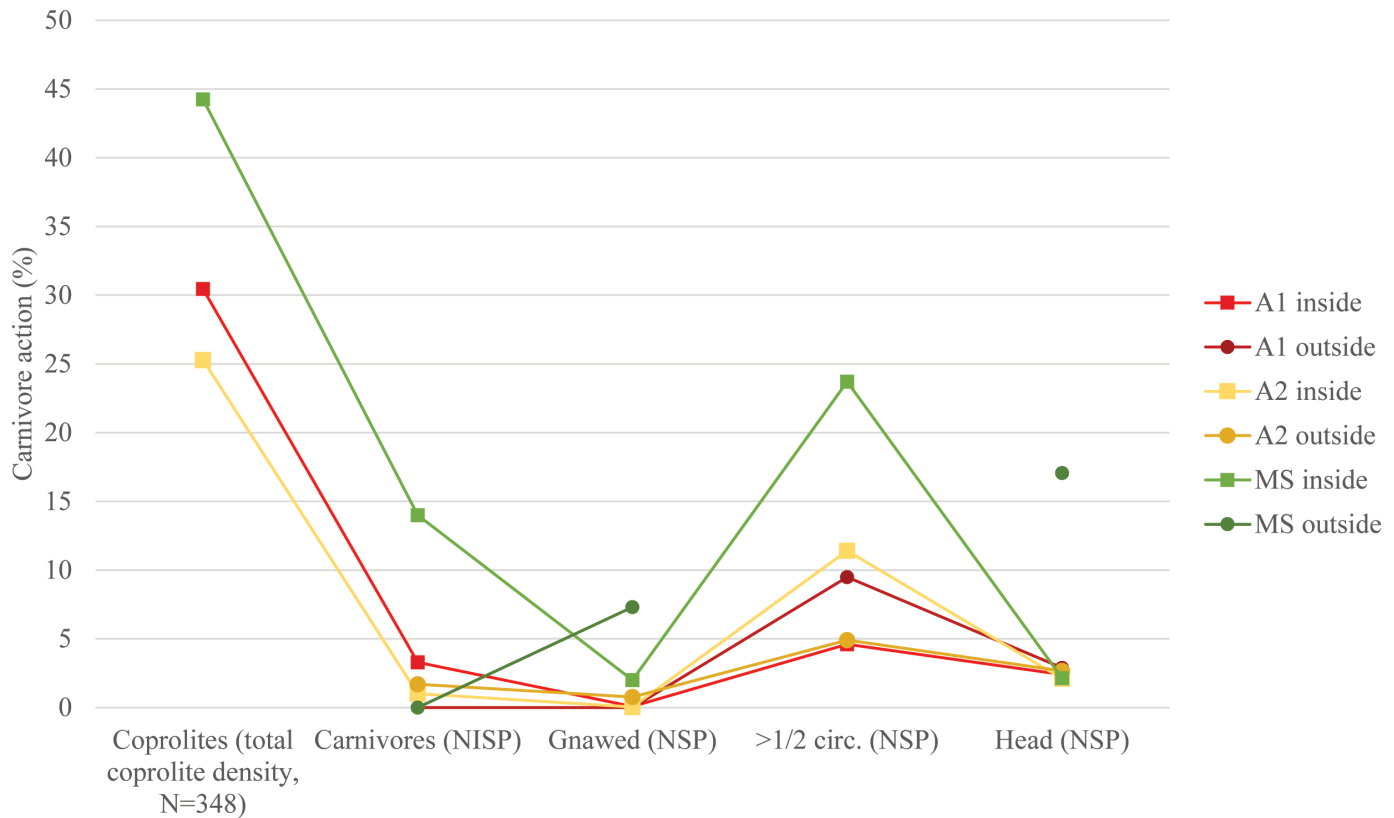


Figure 6. Carnivore action illustrated from data in Table 8. Frequencies of the number of identified specimens (NISP) and total number of specimens (NSP) in Level A1 (red), Level A2 (yellow), and Level MS (green).

AGENTS OF BONE ACCUMULATION

Despite heavy post-depositional attrition, such as abrasion, concretion coverage, and fragmentation, our second line of investigation points to a primary anthropic accumulation of the skeletal remains in the Proto-Aurignacian and a mixed accumulation by humans and carnivores in the Late Mousterian. In the Proto-Aurignacian, the scarcity of anthropic bone alterations such as cut marks and percussion marks might be explained by the post-depositional attrition, or alternatively, part of the assemblage may have been accumulated by carnivores. However, the high density of artifacts and frequent occurrence of burned bones suggest prevalent anthropic activities. The few gnawed skeletal remains were only observed on post-cranial elements in these levels, supporting the hypothesis that they result from carnivores scavenging butchery byproducts. Gnawing damage is commonly recorded on human-generated fauna, especially when large quantities of skeletal remains are piled in refuse areas—such as the uniformly distributed accumulation observed in Level A2 outside the rockshelter (see Figure 4) (Stiner 1994).

In Level MS, a slight increase in carnivore gnaw marks inside the rockshelter (see Table 8: 2%NSP, compared with <0.1%NSP in Levels A1 and A2) suggests a potential role of carnivores in bone accumulation and fragmentation before burial. While it is challenging to confirm if carnivores used the site as a den due to the masking effect of concretion

and post-deposition fragmentation, digested splinters and coprolites provide insights. Although Level MS contains the highest number of coprolites and digested bones on the site, their relative abundance is low, digested splinters accounting for less than 2% of the NSP inside the rockshelter and the volumetric density of coprolites (154g/m³) being only slightly higher than in Level A1 (106g/m³). These data, along with 8%NISP of carnivore remains—below the 20% threshold for den assemblages (Pickering 2002), suggests a nuanced view of carnivore activity. Nevertheless, the presence of carnivore juvenile teeth and a head-dominated assemblage inside the rockshelter supports a possible denning scenario (see Figure 3; SI Table 9). However, definitive conclusions require additional taphonomic analysis of more recent excavation data, including coprolite recovery, to better define these interactions on a larger area of the site.

HUNTING STRATEGIES AT RIPARO BOMBRINI

The paucity of identified specimens and anthropic marks, other than burnt bones, across the three faunal assemblages at Riparo Bombrini considerably limits the depth of discussion possible regarding hunting strategies. Nonetheless, certain patterns warrant consideration as working hypotheses. The overarching pattern of animal exploitation at Riparo Bombrini suggests sustained exploitation of large cer-

TABLE 9. TAPHONOMIC OBSERVATIONS ON CARCASS PROCESSING.*

	Level A1		Level A2		Level MS	
	Inside	Outside	Inside	Outside	Inside	outside
General data						
NISP Cervinae	10	59	12	27	3	13
NISP.lb Caprinae	0	12	0	11	0	0
NISP.lb Capreolinae	0	4	0	0	0	0
NISP.lb Cervinae	3	24	2	14	0	1
NISP.lb Bovinae	5	5	0	7	0	0
NISP.lb Equidae	0	0	2	0	0	0
NSP	3656	832	9001	1422	4852	41
Marrow extraction						
Mean FFI (NISP.lb of Caprinae)	n/a	3.08	n/a	3.4	n/a	n/a
Mean FFI (NISP.lb of Capreolinae)	n/a	5.25	n/a	n/a	n/a	n/a
Mean FFI (NISP.lb of Cervinae)	5.3	3.08	6	2.4	n/a	2
Mean FFI (NISP.lb of Bovinae)	4.4	3.4	n/a	3.1	n/a	n/a
Mean FFI (NISP.lb of Equidae)	n/a	n/a	6	n/a	n/a	n/a
N bone flakes of <i>Cervus</i> sp.	0	9	0	0	0	0
N bone flakes of <i>Capreolus</i> sp.	0	1	0	0	0	0
N bone flakes of <i>Capra</i> sp.	0	1	0	0	0	0
N bone flakes of <i>Sus</i> sp.	0	1	0	0	0	0
N bone flakes of <i>Bos/Bison</i> sp.	0	0	0	1	0	0
N bones of <i>Cervus</i> sp. with percussion marks	0	2	0	0	0	0
N bones of <i>Capra</i> sp. with percussion marks	0	0	0	1	0	0
N bones of <i>Bos/Bison</i> sp. with percussion marks	2	0	0	2	0	0
N bones of <i>Capra</i> sp. with cut marks	0	0	0	1	0	0
N bones of <i>Cervus</i> sp. with fresh fractures**	2	32	0	10	1	2
N bones of <i>Bos/Bison</i> sp. with fresh fractures**	4	4	0	10	0	0
N bones of <i>Capra</i> sp. with fresh fractures**	1	10	0	8	0	0
N bones of <i>Capreolus</i> sp. with fresh fractures**	0	2	0	1	0	0
N bones of <i>Sus</i> sp. with fresh fractures**	0	1	0	1	1	0
N bones of <i>Equus</i> sp. with fresh fractures**	1	0	0	0	0	0
Grease rendering						
%cancellous unburned bones (NSP)	3.5	5.6	5.3	2.2	1.9	4.9
%epiphysial cancellous unburned bones (NSP)	0.8	0.1	0.5	0.6	0.1	2.4
%cancellous bones (NISP of small game)	0	3.1	0	0	0	0
%epiphysial cancellous bone (NISP of small game)	0	0	0	0	0	0
%cancellous bones (NISP of large game)	3.2	4.9	1.5	8.2	0	5
%epiphysial cancellous bone (NISP of large game)	0	1.2	0	4.7	0	0

vids and other medium and large ungulate taxa available in the surrounding environment (see Table 4). Notably, the relative abundance of various ungulate taxa fluctuates across the three assemblages. Level A1, for instance, shows a slightly richer and more evenly distributed taxonomic composition compared to the stratigraphically underlying Level A2. While this difference might be attributed to a narrowing of prey selection from Level A2 to Level A1, it is more probable that these variations are significantly skewed by low NISP tallies. Moreover, the pronounced

presence of red deer in Level A1 could stem from skeletal aggregates identified multiple times via ZooMS, potentially causing taxonomic overrepresentations (see Multivariate Approach with the Integration of ZooMS section below).

Employing ethological and ethnological models alongside the faunal evidence of the most abundant taxa (i.e., red deer, ibex, and *Bos/Bison* sp.) can help flesh out potential hunting and carcass transport strategies adopted at Riparo Bombrini. The consistent representation of red deer and the presence of anthropic marks or fresh fractures with no car-

TABLE 9. TAPHONOMIC OBSERVATIONS ON CARCASS PROCESSING (continued).*

	Level A1		Level A2		Level MS	
	Inside	Outside	Inside	Outside	Inside	outside
Bone fuel (NSP)						
%burned bones	55.0	40.7	51.2	55.9	24.8	24.4
%calcined bones	10.3	6.0	12.1	6.7	1.7	7.3
%cranial unburned bones	2.0	2.6	1.7	1.9	2.1	14.6
%cranial burned bones	0.4	0.2	0.4	0.8	0.1	2.4
%axial post-cranial unburned bones	0.3	2.0	0.4	1.5	0.2	36.6
%axial post-cranial burned bones	0.3	0.1	0.2	0.1	0.0	0.0
%appendicular unburned bones	2.6	9.4	1.4	6.3	1.4	9.8
%appendicular burned bones	1.3	1.9	0.5	2.3	0.1	2.4
%cancellous bones	7.4	4.7	17.1	4.9	2.2	4.9
%cancellous burned bones	3.9	1.4	11.7	2.7	0.4	2.4
%cancellous calcined bones	1.6	0.7	4.5	0.8	0.0	0
%burned long bone diaphysis fragments	1.1	2.4	0.4	1.8	0.1	0

*See SI Table 7 for detailed information on the taphonomic variables.
 **And no carnivore marks.

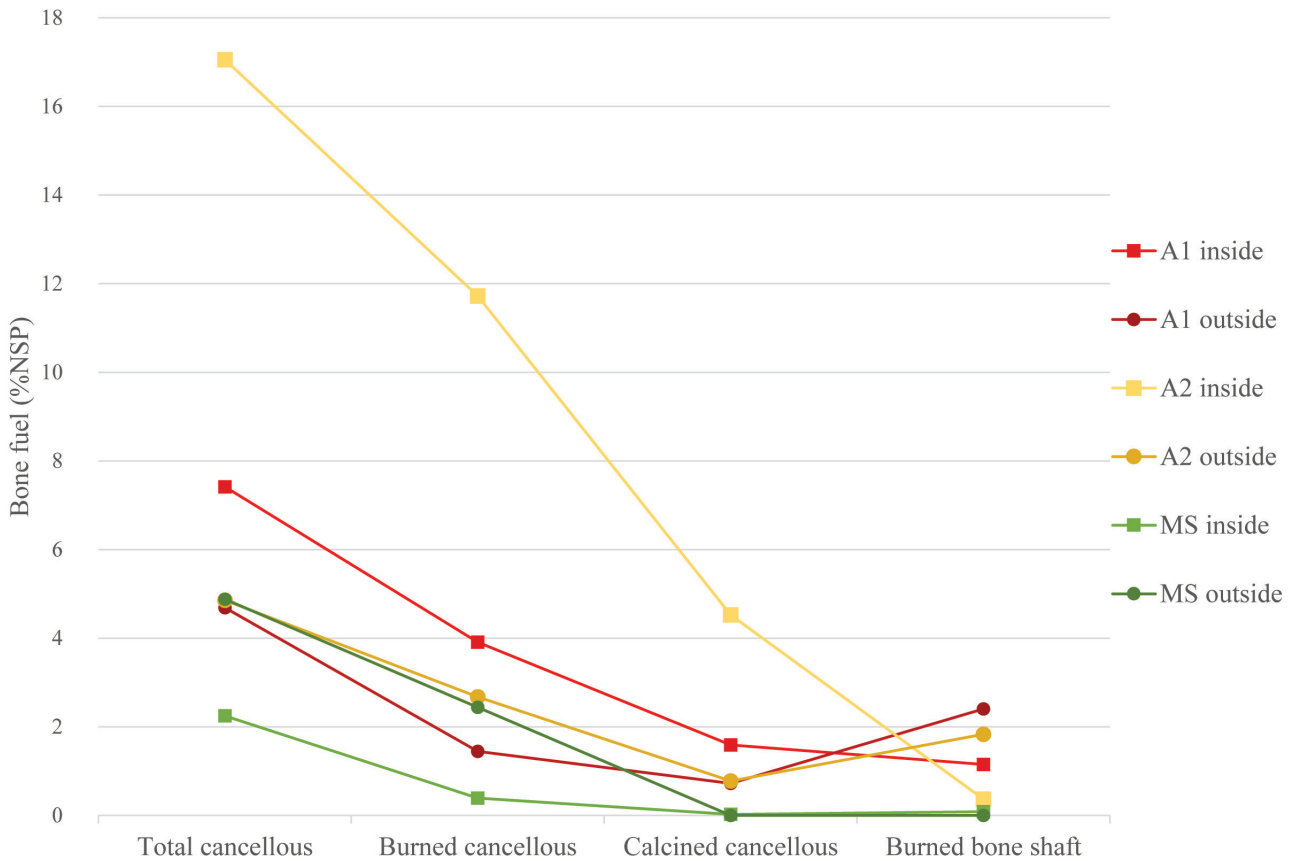


Figure 7. Bone fuel illustrated from data in Table 9. Frequencies of the total number of specimens (NSP) in Level A1 (red), Level A2 (yellow), and Level MS (green).

nivore marks on some skeletal remains across the three levels (see Table 9) suggest the exploitation of this species by human groups throughout the Middle-Upper Paleolithic Transition at Riparo Bombrini. Red deer, being relatively non-migratory, would have been available year-long at the Balzi Rossi. Seasonal changes observed in extant herd composition, particularly the grouping behavior of females for protection and the solitary nature of males except during pre-rut summer gatherings (Steele 2002), could have influenced specific hunting tactics such as collaborative hunts on larger herds. The recovery of adult skeletal elements from all portions (i.e., axial and appendicular) within the three levels suggests that groups of red deer were accessible, providing a stable food source in proximity to the site.

Summer migrations to higher altitudes, commonly observed for the extant red deer populations (Steele 2002), could also have influenced hunting practices at Riparo Bombrini, given its proximity to the Pre-Alps. In Level A2, the presence of deer antler fragments could reflect the opportunistic hunting of solitary prime males during winter or early spring or, alternatively, the gathering of shed antlers. Although direct indicators of seasonality are nearly absent, the presence of an indeterminate fetal bone in Level A2 may also suggest winter/early spring occupations, warranting further investigation in future studies that include a larger faunal sample of the latest excavations at Riparo Bombrini and associated malacofauna.

In the Proto-Aurignacian levels, ibex skeletal remains are also relatively well-represented and exhibit some anthropic alterations (see Table 9). Ibex, typically living in sexually segregated groups for most of the year, may have been accessible in close proximity to the Balzi Rossi during colder seasons and at higher altitudes during warmer months (Acevedo and Cassinello 2009). The latter is also suggested qualitatively by elevated $\delta^{34}\text{S}$ values in two caprine remains from Level A1 (see SI Figure 4). This hypothesis evokes the pattern observed at Fumane cave in north-eastern Italy, where the Proto-Aurignacian levels exhibit a prevalence of ibex and chamois. At Fumane, this narrowed taxonomic diversity aligns with reduced forest covers and lower biomass, conditions tied to the severe climatic shifts of Heinrich 4 Event (Marín-Arroyo et al. 2023).

Finally, Bovines (i.e., bison or aurochs) are similarly abundant to ibex in the Proto-Aurignacian levels. Being gregarious animals, they likely required cooperative hunting strategies. These large ungulates usually group in herds of ten to twenty animals, which can be more or less sedentary depending on the habitat (forested vs. grassland) and available resources (Julien 2011; White et al. 2016).

DIFFERENTIAL CARCASS TREATMENTS

Surface alterations are limited across the faunal assemblages, yet the presence of unburned axial post-cranial (i.e., ribs and vertebrae) and appendicular elements outside the rockshelter in both Proto-Aurignacian levels suggests primary butchery activities such as disarticulation of the axial skeleton. Secondary butchery practices, evidenced by bone

flakes, percussion marks, and fresh fracture angles on long bones without carnivore gnawing, are noted on both sides of the dripline in the Proto-Aurignacian (see Table 9; Figure 8). However, this scenario is expressed with caution since bone flakes and fresh fracture angles could also be the result of trampling or carnivore bone cracking.

Nevertheless, in Level A2, bone flakes near the large hearth are associated with a high abundance of artifacts, likely indicating anthropic long bone cracking in the area. Conversely, such flakes are nearly absent in this area of Level A1, whereas they are present in association with the secondary combustion feature outside the rockshelter. The latter concentration coincides with the highest incidence of fresh fracture angles and percussion marks on the site (see Table 6). The small combustion feature recorded in Level A1 may correspond to shorter occupations of the site, independent of those occurring closer to the rockshelter wall. This hypothesis is supported by the relatively low volumetric density of bone fragments (NSP), comparable to Level MS in this area (see Table 6).

In Level MS, documenting carcass butchering and marrow extraction presents additional challenges to extensive concretion coverage. Despite this, the proportion of fresh fracture angles inside the rockshelter is proportionally comparable to Level A2, suggesting possible bone cracking activities. Outside the dripline, the absence of bone flakes, percussion marks, and cut marks, even on well-preserved remains, also suggests minimal carcass processing. However, the presence of deer ribs in partial anatomical alignment, combined with experimental evidence that deer rib cages can be efficiently disarticulated with direct percussion, leaving most ribs intact, suggests human activity (Vigne 2006). Notably, two deer ribs exhibit fresh and right-angled fractures similar to the experimental patterns (Figure 9), and two red deer femur fragments with helical fractures suggest carcass processing in Level MS.

While grease rendering seems unlikely at Riparo Bombrini – evidenced by preserved collagen in unburned bones and the absence of heated rock accumulations, the primary pre-depositional biotic factor impacting the Proto-Aurignacian faunal assemblages appears to be the use of grease-rich bones (i.e., epiphysal bone) for fuel, given their well-documented combustible properties (Costamagno et al. 2005; Morin 2010; Théry-Parisot et al. 2004). This pattern, previously identified in the Proto-Aurignacian levels (Pothier Bouchard et al. 2020), is particularly pronounced in Level A2 (see Figure 7), supporting our hypothesis that modern humans exploited ungulate carcasses more intensively there compared to Level A1. Moreover, the pattern of bone used as fuel is not observed outside the rockshelter in both Proto-Aurignacian levels. In Level A1, the absence of such activity around the small combustion feature suggests shorter occupations where expedient fuel management would have been used. Conversely, the systematic use of grease-rich elements for fuel in more prolonged occupations suggests a deliberate strategy of curating fuel resources and more organized waste management strategies.



Figure 8. Examples of anthropic marks at Riparo Bombrini. A) Mousterian, from left to right: *Cervus* tibia with fresh fracture and cut marks (BOM15 in Level M4), *Cervus* metatarsal with fresh fracture (BOM 13 in Level M3). B) Protoaurignacian, *Cervus*-*Capreolus* humerus with fresh fracture (BOM02 in Level A1), *Capra*-*Rupicapra* long bone with an impact point (BOM04 in Level A1).

SITE FUNCTION THROUGH TIME

Previous research on Levels A1, A2, and MS at Riparo Bombrini has highlighted varying types of occupation of the site over time (Pothier Bouchard et al. 2020; Riel-Salvatore and Negrino 2018a; Riel-Salvatore et al. 2022). Our study corroborates previous interpretations and helps discuss the hypothesis of three site functions—ephemeral base camp in Level MS, long-term base camp in Level A2, and short-term base camp in Level A1 (Table 10).

In Level MS, the faunal data supports the hypothesis of scant, ephemeral occupations of the site by Neanderthals as

evidenced by the low density of artifacts, scant retouched tools, a truncated lithic *chaîne opératoire*, and alternating occupations with carnivores. This evidence could align with the concept of brief stopping-places described by Daujeard and Moncel (2010) in the Rhone Valley during MIS 6–3, which they suggest to be very short-term camps normally located in-between two long-term residential camps.

Conversely, Levels A1 and A2 indicate continuous use of the site by modern humans as a base camp, evidenced by high artifact densities, extensive lithic retouched tools, spatially organized activities, complete lithic *chaînes opératoires*.



Figure 9. Ceroid ribs in Level MS showing potential stigmata of disarticulation with direct percussion as described by Vigne (2006: 18): (upper) C1.IV/1.486 – direct percussion, (bottom) C1.IV/1.501 – perpendicular angle. Vicino’s fieldnotes indicating their in situ recovery. Stigmata indicated with green dashed circles.

toires, and the presence of at least a few indices of primary and secondary carcass butchery. However, the nature of the occupations of the base camp appears to have changed through time, transitioning from extended and more intensive stays in Level A2 to shorter and less spatially organized occupations in Level A1 (see Table 10).

Level A2 likely saw repeated use of grease-rich bones for fuel within the rockshelter during extended stays, alongside careful waste management that included trash pits (see Figure 4). Outside the rockshelter, the area could have served as a discard site, including a “bone dump,” which is suggested by dense and uniformly distributed skeletal accumulation (Vallerand et al. 2024).

In Level A1, a secondary combustion feature outside the rockshelter with a few pieces of evidence of primary and secondary butchery and no clear pattern of bone fuel suggests independent shorter occupations of the site. Inside the rockshelter, bone fuel use continues with a weaker signal, suggesting less curated management of the grease-rich bones.

SUBSISTENCE, LAND-USE, AND MOBILITY STRATEGIES AT RIPARO BOMBRINI

Our results support and broaden previous hypotheses about mobility and land-use strategies at Riparo Bombrini during the transition, as summarized in Table 11.

The Semi-Sterile Mousterian

Previous research on Level MS advanced the hypothesis that this deposit reflects the adaptation of some of the last Neanderthals in Italy within the context of the Ligurian biogeographical refugium (Riel-Salvatore et al. 2022). Neanderthals could have taken advantage of the proximity of the “I Ciotti” conglomerates to adopt a hyper-local subsistence range, as evidenced by the near absence of circum-local and exotic lithic materials in Level MS. The prevalence of a discoid reduction strategy taking over the Levallois documented in underlying Mousterian levels also suggests increased mobility. The faunal record aligns with this narrative, where Neanderthals appear to have adopted a restricted diet focused on red deer, contrasting with the

TABLE 10. SUMMARY OF FAUNAL AND LITHIC DATA REGARDING SITE FUNCTION AT RIPARO BOMBRINI.

	Level A1	Level A2	Level MS
Comparative taphonomy			
Anthropic Pre-depositional attrition	High	High	Medium
Carnivore Pre-depositional attrition	Low	Low	Medium
<i>In situ</i> Post-depositional attrition	High	High	High
Hypothesis on faunal data			
Agents of bone accumulation	Recurrent human	Recurrent human	Alternating human/carnivore
Seasonality of animal procurement	Absence of seasonality indices	Possible seasonal occupations	Absence of seasonality indices
Animal procurement strategy	Mostly generalist	Mostly generalist	Unclear
Carcass transport strategy	Some possible whole carcasses of small and large ungulates	Some possible whole carcasses of small and large ungulates	Some possible whole carcasses of cervids
Butchery activities	Scarce evidence of primary and secondary inside and outside the rockshelter	Scarce evidence of primary outside, secondary inside and outside the rockshelter	Primary and secondary (no specific spatial data)
Bone fuel management	Presence	Curated	None
Lithic data*			
Technological system	Bladelet-based	Bladelet-based	Discoid flaking
Density of artifacts	High	Highest (outside)	Lowest
Abundance of retouched tools (including bladelets)	High	Highest	Lowest
Chaîne opératoire completeness	Complete	Complete	Partial
Site function hypothesis	Short-term base camp	Long-term base camp	Ephemeral base camp

*Data from Riel-Salvatore and Negrino (2018a), Riel-Salvatore et al. (2022a).

TABLE 11. SUMMARY OF THE SUBSISTENCE AND MOBILITY AT RIPARO BOMBRINI FROM PRESENT AND PREVIOUS RESEARCH.

	Level A1	Level A2	Level MS
Paleoenvironment*	More temperate and mesic	Cold and arid, HE 4	Coldest and most arid
Resource procurement strategies			
Large ungulate exploitation	Relatively close range	Relatively close range	Close range
Small ungulate exploitation	Relatively close range	Relatively close range	n/a
Techno-economic strategy*	Curated	Less curated	Expedient
Chaîne opératoire completeness on local resources (<5km)*	Complete	Complete, more bladelets and finished tools	Complete, mostly flakes and chunks
Chaîne opératoire completeness on circum-local resources (10–20km)*	Partial, bladelets only	Partial, bladelets only	Partial, sporadic flakes
Chaîne opératoire completeness on exotic resources (30–350km)*	Complete, higher frequency of debris of curated tools	Complete, higher frequency of retouched tools (material “stockpiling”)	Partial, sporadic flakes and chunks
Hypotheses on subsistence and mobility			
Degree of mobility	High	Low	Very high
Mobility strategy	Residential	Logistical	Residential
Subsistence range	Extensive	Extensive	Hyper-local
	Strong link with SE France	Strong link with SE France	Weak link with SE France
Diet breadth	Broad	Broadest	Narrow

*Data from previous research (Holt et al. 2019; Riel-Salvatore et al. 2013; 2022; Riel-Salvatore and Negrino 2018a, b; Pothier-Bouchard et al. 2020).

more diversified faunal assemblages characterizing the underlying Mousterian levels at Riparo Bombrini and in the Liguro-Provençal arc throughout the Late Pleistocene (Holt et al. 2019; Valensi and Psathi 2004; Pothier Bouchard 2022). The narrower diet also aligns with the hypothesis that Neanderthals adopted a hyperlocal subsistence and land-use strategy in response to changing ecological conditions and the arrival of new groups in neighboring regions (i.e., Proto-Aurignacian in France, Uluzzian in Italy). However, validating the refugium hypothesis of the last Neanderthals in the Liguro-Provençal arc requires additional fine-grained excavation and comparative studies on contemporaneous sites such as Arma degli Zerbi and Arene Candide (see Riel-Salvatore et al. 2022 for discussion).

Proto-Aurignacian Levels

The Proto-Aurignacian levels mark a significant shift towards extended social and subsistence ranges, coupled with the continuous production of a flexible bladelet-based technocomplex. At Riparo Bombrini, it appears that the vast subsistence range of modern humans was primarily driven by the desire to obtain prime-quality flint, mostly in western and eastern Provence and, to a lesser extent, in eastern Liguria and northern Tuscany. Along the Ligurian corridor, modern humans exploited the locally available raw material of inferior quality with a “readily available” strategy while occupying the residential base camps, and they carried higher-quality flints throughout their seasonal moves (Riel-Salvatore and Negrino 2018a). The flexible Proto-Aurignacian technocomplex allowed the manufacture of polyvalent hunting armatures, which could have facilitated the adoption of a generalist hunting strategy at Riparo Bombrini. The faunal record aligns with this strategy as the hunting spectrums are much broader than the one observed in Level MS, and some ungulate prey species appear to have been hunted in close proximity to the Balzi Rossi.

Previous research has highlighted variability within the Proto-Aurignacian, associating the prolonged stays and the expedient lithic organization in Level A2 with a logistical mobility regimen, contrasting with the shorter occupations and the curated lithic organization in Level A1, linked to more residential mobility (Riel-Salvatore and Negrino 2018a, b). The faunal record does not disagree with these patterns, although limited seasonality indices and carcass transport evidence provided little insight into the specifics of human mobility. Future studies should focus on food availability, particularly how increased snow cover in the nearby Pre-Alps might have enhanced prey availability on the shore during harsher seasons. Nevertheless, the spatial organization of the site requiring waste management (i.e., discarding area outside the living space and curated bone fuel) agrees with the logistical mobility regimen in Level A2, contrasting with the shorter independent occupations outside the rockshelter and the less curated bone fuel in Level A1.

CHANGING HUMAN-ENVIRONMENTAL RELATIONSHIP DURING THE TRANSITION IN THE LIGURO-PROVENÇAL ARC

The data available on faunal composition and skeletal representation during the interval of the transition in the Liguro-Provençal arc suggests continuous exploitation of locally available medium and large ungulates by Neanderthals and modern humans, primarily selecting prime adults and transporting whole carcasses or the meatier parts of larger ungulates back to their base camps (Perez et al. 2022; Pothier Bouchard et al. 2020; Valensi and Psathi 2004). The isotope data obtained in this study align with a general paleoenvironmental portrait of mixed open and forested habitats surrounding Riparo Bombrini associated with the Late Mousterian and the Proto-Aurignacian occupations (Holt et al. 2019; Pothier Bouchard et al. 2020). Foraging groups could have taken advantage of the biogeographic dynamics of a refugium in which warm-adapted taxa cohabited with increasingly higher proportions of cold-adapted taxa, a trend that reached its apex during Heinrich Event (HE) 4 in the Proto-Aurignacian record of Riparo Bombrini. Similar patterns were recently reported for the rest of the Italian Peninsula, where the onset of the HE 4 is generally contemporaneous with Uluzzian sites. Well-documented stratified sites in Italy such as Grotta di Fumane in the northeast and Grotta del Cavallo and Grotta di Castelcivita in the south also exhibit increasing cold-adapted taxa in Uluzzian and Proto-Aurignacian faunal assemblages (Marín-Arroyo et al. 2023; Romandini et al. 2020; Tagliacozzo et al. 2013).

These taxonomic fluctuations, observed across Europe (Vidal-Cordasco et al. 2023), suggest that changes in ungulate taxonomic composition primarily reflect higher-order environmental changes. In southwestern France, the climatic cooling associated with HE 4 correlates with a progressive narrowing of the diet, pushing modern humans to focus largely on reindeer at many Early Aurignacian sites (Rendu et al. 2019). Unlike continental regions, where reliance on a single ungulate species may have caused demographic pulses (Morin 2008), the Liguro-Provençal arc and the Italian peninsula likely benefitted from more stable conditions. At the Balzi Rossi, these conditions could have fostered the patterns of lasting occupations documented for Neanderthals associated with very late “Semi-Sterile” Mousterian (up to shortly before ~42 ky cal BP). In addition, the drastic cooling does not coincide with a technological turnover suggested by some researchers (Riel-Salvatore and Negrino 2018b; cf. Banks et al. 2013). Instead, the Proto-Aurignacian of the Balzi Rossi lasts through HE 4 in Level A2, followed by slightly more mesic conditions up until ~36 ky cal BP. At the same time, the Early Aurignacian is already well established in western regions (Riel-Salvatore and Negrino 2018b).

Despite continuity in taxonomic composition, the transitional faunal assemblages of the Liguro-Provençal arc and its neighboring regions reveal several indices of a shift in human-environmental relationships, especially starting

in the Proto-Aurignacian. Three critical trends related to animal exploitation are discussed here to clarify potential evolutionary implications for modern human adaptations in Europe: 1) the technological change towards long-range weapons, 2) the increased human exploitation of carnivores, and 3) the exploitation of a broader range of animal raw materials for symbolic and technological use (Rendu et al. 2019; Romandini et al. 2020; Soulier 2013).

Long-range Projectile Weaponry

Long-range projectile weaponry has been argued to permit more versatile hunting strategies, potentially reducing hunting parties and enabling solitary hunts. This flexibility arises from the ability to increase the distance between the prey and the hunter, reducing the risks of failure to acquire easily frightened or dangerous game (Churchill and Rhodes 2009; Shea and Sisk 2010; Teyssandier et al. 2010). In the Liguro-Provençal arc, the Proto-Aurignacian is characterized by substantial investment in raw material procurement, lithic production, and tool maintenance. The bladelet-based technology was clearly embedded in large-scale landscape exploitation extending more than 400 kilometers from western Provence to eastern Liguria, which would likely have influenced hunting strategies and prey selection compared to what the thrusting spears so far documented in the Eurasian Mousterian record allowed.

Soulier (2013) attributes the absence of ambush kill sites in the Early Upper Paleolithic record of southwestern France to these technological innovations, contrasting with many Final Mousterian sites (e.g., Marillac, Jonzac, and La Quina), where Neanderthals exploited topographic advantages to mass-hunt reindeer. While no equivalent ambush kill sites have been identified to date in the Final Mousterian of the Liguro-Provençal arc, Valensi and Psathi (2004) mention the close link between the nature of hunted prey and the topographic location of the sites. The absence of mass-kill sites could be explained by its distinctive biogeography, where the most predominant prey taxa, such as red deer exhibit less gregarious and mobile behaviors than cold-adapted taxa. In this context, seasonality could be a better proxy to document collective hunting tactics, considering that the largest aggregations of extant deer populations occur during autumn. According to Valensi and Psathi (2004), Neanderthal groups appear to have exploited large herds of cervids during the rutting season on several sites in the Liguro-Provençal arc (i.e., Grotte du Lazaret, Caverna delle Fate, Arma delle Manie). In the neighboring regions of the Rhone Valley and the Massif Central, Daujeard and colleagues (2012) also identified a close link between Neanderthals' mobility, site occupations, and the seasonal abundance of the hunted species (e.g., fall occupations of the Sainte-Anne I hunting camp).

At Riparo Bombrini, although definitive seasonal indices have yet to be identified, the prolonged modern human occupations in the Proto-Aurignacian levels, particularly Level A2, may have extended during harsher seasons. The versatile hunting strategies associated with long-range weaponry would have facilitated extended stays and mo-

bility shifts, providing greater resilience to climatic instability (Pothier Bouchard et al. 2020; Riel-Salvatore and Negrino 2018b), contrasting with Neanderthal's reliance on the seasonal abundance of resources. Moreover, the intensive use of bones for fuel at Riparo Bombrini could also be linked to these technological changes, paralleling Soulier's (2013) observations on the Proto-Aurignacian of Isturitz in southwestern France, suggesting the adoption of more sedentary lifestyles during colder seasons, much like many extant hunter-gatherers. Patterns of high abundance of burnt bones are documented at several Early Upper Paleolithic sites in eastern and southern Italy (Romandini et al. 2020). While this sudden reliance on bones in fire management may be linked to the global climate cooling of HE 4, it would be worthwhile to investigate the relationship between fuel management and seasonality on additional transitional sites in the Liguro-Provençal arc.

Human-Carnivore Interactions

Changes in the ecological niches of Neanderthals and modern humans can be inferred from their interactions with other large predators. Many transitional sites in France and Italy provide evidence of changing human-carnivore interactions during the Early Upper Paleolithic, possibly related to the emergence of long-range weapons. In southwestern France, Rendu and colleagues (2019) observed the decreasing impact of carnivore predators on Proto-Aurignacian and Early Aurignacian faunal assemblages and the increasing frequency of anthropic marks on a range of carnivore taxa, including bear, hyena, and fox. A similar pattern in the Italian peninsula indicates the exploitation of Ursidae for food and pelts in Mousterian contexts, whereas fox, lynx, and wolf are added to the list of exploited carnivores in the Uluzzian and Proto-Aurignacian levels of Grotta di Fumane (Romandini et al. 2020; Tagliacozzo et al. 2013). These observations suggest a pivotal shift in human-carnivore relationship—while Neanderthals shared their ecological niche with large carnivores like hyenas and wolves, focusing on different age categories of shared prey species (i.e., adults vs. young and old ungulates) (Dusseldorp 2013; Stiner 1994), modern humans appeared to have entered direct competition with them during periods of climatic instability, impacting habitat carrying capacities causing regional declines in hyena populations (Discamps 2014; Rendu et al. 2019). A similar dynamic is noted in the Initial Upper Paleolithic context of Bacho Kiro Cave, where wolf, fox, cave hyena, and cave bear taxa were exploited for skins and fur and personal ornaments (Martisius et al. 2022; Sinet-Mathiot et al. 2023; Smith et al. 2021), possibly pushing back in time this apparent shift in human-carnivore interactions in Europe.

In the Liguro-Provençal arc, documenting these changes is more challenging due to the scarcity of well-preserved Proto-Aurignacian deposits. At Riparo Bombrini, reduced carnivore activities in Levels A1 and A2, in spite of the heavy post-depositional attrition, align with this proposed human-carnivore interaction shift. Additionally, the overlying Early Aurignacian level of the neighboring site of Rip-

aro Mochi includes a few personal ornaments made on carnivore teeth (Tejero and Grimaldi 2015). Valensi and Psathi (2004) documented bear exploitation in several Mousterian faunal assemblages, aligning with the overall pattern across the Italian peninsula, although regional variabilities exist, with the anecdotal discovery of lynx and cave lion bones bearing cut marks at Grotte du Lazaret and Caverna delle Fate.

Broader Range of Animal Raw Material for Symbolic and Technological Use

Many Mousterian faunal assemblages have yielded examples of bone tools such as bone retouchers, knapped bone tools, and smoothers (e.g., Daujeard et al. 2014; Soressi et al. 2013) alongside symbolic uses of prey bird feathers, talons, and bones (e.g., Finlayson et al. 2012; Romandini et al. 2014). A growing body of literature documents continuity in bone retoucher selection and use, and the symbolic utilization of birds of prey across the Middle-Upper Paleolithic transition (e.g., Jéquier et al. 2018; Laroulandie et al. 2020). However, the Final Mousterian and the Early Upper Paleolithic records notably diverge in the diversity of forms and the range of animal raw materials used in both symbolic and functional spheres. In western France, personal ornaments come in different shapes and are made on antler, ivory, carnivore and cervid teeth, fossils, and marine shells. However, ornaments are scarcely documented in the Proto-Aurignacian, whereas they become widespread and regionalized starting in the Early Aurignacian (Soulie 2013). Bone tool types are also diversified, including many pointed objects (i.e., awls and needles), smoothers, and wedges associated with domestic activities such as hide-working, the manufacture of clothing, and woodworking (Soulie 2013; Tartar 2012). Antler is introduced as a material to make projectile armatures, appearing sporadically in southern European Proto-Aurignacian assemblages and prominently (i.e., split-based points) in Early Aurignacian contexts (e.g., Szmidi et al. 2010; Soulie 2014).

In the Liguro-Provençal arc, despite poor skeletal preservation, a bone industry including bone awls and broken needle tips is documented in the Proto-Aurignacian of Riparo Bombrini and the Early Aurignacian of Riparo Mochi (Holt et al. 2019; Tejero and Grimaldi 2015; Pothier Bouchard et al. 2020). Proto-Aurignacian symbolic objects include abundant gastropod shell beads from both sites with a few personal ornaments made of incised bird diaphyses, worked steatite, and grooved fossil belemnite at Riparo Bombrini (Holt et al. 2019). However, those assemblages have so far not yielded proof of *in situ* antler, ivory, or teeth working, whereas the Early Aurignacian of Riparo Mochi documented several split-based points with one ivory bead and a few tooth beads along with the continuous production of gastropod beads (Stiner, 1999; Tejero and Grimaldi 2015). This pattern suggests a slightly narrower range of animal raw materials in the earliest Aurignacian occupations of the Balzi Rossi, consistent with the trends observed in western France.

The shift in human-carnivore interactions and the

broadening of animal raw materials in the earliest Upper Paleolithic may reflect a change in the status of some taxa. For instance, the medium carnivores would have shifted from a status of competitor to sources of raw material (i.e., exploitation of fur) and symbols of identity (i.e., personal ornaments), and possibly a source of food (Rendu et al. 2019; Smith et al. 2021; Soulier 2014). The status of small carnivores such as foxes also changed, from being mostly ignored during the Mousterian to being exploited in the functional and symbolic spheres during the Proto-Aurignacian (Soulie 2013). In the Liguro-Provençal arc, mollusks shift from being strictly a source of food in the Late Mousterian to a primary source of raw material to make beads in the Proto-Aurignacian and the Early Aurignacian (Holt et al. 2019; Stiner 1999).

In sum, the patterns of changing human-environmental relationships, starting in the Proto-Aurignacian and possibly within earlier modern human contexts in Europe, could reflect subsistence adaptations that would have been advantageous towards climate instability. For instance, the reduction in procurement time and risk provided by long-range weapons could have changed how modern humans managed their foraging time by allocating their energy to other specialized or time-consuming tasks (Kuhn and Stiner 2006). In addition, the diversification of symbolic objects could reflect social changes and higher levels of connectedness, often argued to be linked to demographic pressure (Burke 2012; Henshilwood and Marean 2003; Stiner and Kuhn 2006). Stylistic variation and symbolic expression can reflect the need to broadcast identity within extended social networks. In such a scenario, while Neanderthals might have responded to climate variability through demographic fluctuations, modern humans would have had increased demographic robustness, spreading foraging risks over larger territories (Stiner and Kuhn 2006).

MULTIVARIATE APPROACH WITH THE INTEGRATION OF ZOOMS

The multivariate approach, coupled with integrated ZooMS, allowed unprecedentedly detailed insights into the subsistence behaviors of Riparo Bombrini's heavily altered faunal assemblages. The multivariate approach provided a hierarchical organization of taphonomic data that helped clarify issues of equifinality, such as distinguishing the extent of post-depositional attrition and anthropic alterations as sources of the high fragmentation in the Proto-Aurignacian levels. Despite the challenges posed by poor bone preservation, the use of larger taxonomic categories (i.e., medium and large game) to observe how the taphonomic variables vary between more fragile and more robust skeletal remains, and the use of NSP tallies of different bone types (e.g., cancellous and cortical bones), facilitated useful discussions about bone survivorship and taphonomic impact when the use of statistical tests was impossible due to low MNE tallies.

ZooMS, as a complementary analytical tool to archaeological analysis, has so far been primarily applied to the indeterminate fraction of faunal assemblages because it can

TABLE 12. COMPARISON BETWEEN THE SPECIMEN COUNTS IDENTIFIED WITH MORPHOLOGY ALONE AND ZOOMS.*

		Level A1	Level A2	Level MS
Faunal abundance (NISP)	Morphology	12	22	20
	ZooMS	119	96	19
Skeletal frequency (NISPe)	Morphology	12	21	20
	ZooMS	75	52	15
Fetal and juvenile elements (n)	Morphology	0	2	2
	ZooMS	0	0	0
Elements with fresh fracture angles, anthropic, and carnivore alterations (n)	Morphology	0	0	5
	ZooMS	17	15	4

*Number of identified specimens (NISP) and Number of identified specimens of skeletal elements (NISPe).

generate crucial information on the taxonomic identification of unidentifiable bone fragments. The method has also proven beneficial in improving overall taxonomic identifications (e.g., Buckley and Kansa 2011; Buckley et al. 2017; Welker et al. 2015) and highlighting differences in taxonomic composition related to diverse taphonomic patterns (e.g., Ruebens et al. 2022; 2023; Sinet-Mathiot et al. 2019; 2023).

At Riparo Bombrini, our application of ZooMS considerably enhanced skeletal frequencies and the identification of specific agents of skeletal alteration, as shown in Table 12. Our attempt to clarify seasonality and mortality profiles through the sampling of friable fetal and juvenile skeletal remains was unfruitful. This type of sampling has, however, proven successful in better-preserved contexts (Arenas-Sorriquetta et al. 2023).

Furthermore, applying the ZooMS on the unidentifiable fraction considerably increased the NISP tallies of most taxonomic categories, enabling a comprehensive discussion of faunal abundance and taxonomic composition. However, it is crucial to acknowledge that ZooMS does not entirely mitigate interpretive biases associated with NISP, necessitating conceptual and methodological efforts to integrate this method into archaeozoological studies in Paleolithic contexts. For instance, our sampling strategy on the poorly preserved faunal assemblages of Riparo Bombrini demonstrates that the success of ZooMS is primarily influenced by differential preservation. Collagen preservation, contingent on bone density, introduces biases against more fragile bones. Our results show this by the number of ZooMS-identified cortical bones (long bone and indeterminate), accounting for 76% of the total identified ZooMS samples, in contrast with no positive result on juvenile and fetal bones (see Table 11).

In addition, since collagen preserves well in dense corti-

cal bones of large taxa, ZooMS sampling of those abundant types of bone fragments can be influenced by differential bone breakage. These biases mainly concern the interdependence of skeletal remains—i.e., one animal can be counted several times, which exaggerates sample sizes across taxa (Morin et al. 2023). The random ZooMS sampling does not exaggerate all taxonomic categories equally and could create an error propagation phenomenon regarding NISP tallies. Nevertheless, the NISP remains the best quantification unit for discussing faunal abundance and taxonomic composition on heavily fragmented assemblages. In this context, ZooMS can highlight bone fragments of taxonomic categories that might have been absent or underestimated using only morphological identifications. In addition, the issue of the interdependence of skeletal remains can be partly addressed by considering the spatial distribution of faunal remains to locate areas of bone aggregates.

In sum, while ZooMS can aggravate some interpretive biases related to NISP tallies, its influence on the taxonomic and skeletal composition can also reveal anthropic behaviors that would not be possible to identify with morphology alone. However, the full power of the ZooMS as a complementary tool is only revealed when integrated into a complete archaeozoological and taphonomic study. Differential preservation remains the main challenge to interpreting heavily fragmented faunal assemblages. At Riparo Bombrini, the differential bone preservation varied according to bone density and within the different areas of the site. Our window of taxonomic identifications (with morphology and ZooMS) was thus severely biased towards the exterior of the rockshelter. In addition, the loss of collagen in bones affected by anthropic behaviors involving heat (e.g., cooking, grease rendering, and bone fuel) hindered ZooMS identification, which inevitably created taxonomic identifications biased towards unheated skeletal elements.

Nonetheless, the multivariate taphonomic approach helped tackle these many methodological challenges by organizing the variables and structuring our investigation of the different faunal assemblages to extract as much information as possible from a taphonomically challenging site.

CONCLUSION

In conclusion, our study yielded new insights into the patterns of subsistence adaptations of the very last Neanderthals associated with the “Semi-Sterile Mousterian” and the first modern humans of the Proto-Aurignacian at the taphonomically challenging site of Riparo Bombrini. This, in turn, allowed discussion of subsistence behaviors during the transition, for the first time, in the Liguro-Provençal arc. Such fine-grained subsistence data was achieved by applying a multivariate taphonomic approach to our archaeozoological analysis with integrated large-scale ZooMS sampling. Our results attested that the unique topographic and environmental settings of the Liguro-Provençal arc have influenced past subsistence, mobility, and resource management strategies of Neanderthals and modern humans. For instance, the abundant prey availability would have allowed flexible hunting strategies in response to external stresses. This could partly explain the lasting Neanderthal occupations documented in the Balzi Rossi and the subsistence adaptations of the Proto-Aurignacian groups to the HE 4.

The flexible hunting capacities of both human species are shown by the continuous taxonomic diversity documented in the transitional faunal assemblages of the Liguro-Provençal arc, which reflects the local biogeographic dynamics. However, evidence from the faunal and lithic technological records of Riparo Bombrini also suggests changing adaptations to external stresses in the Balzi Rossi. Level MS suggests that the very last Neanderthals to have occupied the site adopted a hyperlocal subsistence and land-use strategy in response to changing ecological conditions and possibly to the arrival of new groups in the neighboring regions (i.e., Proto-Aurignacian in France, Uluzzian in Italy). This working hypothesis should be tested in the future on other sites displaying long stratigraphic sequences that have yet to be investigated (see Riel-Salvatore et al. 2022 for discussion). In contrast, the faunal data of the Proto-Aurignacian levels support the patterns of shifting mobility strategies within a large territory lasting through events of climate instability previously observed at the site (Pothier Bouchard et al. 2020; Riel-Salvatore and Negrino 2018a, b).

Among the scenarios explaining Neanderthals’ demise, cognitive or behavioral inferiority no longer stands. Scenarios integrating behavioral ecology instead highlight the role of subsistence versatility, heightened demography, and social connectedness to explain modern humans’ adaptive success in Europe, which could ultimately have resulted in the competitive exclusion of Neanderthal groups in many regions (e.g., O’Connell 2006; Shea and Sisk 2010; Stiner and Kuhn 2006). The recent discoveries reformulating the chronological timing of modern human dispersals

(i.e., Mandrin in France, Bacho Kiro in Bulgaria, Rani in Germany) also contribute to highlighting the complexity of the coexistence dynamics between the last Neanderthal and first modern human groups in Europe, especially in regions of biogeographic richness and stability (Marín-Arroyo et al. 2023; Mylopotamitaki et al. 2024; Pederzani et al. 2024; Slimak et al. 2022; Smith et al. 2021; Vidal-Cordasco et al. 2023). The diet narrowing, high mobility, and hyper-local adaptation documented in the “Semi-Sterile Mousterian” of the Balzi Rossi could be the expression of lasting pockets of Neanderthal groups and their reduced demography. In contrast, the larger land-use territories, the implementation of long-range weapons allowing flexible hunting tactics, and the changing status of carnivores and several animal raw materials all suggest changing human-environmental interactions that would have increased modern human resilience towards environmental instability.

ACKNOWLEDGMENTS

We wish to thank the Social Sciences and Humanities Research Council of Canada (SSHRC), the Fonds Québécois de Recherche – Société et Culture (FQR-SC), the Mitacs international – Globalink, and the Université de Montréal for financial support and travel grants to Geneviève Pothier-Bouchard, as well as SSHRC grant 435-2017-1520, FQR-SC grant 2016-NP-193048, and CFI JELF grant #37754 to Julien Riel-Salvatore that have supported fieldwork at Riparo Bombrini since 2015, the acquisition of a FTIR instrument, and the ZooMS analyses. We also thank the Royal Society (UF120473) for fellowship funding to Michael Buckley. We thank the Università di Genova for access to materials. We also extend our sincere thanks to Giuliano Doria, director of the *Museo Civico di Storia Naturale di Genova*, who graciously gave us access to the reference collection of herbivore and carnivore skulls. We also thank the European Research Council under the European Union’s Horizon 2020 Research and Innovation Programme (grant agreement number 818299; SUBSILIENCE project; <https://www.subsilience.eu>) for funding the stable isotopic analysis conducted by the Grupo de I+D+i EVOADAPTA (Evolución Humana y Adaptaciones durante la Prehistoria). Fieldwork at Riparo Bombrini is made possible by ongoing collaborations with and administrative support from the *Soprintendenza Archeologia, Belle Arti e Paesaggio per la città metropolitana di Genova e le province di Imperia, La Spezia e Savona*, the *Polo Museale della Liguria*, and the *Museo Preistorico Nazionale dei Balzi Rossi*. The priceless logistical support of the *Istituto Internazionale di Studi Liguri and of Drssa*. Daniela Gandolfi in Bordighera for the Bombrini project is also gratefully acknowledged.

DATA AVAILABILITY

This doi link will provide all the ZooMS raw files used in this study: <https://doi.org/10.5683/SP3/QHLKRU>.



This work is distributed under the terms of a [Creative Commons Attribution-NonCommercial 4.0 Unported License](https://creativecommons.org/licenses/by-nc/4.0/).

REFERENCES

- Acevedo, P., Cassinello, J., 2009. Biology, ecology and status of Iberian ibex *Capra pyrenaica*: a critical review and research prospectus. *Mamm. Rev.* 39, 17–32.
- Adler, D.S., Bar-Oz, G., Belfer-Cohen, A., Bar-Yosef, O., 2006. Ahead of the game: Middle and Upper Palaeolithic hunting behaviors in the southern Caucasus. *Curr. Anthropol.* 47, 89–118.
- Alhaique, F., 2000. Risultati preliminari dell'analisi dei resti faunistici rinvenuti nei livelli del Paleolitico superiore di Riparo Mochi (Balzi Rossi): scavi 1995–96. *Atti del 2*, 125–130.
- Ambrose, S.H., 1990. Preparation and characterization of bone and tooth collagen for isotopic analysis. *J. Archaeol. Sci.* 17, 431–451.
- Arenas-Sorriquetta, E., Marín-Arroyo, A.B., Terlato, G., Torres-Iglesias, L., Agudo Pérez, L., de la Rasilla, M., 2023. Subsistence strategies during the Gravettian in the rock shelter of La Viña (Asturias, N Spain). *Quatern. Sci. Adv.* 12, 100113.
- Banks, W.E., d'Errico, F., Zilhão, J., 2013. Revisiting the chronology of the Proto-Aurignacian and the Early Aurignacian in Europe: a reply to Higham et al.'s comments on Banks et al. (2013). *J. Hum. Evol.* 30, 1–8.
- Barone, R., 1975. Anatomie comparée des mammifères domestiques. Tome premier, ostéologie. Vigot frères, Paris.
- Bar-Oz, G., Dayan, T., 2003. Testing the use of multivariate inter-site taphonomic comparisons: the faunal analysis of Hefzibah in its Epipalaeolithic cultural context. *J. Archaeol. Sci.* 30, 885–900.
- Bar-Oz, G., Munro, N.D., 2004. Beyond cautionary tales: a multivariate taphonomic approach for resolving equifinality in zooarchaeological studies. *J. Taphonomy* 2, 201–220.
- Benazzi, S., Slon, V., Talamo, S., Negrino, F., Peresani, M., Bailey, S.E., Sawyer, S., Panetta, D., Vicino, G., Starnini, E., Mannino, M.A., Salvadori, P.A., Meyer, M., Pääbo, S., Hublin, J.-J., 2015. The makers of the Protoaurignacian and implications for Neandertal extinction. *Science* 348, 793–796.
- Bignon, O., 2006. Approche morphométrique des dents jugales déciduales d'*Equus caballus arcelini* (sensu lato, Guadelli 1991): critères de détermination et estimation de l'âge d'abattage. *C. R. Palevol* 5, 1005–1020.
- Blasco, R., Fernández Peris, J., 2012. A uniquely broad spectrum diet during the Middle Pleistocene at Bolomor Cave (Valencia, Spain). *Quatern. Int.* 252, 16–31.
- Blumenschine, R.J., 1995. Percussion marks, tooth marks, and experimental determinations of the timing of hominid and carnivore access to long bones at FLK *Zinj-anthropus*, Olduvai Gorge, Tanzania. *J. Hum. Evol.* 29, 21–51.
- Blumenschine, R.J., Marean, C.W., Capaldo, S.D., 1996. Blind tests of inter-analyst correspondence and accuracy in the identification of cut marks, percussion marks, and carnivore tooth marks on bone surfaces. *J. Archaeol. Sci.* 23, 493–507.
- Bocherens, H., 2009. Neanderthal dietary habits: review of the isotopic evidence. In: Hublin, J.-J., Richards, M.P. (Eds.), *The Evolution of Hominin Diets: Integrating Approaches to the Study of Palaeolithic Subsistence. Vertebrate Paleobiology and Paleoanthropology*. Springer Netherlands, Dordrecht, pp. 241–250.
- Brain, C.K., 1981. *The Hunters or the Hunted? An Introduction to African Cave Taphonomy*. University of Chicago Press, Chicago.
- Brown, S., Higham, T., Slon, V., Pääbo, S., Meyer, M., Douka, K., Brock, F., Comeskey, D., Procopio, N., Shunkov, M., Derevianko, A., Buckley, M., 2016. Identification of a new hominin bone from Denisova Cave, Siberia using collagen fingerprinting and mitochondrial DNA analysis. *Sci. Rep.* 6, 23559.
- Brown, W.A.B., Chapman, N.G., 1991. The dentition of red deer (*Cervus elaphus*): a scoring scheme to assess age from wear of the permanent molariform teeth. *J. Zool.* 224, 519–536.
- Brugal, J.-P., Fourvel, J.-B., Fosse, P., 2017. Premières observations sur les guildes de carnivores de la grotte de l'Observatoire. *Bull. Musée Anthropol. Préhist Monaco* 57, 47–60.
- Buckley, M., Collins, M., Thomas-Oates, J., Wilson, J.C., 2009. Species identification by analysis of bone collagen using matrix-assisted laser desorption/ionisation time-of-flight mass spectrometry. *Rapid Commun. Mass Spectrom.* 23, 3843–3854.
- Buckley, M., Harvey, V.L., Chamberlain, A.T., 2017. Species identification and decay assessment of Late Pleistocene fragmentary vertebrate remains from Pin Hole Cave (Creswell Crags, UK) using collagen fingerprinting. *Boreas* 46, 402–411.
- Buckley, M., Kansa, S.W., 2011. Collagen fingerprinting of archaeological bone and teeth remains from Domuztepe, South Eastern Turkey. *Archaeol. Anthropol. Sci.* 3, 271–280.
- Buckley, M., Larkin, N.R., Collins, M.J., 2011. Mammoth and mastodon collagen sequences; survival and utility. *Geochim. Cosmochim. Acta* 75, 2007–2016.
- Buckley, M., Whitcher Kansa, S., Howard, S., Campbell, S., Thomas-Oates, J., Collins, M., 2010. Distinguishing between archaeological sheep and goat bones using a single collagen peptide. *J. Archaeol. Sci.* 37, 13–20.
- Bunn, H.T., 1986. Patterns of skeletal representation and hominid subsistence activities at Olduvai Gorge, Tanzania, and Koobi Fora, Kenya. *J. Hum. Evol.* 15, 673–690.
- Burke, A., 2000. Preface: hunting in the Middle Palaeolithic. *Int. J. Osteoarchaeol.* 10, 281–285.
- Burke, A., 2012. Spatial abilities, cognition and the pattern of Neanderthal and modern human dispersals. *Quatern. Int.* 247, 230–235.
- Carden, R.F., Hayden, T.J., 2006. Epiphyseal fusion in the postcranial skeleton as an indicator of age at death of European fallow deer (*Dama dama dama*, Linnaeus, 1758). In: Ruscillo, D. (Ed.), *Recent Advances in Ageing and Sexing Animal Bones*. Oxbow Books, Oxford, pp.

- 227–236.
- Carter, R.J., 2006. A method to estimate the ages at death of red deer (*Cervus elaphus*) and roe deer (*Capreolus capreolus*) from developing mandibular dentition and its application to Mesolithic NW Europe. In: Ruscillo, D. (Ed.), *Recent Advances in Ageing and Sexing Animal Bones*. Oxbow Books, Oxford, pp. 40–61.
- Carvalho, M., Bicho, N., 2022. Complexity in the Middle to Upper Paleolithic transition in peninsular southern Europe and application of refugium concepts. *J. Quatern. Sci.* 37, 380–393.
- Churchill, S.E., Rhodes, J.A., 2009. The evolution of the human capacity for “killing at a distance”: the human fossil evidence for the evolution of projectile weaponry. In: Hublin, J.-J., Richards, M.P. (Eds.), *The Evolution of Hominin Diets: Integrating Approaches to the Study of Palaeolithic Subsistence*. Vertebrate Paleobiology and Paleoanthropology. Springer Netherlands, Dordrecht, pp. 201–210.
- Collins, M.J., Galley, P., 1998. Towards an optimal method of archaeological collagen extraction: the influence of pH and grinding. *Anc. Biomol.* 2, 209–223.
- Cortés-Sánchez, M., Morales-Muñiz, A., Simón-Vallejo, M.D., Lozano-Francisco, M.C., Vera-Peláez, J.L., Finlayson, C., Rodríguez-Vidal, J., Delgado-Huertas, A., Jiménez-Espejo, F.J., Martínez-Ruiz, F., Martínez-Aguirre, M.A., Pascual-Granged, A.J., Bergadá-Zapata, M.M., Gibaja-Bao, J.F., Riquelme-Cantal, J.A., López-Sáez, J.A., Rodrigo-Gámiz, M., Sakai, S., Sugisaki, S., Finlayson, G., Fa, D.A., Bicho, N.F., 2011. Earliest known use of marine resources by Neanderthals. *PLoS One* 6, e24026.
- Costamagno, S., 2013. Bone grease rendering in Mousterian contexts: the case of Noisetier Cave (Fréchet-Aure, Hautes-Pyrénées, France). In: Clark, J.L., Speth, J.D. (Eds.), *Zooarchaeology and Modern Human Origins: Human Hunting Behavior during the Later Pleistocene*. Vertebrate Paleobiology and Paleoanthropology. Springer Netherlands, Dordrecht, pp. 209–225.
- Costamagno, S., Bourguignon, L., Soulier, M.-C., Meignen, L., Beauval, C., Rendu, W., Mussini, C., Mann, A., Maureille, B., 2015. Bone retouchers and site function in the Quina Mousterian: the case of Les Pradelles (Marillac-le-France, France). In: Hutson, J.M., García-Moreno, A., Noack, E.S., Turner, E., Villaluenga, A., Gaudzinski-Windheuser, S. (Eds.), *Retouching the Palaeolithic: Becoming Human and the Origins of Bone Tool Technology*, International Workshop, The Origins of Bone Tool Technologies. RGZM Press, Hannover, Germany, pp. 165–195.
- Costamagno, S., Théry-Parisot, I., Brugal, J.-P., Guibert, R., 2005. Taphonomic consequences of the use of bones as fuel. Experimental data and archaeological applications. In: O'Connor, T. (ed.), *Biosphere to Lithosphere*, Proceedings of the 9th Conference of the International Council of Archaeozoology. Oxbow Books, Oxford. pp. 51–62.
- d'Errico, F., Vanhaeren, M., 2002. Criteria for identifying red deer (*Cervus elaphus*) age and sex from their canines. Application to the study of Upper Palaeolithic and Mesolithic ornaments. *J. Archaeol. Sci.* 29, 211–232.
- Daujeard, C., Fernandes, P., Guadelli, J.-L., Moncel, M.-H., Santagata, C., Raynal, J.-P., 2012. Neanderthal subsistence strategies in Southeastern France between the plains of the Rhone Valley and the mid-mountains of the Massif Central (MIS 7 to MIS 3). *Quatern. Int.* 252, 32–47.
- Daujeard, C., Moncel, M.-H., Fiore, I., Tagliacozzo, A., Bindon, P., Raynal, J.-P., 2014. Middle Paleolithic bone retouchers in Southeastern France: variability and functionality. *Quatern. Int.* 326, 492–518.
- DeNiro, M.J., 1985. Postmortem preservation and alteration of in vivo bone collagen isotope ratios in relation to palaeodietary reconstruction. *Nature* 317, 806–809.
- Discamps, E., 2014. Ungulate biomass fluctuations endured by Middle and Early Upper Paleolithic societies (SW France, MIS 5-3): the contributions of modern analogs and cave hyena paleodemography. *Quatern. Int.* 337, 64–79.
- Discamps, E., Costamagno, S., 2015. Improving mortality profile analysis in zooarchaeology: a revised zoning for ternary diagrams. *J. Archaeol. Sci.* 58, 62–76.
- Discamps, E., Jaubert, J., Bachellerie, F., 2011. Human choices and environmental constraints: deciphering the variability of large game procurement from Mousterian to Aurignacian times (MIS 5-3) in southwestern France. *Quatern. Sci. Rev.* 30, 2755–2775.
- Domínguez-Rodrigo, M., 2009. Taphonomie des sites plio-pléistocènes d'Afrique orientale. Apport de l'expérimentation. *Nouv. archéol.* 118, 6–11.
- Drucker, D.G., Bridault, A., Hobson, K.A., Szuma, E., Boucherens, H., 2008. Can carbon-13 in large herbivores reflect the canopy effect in temperate and boreal ecosystems? Evidence from modern and ancient ungulates. *Palaeogeogr. Palaeoclimatol. Palaeoecol.* 266, 69–82.
- Drucker, D.G., Naito, Y.I., Péan, S., Prat, S., Crépin, L., Chikaraishi, Y., Ohkouchi, N., Puaud, S., Lázníčková-Galetová, M., Patou-Mathis, M., Yanevich, A., Boucherens, H., 2017. Isotopic analyses suggest mammoth and plant in the diet of the oldest anatomically modern humans from far southeast Europe. *Sci. Rep.* 7, 6833.
- Dusseldorp, G.L., 2013. Neanderthals and cave hyenas: co-existence, competition or conflict? In: Clark, J.L., Speth, J.D. (Eds.), *Zooarchaeology and Modern Human Origins: Human Hunting Behavior during the Later Pleistocene*. Vertebrate Paleobiology and Paleoanthropology. Springer Netherlands, Dordrecht, pp. 191–208.
- Finlayson, C., Brown, K., Blasco, R., Rosell, J., Negro, J.J., Bortolotti, G.R., Finlayson, G., Marco, A.S., Pacheco, F.G., Vidal, J.R., 2012. Birds of a feather: Neanderthal exploitation of raptors and corvids. *PLoS One* 7, e45927.
- Finlayson, C., Giles Pacheco, F., Rodríguez-Vidal, J., Fa, D.A., María Gutierrez López, J., Santiago Pérez, A., Finlayson, G., Allue, E., Baena Preysler, J., Cáceres, I., Carrión, J.S., Fernández Jalvo, Y., Gleed-Owen, C.P., Jiménez Espejo, F.J., López, P., Antonio López Sáez, J.,

- Antonio Riquelme Cantal, J., Sánchez Marco, A., Giles Guzman, F., Brown, K., Fuentes, N., Valarino, C.A., Villalpando, A., Stringer, C.B., Martínez Ruiz, F., Sakamoto, T., 2006. Late survival of Neanderthals at the southernmost extreme of Europe. *Nature* 443, 850–853.
- Fiorenza, L., Benazzi, S., Henry, A.G., Salazar-García, D.C., Blasco, R., Picin, A., Wroe, S., Kullmer, O., 2015. To meat or not to meat? New perspectives on Neanderthal ecology. *Am. J. Phys. Anthropol.* 156, 43–71.
- Fisher, Jr, J.W., 1995. Bone surface modifications in zooarchaeology. *J. Archaeol. Method and Theory* 2, 7–68.
- Gaudzinski, S., 2006. Monospecific or species-dominated faunal assemblages during the Middle Paleolithic in Europe. In: Hovers, E., Kuhn, S.L. (Eds.), *Transitions Before the Transition. Interdisciplinary Contributions to Archaeology*. Springer US, Boston, pp. 137–147.
- Gaudzinski, S., Roebroeks, W., 2000. Adults only. Reindeer hunting at the Middle Palaeolithic site Salzgitter Lebenedt, northern Germany. *J. Hum. Evol.* 38, 497–521.
- Gipson, P.S., Ballard, W.B., Nowak, R.M., Mech, L.D., 2000. Accuracy and precision of estimating age of gray wolves by tooth wear. *J. Wildl. Manag.* 64, 752–758.
- Grant, A., 1982. The use of tooth wear as a guide to the age of domestic ungulates. In: Wilson, B., Grigson, C., Payne, S. (Eds.), *Ageing and Sexing Animal Bones From Archaeological Sites*. British Archaeological Reports 109, Oxford, 91–108.
- Grayson, D.K., 1984. *Quantitative Zooarchaeology: Topics in the Analysis of Archaeological Faunas*. Academic Press, Orlando.
- Grayson, D.K., Delpech, F., 1998. Changing diet breadth in the Early Upper Palaeolithic of southwestern France. *J. Archaeol. Sci.* 25, 1119–1129.
- Grayson, D.K., Delpech, F., 2002. Specialized early Upper Palaeolithic hunters in southwestern France? *J. Archaeol. Sci.* 29, 1439–1449.
- Grimaldi, S., Porraz, G., Santaniello, F., 2014. Raw material procurement and land use in the northern Mediterranean Arc: insight from the first Proto-Aurignacian of Riparo Mochi (Balzi Rossi, Italy). *Quartär* 61, 113–127.
- Grimaldi, S., Santaniello, F., 2014. New insights into Final Mousterian lithic production in western Italy. *Quatern. Int.* 350, 116–129.
- Guillaud, E., Béarez, P., Daujeard, C., Defleur, A.R., Desclaux, E., Roselló-Izquierdo, E., Morales-Muñiz, A., Moncel, M.-H., 2021. Neanderthal foraging in freshwater ecosystems: a reappraisal of the Middle Paleolithic archaeological fish record from continental Western Europe. *Quatern. Sci. Rev.* 252, 106731.
- Hardy, B.L., Moncel, M.-H., 2011. Neanderthal use of fish, mammals, birds, starchy plants and wood 125-250,000 Years Ago. *PLoS One* 6, e23768.
- Henry, A.G., Brooks, A.S., Piperno, D.R., 2011. Microfossils in calculus demonstrate consumption of plants and cooked foods in Neanderthal diets (Shanidar III, Iraq; Spy I and II, Belgium). *Proc. Nat. Acad. Sci. U.S.A.* 108, 486–491.
- Henshilwood, C.S., Marean, C.W., 2003. The origin of modern human behavior: critique of the models and their test implications. *Curr. Anthropol.* 44, 627–651.
- Holt, B., Negrino, F., Riel-Salvatore, J., Formicola, V., Arelano, A., Arobba, D., Boschian, G., Churchill, S.E., Cristiani, E., Di Canzio, E., Vicino, G., 2019. The Middle-Upper Paleolithic transition in northwest Italy: new evidence from Riparo Bombrini (Balzi Rossi, Liguria, Italy). *Quatern. Int.* 508, 142–152.
- Jéquier, C., Peresani, M., Livraghi, A., Romandini, M., 2018. Same but different: 20,000 years of bone retouchers from northern Italy. A diachronologic approach from Neanderthals to Anatomically Modern Humans. In: Hutson, J.M., García-Moreno, A., Noack, E., Turner, E., Villaluenga, A., Gaudzinski-Windheuser, S. (Eds.), *Retouching the Palaeolithic: Becoming Human and the Origins*. Römisch-Germanischen Zentralmuseums, Mainz, pp. 269–285.
- Jones, J.R., Richards, M.P., Straus, L.G., Reade, H., Altuna, J., Mariezkurrena, K., Marín-Arroyo, A.B., 2018. Changing environments during the Middle-Upper Palaeolithic transition in the eastern Cantabrian Region (Spain): direct evidence from stable isotope studies on ungulate bones. *Sci. Rep.* 8, 14842.
- Julien, M.-A., 2011. *Chasseurs de bisons: apports de l'archéozoologie et de la biogéochimie isotopique à l'étude paléthnographique et paléothologique du gisement épigravettien d'Amvrosievka (Ukraine)*. Muséum national d'histoire naturelle and Université de Montréal, Paris.
- Klein, R., Allwarden, K., Wolf, C., 1983. The calculation and interpretation of ungulate age profiles from dental crown heights (North America red deer). In: Bailey, G. (Ed.), *Hunter-Gatherer Economy in Prehistory: A European Perspective*. Cambridge University Press, Cambridge, UK, pp. 47–57.
- Klein, R.G., Cruz-Urbe, K., 1984. *The Analysis of Animal Bones from Archeological Sites*. University of Chicago Press, Chicago.
- Kuhn, S.L., Stiner, M.C., 2006. What's a mother to do? The division of labor among Neandertals and Modern Humans in Eurasia. *Curr. Anthropol.* 47, 953–981.
- Laroulandie, V., Morin, E., Soulier, M.-C., Castel, J.-C., 2020. Bird procurement by humans during the Middle and early Upper Paleolithic of Europe: new data for the Aurignacian of southwestern France. *Quatern. Int.* 543, 16–24.
- Levine, M.A., 1982. The use of crown height measurements and eruption-wear sequences to age horse teeth. In: Wilson, B., Grigson, C., Payne, S. (Eds.), *Ageing and Sexing Animal Bones from Archaeological Sites*. British Archaeological Reports 109, Oxford, pp. 223–250.
- Longin, R., 1971. New method of collagen extraction for radiocarbon dating. *Nature* 230, 241–242.
- Lyman, R.L., 1994. *Vertebrate Taphonomy*. Cambridge University Press, Cambridge, UK.
- Lyman, R.L., 2008. *Quantitative Paleozoology*. Cambridge University Press Cambridge, UK.
- Magnell, O., 2006. Tooth wear in wild boar (*Sus scrofa*). In:

- Ruscillo, D. (Ed.), Recent Advances in Ageing and Sexing Animal Bones. Oxbow Books, Oxford, pp. 189–203.
- Marean, C.W., 1991. Measuring the post-depositional destruction of bone in archaeological assemblages. *J. Archaeol. Sci.* 18, 677–694.
- Marean, C.W., 1998. A critique of the evidence for scavenging by Neanderthals and early modern humans: new data from Kobeh Cave (Zagros Mountains, Iran) and Die Kelders Cave 1 Layer 10 (South Africa). *J. Hum. Evol.* 35, 111–136.
- Marín-Arroyo, A.B., Terlato, G., Vidal-Cordasco, M., Pearsani, M., 2023. Subsistence of early anatomically modern humans in Europe as evidenced in the Protoaurignacian occupations of Fumane Cave, Italy. *Sci. Rep.* 13, 3788.
- Mariotti Lippi, M., Aranguren, B., Arrighi, S., Attolini, D., Benazzi, S., Boschini, F., Florindi, S., Moroni, A., Negrino, F., Pallecchi, P., Pisaneschi, L., Riel-Salvatore, J., Ronchitelli, A., Revedin, A., 2023. New evidence of plant food processing in Italy before 40ka. *Quatern. Sci. Rev.* 312, 108161.
- Marques, M.P.M., Mamede, A.P., Vassalo, A.R., Makhoul, C., Cunha, E., Gonçalves, D., Parker, S.F., Batista de Carvalho, L.A.E., 2018. Heat-induced bone diagenesis probed by vibrational spectroscopy. *Sci. Rep.* 8, 15935.
- Martisius, N.L., Spasov, R., Smith, G.M., Enderova, E., Sinet-Mathiot, V., Welker, F., Aldeias, V., Horta, P., Marreiros, J., Rezek, Z., McPherron, S.P., Sirakov, N., Sirakova, S., Tsanova, T., Hublin, J.-J., 2022. Initial Upper Paleolithic bone technology and personal ornaments at Bacho Kiro Cave (Bulgaria). *J. Hum. Evol.* 167, 103198.
- Mellars, P., 1996. *The Neanderthal Legacy: An Archaeological Perspective from Western Europe*. Princeton University Press, Princeton.
- Metcalfe, D., Jones, K.T., 1988. A reconsideration of animal body-part utility indices. *Am. Antiq.* 53, 486–504.
- Morin, E., 2008. Evidence for declines in human population densities during the early Upper Paleolithic in western Europe. *Proc. Nat. Acad. Sci. U.S.A.* 105, 48–53.
- Morin, E., 2010. Taphonomic implications of the use of bone as fuel. *Paléthnologie* 2, 209–217.
- Morin, E., Meier, J., Guennouni, K.E., Moigne, A.-M., Lebreton, L., Rusch, L., Valensi, P., Conolly, J., Cochard, D., 2019. New evidence of broader diets for archaic *Homo* populations in the northwestern Mediterranean. *Sci. Adv.* 5, eaav9106.
- Morin, E., Oldfield, E.-M., Baković, M., Bordes, J.-G., Castel, J.-C., Crevecoeur, I., Rougier, H., Monnier, G., Tostevin, G., Buckley, M., 2023. A double-blind comparison of morphological and collagen fingerprinting (ZooMS) methods of skeletal identifications from Palaeolithic contexts. *Sci. Rep.* 13, 18825.
- Morin, E., Ready, E., Boileau, A., Beauval, C., Coumont, M.-P., 2017. Problems of identification and quantification in archaeozoological analysis, part II: presentation of an alternative counting method. *J. Archaeol. Method Theory* 24, 938–973.
- Morin, E., Soulier, M.-C., 2017. New criteria for the archaeological identification of bone grease processing. *Am. Antiq.* 82, 96–122.
- Münzel, S.C., Conard, N.J., 2004. Change and continuity in subsistence during the Middle and Upper Palaeolithic in the Ach Valley of Swabia (south-west Germany). *Int. J. Osteoarchaeol.* 14, 225–243.
- Mylopotamitaki, D., Weiss, M., Fewlass, H., Zavala, E.I., Rougier, H., Sümer, A.P., Hajdinjak, M., Smith, G.M., Ruebens, K., Sinet-Mathiot, V., Pederzani, S., Essel, E., Harking, F.S., Xia, H., Hansen, J., Kirchner, A., Lauer, T., Stahlschmidt, M., Hein, M., Talamo, S., Wacker, L., Meller, H., Dietl, H., Orschiedt, J., Olsen, J.V., Zeberg, H., Prüfer, K., Krause, J., Meyer, M., Welker, F., McPherron, S.P., Schüller, T., Hublin, J.-J., 2024. *Homo sapiens* reached the higher latitudes of Europe by 45,000 years ago. *Nature* 626, 341–346.
- Naito, Y.I., Chikaraishi, Y., Drucker, D.G., Ohkouchi, N., Semal, P., Wißing, C., Bocherens, H., 2016. Ecological niche of Neanderthals from Spy Cave revealed by nitrogen isotopes of individual amino acids in collagen. *J. Hum. Evol.* 93, 82–90.
- Negrino, F., Riel-Salvatore, J., 2018. From Neanderthals to Anatomically Modern Humans in Liguria (Italy): the current state of knowledge. In: Borgia, V., Cristiani, E. (Eds.), *Palaeolithic Italy. Advanced Studies on Early Human Adaptations in the Apennine Peninsula*. Sidestone Press Academics, Leiden, Netherlands, pp. 159–180.
- Nehlich, O., 2015. The application of sulphur isotope analyses in archaeological research: a review. *Earth Sci. Rev.* 142, 1–17.
- Nehlich, O., Richards, M.P., 2009. Establishing collagen quality criteria for sulphur isotope analysis of archaeological bone collagen. *Archaeol. Anthropol. Sci.* 1, 59–75.
- Niven, L.B., 2006. The role of woolly rhinoceros and woolly mammoth in Paleolithic economies at Vogelherd cave, Germany. In: Haws, J.A., Hockett, B.S., Brugal, J.-P. (Eds.), *Paleolithic Zooarchaeology in Practice*, BAR International Series 1564. Archaeopress, Oxford, pp. 73–85.
- O’Connell, J.F., 2006. How did modern humans displace Neanderthals? Insights from hunter-gatherer ethnography and archaeology. In: Conard, N.J. (Ed.), *When Neanderthals and Modern Humans Met*. Kerns Verlag, Tübingen, pp. 43–64.
- Outram, A.K., 2001. A new approach to identifying bone marrow and grease exploitation: why the indeterminate fragments should not be ignored. *J. Archaeol. Sci.* 28, 401–410.
- Pales, L., Garcia, M.-A., 1981. *Atlas ostéologique pour servir à l’identification des mammifères du quaternaire*. Editions du Centre national de la recherche scientifique, Paris.
- Payne, S., 1987. Reference codes for wear states in the mandibular cheek teeth of sheep and goats. *J. Archaeol. Sci.* 14, 609–614.
- Pederzani, S., Britton, K., Trost, M., Fewlass, H., Bourgon,

- N., McCormack, J., Jaouen, K., Dietl, H., Döhle, H.-J., Kirchner, A., Lauer, T., Le Corre, M., McPherron, S.P., Meller, H., Mylopotamitaki, D., Orschiedt, J., Rougier, H., Ruebens, K., Schüler, T., Sinet-Mathiot, V., Smith, G.M., Talamo, S., Tütken, T., Welker, F., Zavala, E.I., Weiss, M., Hublin, J.-J., 2024. Stable isotopes show *Homo sapiens* dispersed into cold steppes ~45,000 years ago at Ilsenhöhle in Ranis, Germany. *Nature Ecol. Evol.* 8, 578–588.
- Perez, A., Santaniello, F., Hohenstein, U.T., Grimaldi, S., 2022. The faunal assemblage from the Riparo Mochi site (Balzi Rossi): new insights on the Mousterian-Aurignacian human-environment relationship. *Alp. Mediterr. Quatern.* 35, 135–155.
- Pickering, T.R., 2002. Reconsideration of criteria for differentiating faunal assemblages accumulated by hyenas and hominids. *Int. J. Osteoarchaeol.* 12, 127–141.
- Porraz, G., Negrino, F., 2008. Espaces économiques et approvisionnement minéral au Paléolithique moyen dans l'aire liguro-provençale. *Bull. Musée Anthropol. Préhist. Monaco* 1, 29–40.
- Porraz, G., Simon, P., Pasquini, A., Onoratini, G., 2010. Identité technique et comportements économiques des groupes protoaurignaciens à la grotte de l'Observatoire (Principauté de Monaco). *Gall. préhist.* 52, 33–59.
- Pothier-Bouchard, G., 2022. A ZooMS-Informed Archaeozoological and Taphonomic Analysis Comparing Neanderthal and *Homo sapiens* Subsistence Behaviours in Northwest Italy. Ph.D. Dissertation. Université de Montréal.
- Pothier-Bouchard, G., Mentzer, S.M., Riel-Salvatore, J., Hodgkins, J., Miller, C.E., Negrino, F., Wogelius, R., Buckley, M., 2019. Portable FTIR for on-site screening of archaeological bone intended for ZooMS collagen fingerprint analysis. *J. Archaeol. Sci. Rep.* 26, 101862.
- Pothier-Bouchard, G., Riel-Salvatore, J., Negrino, F., 2023. Archéozoologie, taphonomie et application du ZooMS sur la faune protoaurignacienne de Riparo Bombrini. *Rivista di Scienze Preistoriche LXXIII*, 973–980.
- Pothier-Bouchard, G., Riel-Salvatore, J., Negrino, F., Buckley, M., 2020. Archaeozoological, taphonomic and ZooMS insights into the Protoaurignacian faunal record from Riparo Bombrini. *Quatern. Int.* 551, 243–263.
- Power, R.C., Salazar-García, D.C., Rubini, M., Darlas, A., Harvati, K., Walker, M., Hublin, J.-J., Henry, A.G., 2018. Dental calculus indicates widespread plant use within the stable Neanderthal dietary niche. *J. Hum. Evol.* 119, 27–41.
- Rampelli, S., Turrone, S., Mallol, C., Hernandez, C., Galván, B., Sistiaga, A., Biagi, E., Astolfi, A., Brigidi, P., Benazzi, S., Lewis, C.M., Warinner, C., Hofman, C.A., Schnorr, S.L., Candela, M., 2021. Components of a Neanderthal gut microbiome recovered from fecal sediments from El Salt. *Commun. Biol.* 4, 1–10.
- Reitz, E.J., Wing, E.S., 2008. *Zooarchaeology*. Cambridge University Press, Cambridge, UK.
- Rendu, W., Costamagno, S., Meignen, L., Soulier, M.-C., 2012. Monospecific faunal spectra in Mousterian contexts: implications for social behavior. *Quatern. Int.* 247, 50–58.
- Rendu, W., Renou, S., Soulier, M.-C., Rigaud, S., Roussel, M., Soressi, M., 2019. Subsistence strategy changes during the Middle to Upper Paleolithic transition reveals specific adaptations of human populations to their environment. *Sci. Rep.* 9, 15817.
- Richards, M.P., Trinkaus, E., 2009. Isotopic evidence for the diets of European Neanderthals and early modern humans. *Proc. Nat. Acad. Sci. U.S.A.* 106, 16034–16039.
- Riel-Salvatore, J., Ludeke, I.C., Negrino, F., Holt, B.M., 2013. A spatial analysis of the late Mousterian levels of Riparo Bombrini (Balzi Rossi, Italy). *Can. J. Archaeol.* 37, 70–92.
- Riel-Salvatore, J., Negrino, F., 2009. Early Upper Paleolithic population dynamics and raw material procurement patterns in Italy. In: Camps, M., Szmíd, C. (Eds.), *The Mediterranean From 50000 to 25000 BP – Turning Points and New Directions*. Oxbow Books, Oxford, pp. 211–230.
- Riel-Salvatore, J., Negrino, F., 2018a. Proto-Aurignacian lithic technology, mobility, and human niche construction: a case study from Riparo Bombrini, Italy. In: Robinson, E., Sellet, F. (Eds.), *Lithic Technological Organization and Paleoenvironmental Change, Studies in Human Ecology and Adaptation, Volume 9*. Springer, Cham, pp. 163–187.
- Riel-Salvatore, J., Negrino, F., 2018b. Human adaptations to climatic change in Liguria across the Middle-Upper Paleolithic transition. *J. Quatern. Sci.* 3, 313–322.
- Riel-Salvatore, J., Negrino, F., Pothier Bouchard, Geneviève, Vallerand, A., Costa, S., Benazzi, S., 2022. The “Semi-Sterile Mousterian” of Riparo Bombrini: evidence of a late-lasting Neanderthal refugium in Liguria? *J. Quatern. Sci.* 37, 268–282.
- Romandini, M., 2017. La Grotte de l'Observatoire (Monaco) Industrie sur matières dures animales, objets de parure et observations archéozoologiques. *Bull. Musée Anthropol. Préhist Monaco* 57, 75–96.
- Romandini, M., Crezzini, J., Bortolini, E., Boscato, P., Boschin, F., Carrera, L., Nannini, N., Tagliacozzo, A., Terlato, G., Arrighi, S., Badino, F., Figus, C., Lugli, F., Marciani, G., Oxilia, G., Moroni, A., Negrino, F., Peresani, M., Riel-Salvatore, J., Ronchitelli, A., Spinapolice, E.E., Benazzi, S., 2020. Macromammal and bird assemblages across the late Middle to Upper Palaeolithic transition in Italy: an extended zooarchaeological review. *Quatern. Int.* 551, 188–223.
- Romandini, M., Peresani, M., Laroulandie, V., Metz, L., Pa-stoors, A., Vaquero, M., Slimak, L., 2014. Convergent evidence of eagle talons used by late Neanderthals in Europe: a further assessment on symbolism. *PLoS One* 9, e101278.
- Romandini, M., Silvestrini, S., Real, C., Lugli, F., Tassoni, L., Carrera, L., Badino, F., Bortolini, E., Marciani, G., Delpiano, D., Piperno, M., Collina, C., Peresani, M., Benazzi, S., 2023. Late Neanderthal “menu” from northern to southern Italy: freshwater and terrestrial animal

- resources. *Quatern. Sci. Rev.* 315, 108233.
- Rossoni-Notter, E., Notter, O., Simon, P., 2017. Mousterian in Balzi Rossi (Ventimiglia, Liguria, Italy): new insights and old collections. *Quatern. Int.* 435, 21–57.
- Rossoni-Notter, E., Simon, P., 2016. Péroarchéologie et techno-économie: pour une valorisation des collections moustériennes des Balzi Rossi (Grimaldi, Vintimille, Ligurie, Italie). In: Tomasso, A., Binder, D., Martino, G., Porraz, G., Simon, P., Naudinot, N. (Eds.), *Ressources lithiques, productions et transferts entre Alpes et Méditerranée, Actes de la journée de la Société préhistorique française de Nice, 28-29 March 2013. Séance de la Société préhistorique française 5*, pp. 145–175.
- Ruebens, K., Sinet-Mathiot, V., Talamo, S., Smith, G.M., Welker, F., Hublin, J.-J., McPherron, S.P., 2022. The Late Middle Palaeolithic Occupation of Abri du Maras (Layer 1, Neronian, Southeast France): integrating lithic analyses, ZooMS and radiocarbon dating to reconstruct Neanderthal hunting behaviour. *J. Paleolit. Archaeol.* 5, 4.
- Ruebens, K., Smith, G.M., Fewlass, H., Sinet-Mathiot, V., Hublin, J.-J., Welker, F., 2023. Neanderthal subsistence, taphonomy and chronology at Salzgitter-Lebenstedt (Germany): a multifaceted analysis of morphologically unidentifiable bone. *J. Quatern. Sci.* 38, 471–487.
- Schmid, E., 1972. Atlas of Animal Bones. For Prehistorians, Archaeologists and Quaternary Geologists. *Knochenatlas. Für Prähistoriker, Archäologen und Quartärgeologen*. Elsevier, Amsterdam.
- Shea, J.J., Sisk, M.L., 2010. Complex projectile technology and *Homo sapiens* dispersal into western Eurasia. *Paleo-Anthropology* 2010, 100–122.
- Sinet-Mathiot, V., Rendu, W., Steele, T.E., Spasov, R., Madelaine, S., Renou, S., Soulier, M.-C., Martisius, N.L., Aldeias, V., Enderova, E., Goldberg, P., McPherron, S.J.P., Rezek, Z., Sandgathe, D., Sirakov, N., Sirakova, S., Soressi, M., Tsanova, T., Turq, A., Hublin, J.-J., Welker, F., Smith, G.M., 2023. Identifying the unidentified fauna enhances insights into hominin subsistence strategies during the Middle to Upper Palaeolithic transition. *Archaeol. Anthropol. Sci.* 15, 139.
- Sinet-Mathiot, V., Smith, G.M., Romandini, M., Wilcke, A., Peresani, M., Hublin, J.-J., Welker, F., 2019. Combining ZooMS and zooarchaeology to study Late Pleistocene hominin behaviour at Fumane (Italy). *Sci. Rep.* 9, 1–13.
- Sistiaga, A., Mallol, C., Galván, B., Summons, R.E., 2014. The Neanderthal meal: a new perspective using faecal biomarkers. *PLoS One* 9, e101045.
- Slimak, L., Zanolli, C., Higham, T., Frouin, M., Schwenninger, J.-L., Arnold, L.J., Demuro, M., Douka, K., Mercier, N., Guérin, G., Valladas, H., Yvorra, P., Giraud, Y., Seguin-Orlando, A., Orlando, L., Lewis, J.E., Muth, X., Camus, H., Vandevelde, S., Buckley, M., Mallol, C., Stringer, C., Metz, L., 2022. Modern human incursion into Neanderthal territories 54,000 years ago at Mandrin, France. *Sci. Adv.* 8, eabj9496.
- Smith, G.M., Spasov, R., Martisius, N.L., Sinet-Mathiot, V., Aldeias, V., Rezek, Z., Ruebens, K., Pederzani, S., McPherron, S.P., Sirakova, S., Sirakov, N., Tsanova, T., Hublin, J.-J., 2021. Subsistence behavior during the Initial Upper Paleolithic in Europe: site use, dietary practice, and carnivore exploitation at Bacho Kiro Cave (Bulgaria). *J. Hum. Evol.* 161, 103074.
- Soressi, M., McPherron, S.P., Lenoir, M., Dogandžić, T., Goldberg, P., Jacobs, Z., Maignot, Y., Martisius, N.L., Miller, C.E., Rendu, W., 2013. Neandertals made the first specialized bone tools in Europe. *Proc. Nat. Acad. Sci. U.S.A.* 110, 14186–14190.
- Soulier, M.-C., 2013. *Entre alimentaire et technique : l'exploitation animale aux débuts du paléolithique supérieur : stratégies de subsistance et chaînes opératoires de traitement du gibier à Isturitz, La Quina aval, Roc-de-Combe et Les Abeilles*. Ph.D. Dissertation. Université Toulouse le Mirail - Toulouse II.
- Soulier, M.-C., 2014. Food and technical exploitation of mammals during the early Upper Palaeolithic at Les Abeilles (Haute-Garonne, France). *Paléo* 25, 287–307.
- Speth, J.D., Tchernov, E., 2001. Neandertal hunting and meat-processing in the Near East. In: Stanford, C.B., Bunn, H.T. (Eds.), *Meat-Eating and Human Evolution*. Oxford University Press, Oxford, pp. 52–72.
- Steele, T.E., 2002. *Red Deer: Their Ecology and How They Were Hunted by Late Pleistocene Hominids in Western Europe*. Ph.D. Dissertation. Stanford University.
- Stiner, M.C., 1994. *Honor Among Thieves: A Zooarchaeological Study of Neandertal Ecology*. Princeton University Press, Princeton, N.J.
- Stiner, M.C., 1998. Mortality analysis of Pleistocene bears and its paleoanthropological relevance. *J. Hum. Evol.* 34, 303–326.
- Stiner, M.C., 1999. Palaeolithic mollusc exploitation at Riparo Mochi (Balzi Rossi, Italy): food and ornaments from the Aurignacian through Epigravettian. *Antiquity* 73, 735–754.
- Stiner, M.C., 2001. Thirty years on the “Broad Spectrum Revolution” and paleolithic demography. *Proc. Nat. Acad. Sci. U.S.A.* 98, 6993–6996.
- Stiner, M.C., Kuhn, S.L., 2006. Changes in the ‘connectedness’ and resilience of Paleolithic societies in Mediterranean ecosystems. *Hum. Ecol.* 34, 693–712.
- Stiner, M.C., Kuhn, S.L., Weiner, S., Bar-Yosef, O., 1995. Differential burning, recrystallization, and fragmentation of archaeological bone. *J. Archaeol. Sci.* 22, 223–237.
- Szmidt, C.C., Normand, C., Burr, G.S., Hodgins, G.W.L., LaMotta, S., 2010. AMS ¹⁴C dating the Protoaurignacian/Early Aurignacian of Isturitz, France. Implications for Neanderthal–modern human interaction and the timing of technical and cultural innovations in Europe. *J. Archaeol. Sci.* 37, 758–768.
- Tagliacozzo, A., Romandini, M., Fiore, I., Gala, M., Peresani, M., 2013. Animal exploitation strategies during the Uluzzian at Grotta di Fumane (Verona, Italy). In: Clark, J.L., Speth, J.D. (Eds.), *Zooarchaeology and Modern Human Origins: Human Hunting Behavior during the Later Pleistocene. Vertebrate Paleobiology and Paleoanthropology*. Springer Netherlands, Dordrecht, pp.

- 129–150.
- Tartar, E., 2012. The recognition of a new type of bone tools in Early Aurignacian assemblages: implications for understanding the appearance of osseous technology in Europe. *J. Archaeol. Sci.* 39, 2348–2360.
- Tejero, J.-M., Grimaldi, S., 2015. Assessing bone and antler exploitation at Riparo Mochi (Balzi Rossi, Italy): implications for the characterization of the Aurignacian in South-western Europe. *J. Archaeol. Sci.* 61, 59–77.
- Teyssandier, N., Bon, F., Bordes, J.-G., 2010. Within projectile range: some thoughts on the appearance of the Aurignacian in Europe. *J. Anthropol. Res.* 66, 209–229.
- Théry-Parisot, I., Costamagno, S., Brugal, J.-P., Fosse, P., Guilbert, R., 2004. The use of bone as fuel during the Palaeolithic, experimental study of bone combustible properties. In: Mulville, J., Outram, A.K. (Eds.), *Proceedings of the 9th Conference of the International Council of Archaeozoology*. Presented at the Zooarchaeology of Eats, Oils, Milk and Dairying, Durham. Oxbow Books, Oxford, pp. 50–59.
- Thieme, H., 1997. Lower Palaeolithic hunting spears from Germany. *Nature* 385, 807–810.
- Tomasso, A., Porraz, G., 2016. Hunter-gatherer mobility and embedded raw-material procurement strategies in the Mediterranean Upper Paleolithic. *Evol. Anthropol.* 25, 164–174.
- Valensi, P., 2009. Evolution des peuplements mammaliens en Europe méditerranéenne occidentale durant le Pléistocène moyen et supérieur. Un exemple régional : les Alpes du Sud françaises et italiennes. *Quaternaire* 20, 551–567.
- Valensi, P., Psathi, E., 2004. Faunal exploitation during the Middle Palaeolithic in south-eastern France and north-western Italy. *Int. J. Osteoarchaeol.* 14, 256–272.
- Vallerand, A., Negrino, F., Riel-Salvatore, J., 2024. *Homo sapiens* and Neanderthal use of space at Riparo Bombrini (Liguria, Italy). *J. Archaeol. Method Theory* 30, 1292–1332.
- van Klinken, G.J., 1999. Bone collagen quality indicators for palaeodietary and radiocarbon measurements. *J. Archaeol. Sci.* 26, 687–695.
- Vehik, S.C., 1977. Bone fragments and bone grease manufacturing: a review of their archaeological use and potential. *Plains Anthropol.* 22, 169–182.
- Vidal-Cordasco, M., Terlato, G., Ocio, D., Marín-Arroyo, A.B., 2023. Neanderthal coexistence with *Homo sapiens* in Europe was affected by herbivore carrying capacity. *Sci. Adv.* 9, eadi4099.
- Vigne, J.-D., 2006. Découpe du cerf (*Cervus elaphus*) au Mésolithique moyen, à Noyen-sur-Seine (Seine-et-Marne): analyses tracéologique et expérimentale. *Rev. paléobiol.* 24, 69.
- Villa, P., Mahieu, E., 1991. Breakage patterns of human long bones. *J. Hum. Evol.* 21, 27–48.
- Welker, F., Soressi, M., Rendu, W., Hublin, J.-J., Collins, M., 2015. Using ZooMS to identify fragmentary bone from the late Middle/Early Upper Palaeolithic sequence of Les Cottes, France. *J. Archaeol. Sci.* 54, 279–286.
- White, M., Pettitt, P., Schreve, D., 2016. Shoot first, ask questions later: interpretative narratives of Neanderthal hunting. *Quatern. Sci. Rev.* 140, 1–20.
- Wißing, C., Rougier, H., Baumann, C., Comeyne, A., Crevecoeur, I., Drucker, D.G., Gaudzinski-Windheuser, S., Germonpré, M., Gómez-Olivencia, A., Krause, J., Mathies, T., Naito, Y.I., Posth, C., Semal, P., Street, M., Boucherens, H., 2019. Stable isotopes reveal patterns of diet and mobility in the last Neanderthals and first modern humans in Europe. *Sci. Rep.* 9, 4433.
- Yravedra, J., Gómez-Castanedo, A., Aramendi-Picado, J., Montes-Barquín, R., Sanguino-González, J., 2016. Neanderthal and *Homo sapiens* subsistence strategies in the Cantabrian region of northern Spain. *Archaeol. Anthropol. Sci.* 8, 779–803.
- Zeder, M.A., 2006. Reconciling rates of long bone fusion and tooth eruption and wear in sheep (*Ovis*) and goat (*Capra*). In: Ruscillo, D. (Ed.), *Recent Advances in Ageing and Sexing Animal Bones*. Oxbow Books, Oxford, pp. 87–118.
- Zilhão, J., Angelucci, D.E., Igreja, M.A., Arnold, L.J., Badal, E., Callapez, P., Cardoso, J.L., d’Errico, F., Daura, J., Demuro, M., Deschamps, M., Dupont, C., Gabriel, S., Hoffmann, D.L., Legoinha, P., Matias, H., Soares, A.M.M., Nabais, M., Portela, P., Queffelec, A., Rodrigues, F., Souto, P., 2020. Last Interglacial Iberian Neanderthals as fisher-hunter-gatherers. *Science* 367, eaaz7943.

Special Issue: Integrating ZooMS and Zooarchaeology: Methodological Challenges and Interpretive Potentials

Supplement 1: Comparing Neanderthal and Modern Human Subsistence at Riparo Bombrini: An Integrated Archaeozoological, Multivariate Taphonomic, and ZooMS Analysis

GENEVIÈVE POTHIER-BOUCHARD*

Département des sciences historiques, Pavillon Charles-De Koninck, Université Laval, 1030 avenue des Sciences-Humaines, G1V 0A6, Québec; and, Département d'anthropologie, Pavillon Lionel-Groulx, Université de Montréal, 3150 Jean-Brillant, H3T 1N8, Montréal, CANADA; genevieve.pothier-bouchard.1@ulaval.ca

ARIANE BURKE

Département d'anthropologie, Pavillon Lionel-Groulx, Université de Montréal, 3150 Jean-Brillant, H3T 1N8, Montréal, CANADA; a.burke@umontreal.ca

MICHAEL BUCKLEY

Manchester Institute of Biotechnology, School of Natural Sciences, University of Manchester, 131 Princess Street, M1 7DN, Manchester, UNITED KINGDOM; M.Buckley@manchester.ac.uk

FABIO NEGRINO

Dipartimento di Antichità, Filosofia, Storia, Università degli Studi di Genova, Via Balbi, 2, 16126, Genova, ITALY; fabio.negrino@unige.it

AMÉLIE VALLERAND

Département d'anthropologie, Pavillon Lionel-Groulx, Université de Montréal, 3150 Jean-Brillant, H3T 1N8, Montréal, CANADA; amelie.vallerand@umontreal.ca

ANA B. MARÍN-ARROYO

Departamento Ciencias Históricas, Universidad de Cantabria, Avda. de los Castros 52, 39005, Santander, SPAIN; anabelen.marin@unican.es

JULIEN RIEL-SALVATORE

Département d'anthropologie, Pavillon Lionel-Groulx, Université de Montréal, 3150 Jean-Brillant, H3T 1N8, Montréal, CANADA; julien.riel-salvatore@umontreal.ca

SUPPLEMENT 1

This supplementary material includes: Supplementary Text, Supplementary Figures 1–4, and Supplementary Tables 1–19.

NEANDERTHAL AND MODERN HUMAN OCCUPATIONS AT RIPARO BOMBRINI

Riparo Bombrini is a rockshelter located in the Balzi Rossi site complex in northwest Italy. The site corresponds to the easternmost edge of a long talus slope opening in front of the cave complex (SI Figure 1). Due to its small size, Riparo Bombrini is one of the few sites to have been overlooked by the coarse excavations of the 19th century when the Balzi Rossi became famous for their multiple Upper Paleolithic burial discoveries (see Formicola and Holt 2015). Émile Rivière first acknowledged the site in 1871 during the construction of the Genoa-Marseille railway, which truncated the talus in front of Grotta del Caviglione,

exposing rich archaeological deposits and simultaneously destroying the northern part of Riparo Bombrini. While E. Rivière excavated through the transitional deposits without singling them out in Grotta del Caviglione, his disinterest in the adjacent rockshelters (Riparo Mochi forming the western edge of the Caviglione talus slope) fortunately preserved their transitional deposits.

Consequently, the long stratigraphic sequence documented at Riparo Mochi is today considered a reference point to discuss the early arrival of modern humans in Mediterranean Europe (Douka et al. 2012; Kuhn and Stiner 1998). A dating program during the 2002–2005 excavations at Riparo Bombrini also helped assess the general strati-

graphic correspondence between Riparo Mochi and Riparo Bombrini (Holt et al. 2019), indicating that these rockshelters were part of a large talus slope opening in front of Grotta del Caviglione that was recurrently occupied during the Late Pleistocene.

Along with Riparo Mochi, Riparo Bombrini is thus the only site in the Balzi Rossi to have preserved *in situ* Late Mousterian and Proto-Aurignacian deposits to have been excavated with modern methods. The site was excavated in three phases, using fine-grained methods to systematically document the spatial coordinates of artifacts and water sieving. A first limited excavation in 1976 of six square meters outside the shelter itself yielded rich Late Mousterian and Proto-Aurignacian deposits and a deciduous *Homo sapiens* incisor in level A2 (Benazzi et al. 2015; Formicola 1989; Vicino 1984). Subsequently, more extensive controlled excavations from 2002–2005 were organized on both sides of the 1976 excavation pit to investigate the nature and the chronology of the transitional deposit across the entire site (Higham et al. 2014; Holt et al. 2019; Riel-Salvatore et al. 2013). Finally, two of the authors (FN and JRS) conducted excavations on a more extensive area inside the dripline from 2015–2019 to clarify the formation history of the site and the nature and temporality of the Middle-Upper Paleolithic transition at Riparo Bombrini (Negrino and Riel-Salvatore 2018; Riel-Salvatore and Negrino 2018a, b; Riel-Salvatore et al. 2022b).

The robust chronological framework for the transitional occupations of Riparo Bombrini reveals very recent Mousterian levels (i.e., M7-MS) dated 45–42 ky cal BP. The top Mousterian Levels MS1 and MS2 (grouped into one Level MS for the purpose of this study), while not directly dated yet, have been correlated to a period covering the cold interval between the GI-11 and GI-10 (~43–42 ky cal BP) with the overlying Proto-Aurignacian levels (A1 and A2) dated between 42–36ky cal BP, acting as *terminus ante quem* (Benazzi et al. 2015; Holt et al. 2019) (SI Figure 2).

Paleoenvironmental data, including sedimentology, palynology, and microfauna, indicate overall temperate conditions and forested environments in Mousterian Levels M7-M1 (Arobba and Caramiello 2009; Holt et al. 2019). The overlying Levels MS1-MS2 document a climatic shift towards increasingly cold and arid conditions. These levels (hereafter merged in one “Level MS” as they are undifferentiated outside the dripline) correspond to a 30CM to 40cm thick orangish clayey loam that incorporates large limestone blocks resulting from the partial collapse of the rockshelter roof as a result of increasing freeze-thaw action. Level MS is also characterized by some episodes of water action, as shown by an erosion channel against the rockshelter wall. This level, also called the ‘Semi-Sterile Mousterian,’ corresponds to the last traces of Neanderthal occupations on the site and shows much lower densities of artifacts than the underlying Mousterian deposits. It is probable they correspond to Level H at Riparo Mochi, though it is less clearly defined there (Alhaique et al. 2000; Bietti and Negrino 2007; Kuhn and Stiner 1992; Perez et al. 2022).

The climatic deterioration continues in the Proto-Aurignacian levels, which began accumulating under much colder and more arid conditions. Levels A1 and A2 form a yellowish clayey loam deposit varying from 10cm to 30cm thick each. Both levels contain rich assemblages with overlying “cuvette-type” hearths and discarding features. Slightly different environmental conditions are recorded between Level A2 and Level A1. The latter corresponds to somewhat more temperate and mesic conditions than the first, which is chronologically associated with the cold phase of the Heinrich Event 4 (HE 4). These paleoenvironmental data are also visible in the macrofaunal record with more abundant warm-adapted taxa (i.e., Suidae and Cervidae) in the Mousterian Levels M7-M1 and increasing abundance of cold-adapted taxa (i.e., Bovinae, Equidae, and Caprinae) in Levels MS, A2, and A1 (Holt et al. 2019; Pothier-Bouchard et al. 2020). The continuous presence of red deer in all levels also agrees with the refugium biogeographical settings of Liguria during the Upper Pleistocene, characterized by mixed open and forested environments during colder phases (Riel-Salvatore et al. 2022). Furthermore, anthracological data indicate that human groups primarily collected wood from shrubby species available close to the site in both Mousterian and Proto-Aurignacian levels (Holt et al. 2019).

Previous research on the transitional levels at Riparo Bombrini (i.e., MS, A2, A1) highlighted contrasting occupations of the site. Level MS was described as “semi-sterile” in the past to emphasize the paucity of artifacts in this thick deposit (Bietti and Negrino 2007). Nevertheless, new data from the 2015–2019 excavations has considerably increased the artifactual and faunal corpus, allowing updating behavioral and biogeographical interpretations of this level. The most striking new evidence includes the discovery of an ovoidal combustion area directly underlying the Proto-Aurignacian hearths close to the rockshelter back wall. The combustion area is also associated with most artifacts recorded in Level MS and the highest density of red ochre recovered throughout the Mousterian levels. The renewed analyses warrant testing the hypothesis that Level MS corresponds to Neanderthals’ adaption to an ecologically stable micro-refugium manifested by increased mobility in a restrained territory. This “hyperlocal” adaptation is also marked by opportunistic lithic exploitation of locally sourced raw material (<5km) and the exclusive use of very flexible knapping methods (i.e., Discoid technology).

The Proto-Aurignacian Levels A1 and A2 are both rich in artifacts and faunal remains. The combination of different factors, including the density of archaeological remains, the overlying cuvette-type hearths and possible trash pits, and the curated bladelet-based technology, was interpreted to indicate the continuous occupation of the site by modern humans in both levels. Furthermore, variability between the two levels in the bladelet production and lithic resource management was interpreted as the manifestation of changing mobility strategies (*sensu* Binford) in response to paleoclimatic instability. The colder Level A2 was thus associated with logistical mobility strategies, whereas the

slightly warmer Level A1 was characterized with more residential strategies (Riel-Salvatore and Negrino 2018a). Our previous archaeozoological analysis showed stability in hunting strategies despite the mobility shift, attesting to the flexibility of modern humans' hunting technology (Pothier-Bouchard et al. 2020). Although general patterns of site organization and fuel management identified in the faunal record were associated with these changing land-use and mobility strategies, our previous analysis did not include assemblages from outside the dripline, which could have obscured crucial evidence about practices such as waste management and spatially segregated butchering activities.

THE FAUNAL ASSEMBLAGES OF RIPARO BOMBRINI

The 1976 salvage excavation was carried out with various degrees of resolution within the stratigraphy due to the limited time frame to finalize the work (Vicino 1984). Vicino thus recorded the Proto-Aurignacian levels (A1 and A2) using the most fine-grained methods available at the time, i.e., by excavating one square-meter units in 5cm thick arbitrary spits and individually plotting in three dimensions all artifacts, diagnostic bones, and non-diagnostic bones larger than ten centimeters. The sediments were also water-sieved on-site, providing fine-grained faunal assemblages. However, Vicino accelerated the excavation of the Mousterian levels, including Level MS, to reach the expected depth of the salvage excavation pit. His spits varied from 5cm to 10cm, and he reported having collected only the visible fragments while putting aside all the sediment spits by spits for future analysis, therefore, not systematically recording smaller, non-diagnostic artifacts and skeletal remains. These sediments are currently being water-sieved at the University of Genoa (Italy) under the supervision of F. Negrino and should bring better light to the taphonomic factors acting on the Mousterian faunal assemblages outside the rockshelter in the future. As for now, the Mousterian faunal assemblages from 1976 are characterized by larger diagnostic elements and a few bone fragments of varying sizes recovered during Vicino's fieldwork.

The team excavating the 2002–2005 deposits used similar methods to Vicino's original fine-grained fieldwork. The square-meter units were excavated with arbitrary spits of 5cm thick, and diagnostic artifacts were systematically piece-plotted three-dimensionally along with faunal remains larger than 5cm. All sediments were also water-screened using 2cm mesh sieves, and small fractions of bones, ochre, lithic, shells, and others were retained for analysis (Riel-Salvatore et al. 2013). The 2015–2019 deposits started with the same excavation methods as before. From 2016, we operated with small changes to maximize the taphonomic resolution of the faunal remains by subdividing the square-meter units into 50cm subunits, piece-plotting bone fragments larger than 2cm, and collecting the smaller fraction (>1cm) of coprolites from the sieve. The team also acquired a total station in 2018 that allowed georeferencing the site and the different structures on the site and digitiz-

ing the spatial distribution of all piece-plotted finds from 1976 and later within the ArcGIS software.

The faunal remains recovered during the 1976 salvage excavation were never formally analyzed and published. However, this collection accounts for a large part of the faunal remains recovered on the site, especially regarding the Proto-Aurignacian levels. This four-square-meter area is located outside the rockshelter, delimited by the dripline, and comprises thicker deposits than those excavated inside the rockshelter (SI Figure 2). Consequently, these faunal assemblages are of great interest to tackle the levels corresponding to the transition at Riparo Bombrini despite the varying degree of recovery resolution. Furthermore, the 1976 collections are the only ones that document both Proto-Aurignacian layers and the Semi-Sterile Mousterian outside the rockshelter (see Pothier-Bouchard et al. 2020 for discussion).

A. Arellano (Musée de Préhistoire Régionale de Menton, France) examined the faunal remains recovered during the 2002–2005 archaeological campaigns. Her work provided the first portrait of the vertebrate taxonomic composition on the site (Holt et al. 2019; Riel-Salvatore and Negrino 2018a b). This first formal archaeozoological analysis focused on the faunal remains recovered from a five-square-meter trench (square-meter units A1 to EE1) and helped to discuss the paleoenvironmental implications of the macrofauna in the two Proto-Aurignacian and nine Mousterian levels along with other paleoenvironmental data (Holt et al. 2019; Riel-Salvatore and Negrino 2018b; Riel-Salvatore et al. 2013). However, the high level of skeletal fragmentation on the site (more than 93% of the fauna was described as measuring less than 2cm) severely hindered morphological taxonomic identification.

In 2015, therefore, we initiated an exhaustive archaeozoological and taphonomic study with integrated ZooMS to re-analyze the 2002–2005 faunal remains along with the implementation of newly recovered remains as part of the new five-year excavation project at Riparo Bombrini. Our main objectives were to examine site formation processes and provide a detailed picture of the variability of the hunting and subsistence strategies employed by human groups occupying Riparo Bombrini during the Middle-Upper Paleolithic transition. Our first archaeozoological study focused on a sample of the Proto-Aurignacian assemblages recovered from 2002–2005, 2015, and 2016. This study revealed the importance of integrating ZooMS as a tool for countering poor taxonomic identification due to fragmentation. It also highlighted the differential state of preservation of the faunal remains on the site, which needs to be factored into the interpretation of the assemblages (Pothier-Bouchard et al. 2019, 2020).

STABLE ISOTOPIC ANALYSIS

Carbon and nitrogen stable isotope measurements were calibrated to the VPDB and AIR (atmospheric N₂) scales, and quality checked using in-house standards IA-R068 (soy protein, accepted values: $\delta^{13}\text{C} = -25.22\text{‰VPDB}$ and $\delta^{15}\text{N} = 0.99\text{‰AIR}$), IA-R038 (L-alanine, accepted values:

$\delta^{13}\text{C}=-24.99\%$ VPDB and $\delta^{15}\text{N}=-0.65\%$ AIR), IA-R069 (tuna protein, accepted values: $\delta^{13}\text{C}=-18.88\%$ VPDB and $\delta^{15}\text{N}=11.60\%$ AIR), and a mixture of IAEA-C7 (oxalic acid, $\delta^{13}\text{C}=-14.48\%$ VPDB) and in-house standard IA-R046 (ammonium sulfate, $\delta^{15}\text{N}=22.04\%$ AIR). The accepted values of in-house standards were obtained via calibration against international reference materials: IA-R068, IA-R038, and IA-R069 against IAEA-CH6 (sucrose, $\delta^{13}\text{C}=-10.449\%$ VPDB) and IAEA-N-1 (ammonium sulfate, $\delta^{15}\text{N}=0.40\%$ AIR). During the analysis of Axlor Bombrini samples, IA-R069 gave values of $\delta^{13}\text{C}=-18.90 \pm 0.04\%$ VPDB (1 SD, n=6) and $\delta^{15}\text{N}=-0.65 \pm 0.03\%$ AIR (1 SD, n=6). The average reproducibility of samples measured in duplicate was 0.04% for $\delta^{13}\text{C}$ and 0.01% for $\delta^{15}\text{N}$.

For sulfur stable isotope analysis, calibration to the VCDT (Vienna Cañon Diablo Troilite) scale and correction for ^{18}O contribution were conducted using in-house standards IA-R061 (barium sulfate, $\delta^{34}\text{S}=20.33\%$ VCDT), IA-R025 (barium sulfate, $\delta^{34}\text{S}=8.53\%$ VCDT), and IA-R026 (silver sulfide, $\delta^{34}\text{S}=3.96\%$ VCDT). Accepted values for these in-house standards were obtained by calibrating against international reference materials NBS-17 (barium sulfide, $\delta^{34}\text{S}=5.25\%$ VCDT) and IAEA-S-1 (silver sulfide, $\delta^{34}\text{S}=-0.30\%$ VCDT). IA-R061, IAEA-SO-5 (barium sulphate, $\delta^{34}\text{S}=20.3\%$ VCDT), IA-R068 (soy protein, $\delta^{34}\text{S}=5.25\%$ VCDT), and IA-R069 (tuna protein, $\delta^{34}\text{S}=18.91\%$ VCDT) were used as quality-control standards. The accepted values of IA-R068 and IA-R069 were obtained via calibration using the international reference materials NBS-17 and IAEA-SO-5. During the analysis of Axlor samples, the following values were obtained for the quality-control standards: IA-R061 $\delta^{34}\text{S}=20.32 \pm 0.08\%$ VCDT (1 SD, n=6), IAEA-SO-5 $\delta^{34}\text{S}=0.47 \pm 0.07\%$ VCDT (1 SD, n=2), IA-068 $\delta^{34}\text{S}=5.17 \pm 0.15\%$ VCDT (1 SD, n=4), and IA-R069 $\delta^{34}\text{S}=18.85 \pm 0.10\%$ VCDT (1 SD, n=4).

REFERENCES

Alhaique, F., 2000. Risultati preliminari dell'analisi dei resti faunistici rinvenuti nei livelli del Paleolitico superiore di Riparo Mochi (Balzi Rossi): scavi 1995–96. *Atti del 2*, 125–130.

Arobba, D., Caramiello, R., 2009. Analisi paleobotanica sui sedimenti del riparo Bombrini (Balzi Rossi, Ventimiglia). *Bull. Musée Anthropol. Préhist. Monaco* 49, 41–48.

Bar-Oz, G., Dayan, T., 2003. Testing the use of multivariate inter-site taphonomic comparisons: the faunal analysis of Hefzibah in its Epipalaeolithic cultural context. *J. Archaeol. Sci.* 30, 885–900.

Bar-Oz, G., Munro, N.D., 2004. Beyond cautionary tales: a multivariate taphonomic approach for resolving equifinality in zooarchaeological studies. *J. Taphonomy* 2, 201–220.

Behrensmeyer, A.K., 1991. Terrestrial Vertebrate Accumulations. In: Allison, P.A., Briggs, A.W. (Eds.), *Taphonomy: Releasing the Data Locked in the Fossil Record*. Plenum, New York, pp. 291–335.

Benazzi, S., Slon, V., Talamo, S., Negrino, F., Peresani, M.,

Bailey, S.E., Sawyer, S., Panetta, D., Vicino, G., Starnini, E., Mannino, M.A., Salvadori, P.A., Meyer, M., Pääbo, S., Hublin, J.-J., 2015. The makers of the Protoaurignacian and implications for Neandertal extinction. *Science* 348, 793–796.

Bietti, A., Negrino, F., 2007. “Transitional” industries from Neandertals to Anatomically Modern Humans in continental Italy: present state of knowledge. In: Riel-Salvatore, J., Clark, G.A. (Eds.), *New Approaches to the Study of Early Upper Paleolithic ‘Transitional’ Industries in Western Eurasia*. British Archaeological Reports International Series 1620, Oxford, pp. 41–60.

Brown, S., Higham, T., Slon, V., Pääbo, S., Meyer, M., Douka, K., Brock, F., Comeskey, D., Procopio, N., Shunkov, M., Derevianko, A., Buckley, M., 2016. Identification of a new hominin bone from Denisova Cave, Siberia using collagen fingerprinting and mitochondrial DNA analysis. *Sci. Rep.* 6, 23559.

Brugal, J.-P., Fourvel, J.-B., Fosse, P., 2017. Premières observations sur les guildes de carnivores de la grotte de l’Observatoire. *Bull. Musée Anthropol. Préhist. Monaco* 57, 47–60.

Buckley, M., Collins, M., Thomas-Oates, J., Wilson, J.C., 2009. Species identification by analysis of bone collagen using matrix-assisted laser desorption/ionisation time-of-flight mass spectrometry. *Rapid Commun. Mass Spectrom.* 23, 3843–3854.

Buckley, M., Harvey, V.L., Chamberlain, A.T., 2017. Species identification and decay assessment of Late Pleistocene fragmentary vertebrate remains from Pin Hole Cave (Creswell Crags, UK) using collagen fingerprinting. *Boreas* 46, 402–411.

Buckley, M., Larkin, N.R., Collins, M.J., 2011. Mammoth and mastodon collagen sequences; survival and utility. *Geochim. Cosmochim. Acta* 75, 2007–2016.

Buckley, M., Whitcher Kansa, S., Howard, S., Campbell, S., Thomas-Oates, J., Collins, M., 2010. Distinguishing between archaeological sheep and goat bones using a single collagen peptide. *J. Archaeol. Sci.* 37, 13–20.

Costamagno, S., 2013. Bone grease rendering in Mousterian contexts: the case of Noisetier Cave (Fréchet-Aure, Hautes-Pyrénées, France). In: Clark, J.L., Speth, J.D. (Eds.), *Zooarchaeology and Modern Human Origins: Human Hunting Behavior during the Later Pleistocene*. Vertebrate Paleobiology and Paleoanthropology. Springer Netherlands, Dordrecht, pp. 209–225.

Daujeard, C., Fernandes, P., Guadelli, J.-L., Moncel, M.-H., Santagata, C., Raynal, J.-P., 2012. Neanderthal subsistence strategies in Southeastern France between the plains of the Rhone Valley and the mid-mountains of the Massif Central (MIS 7 to MIS 3). *Quatern. Int.* 252, 32–47.

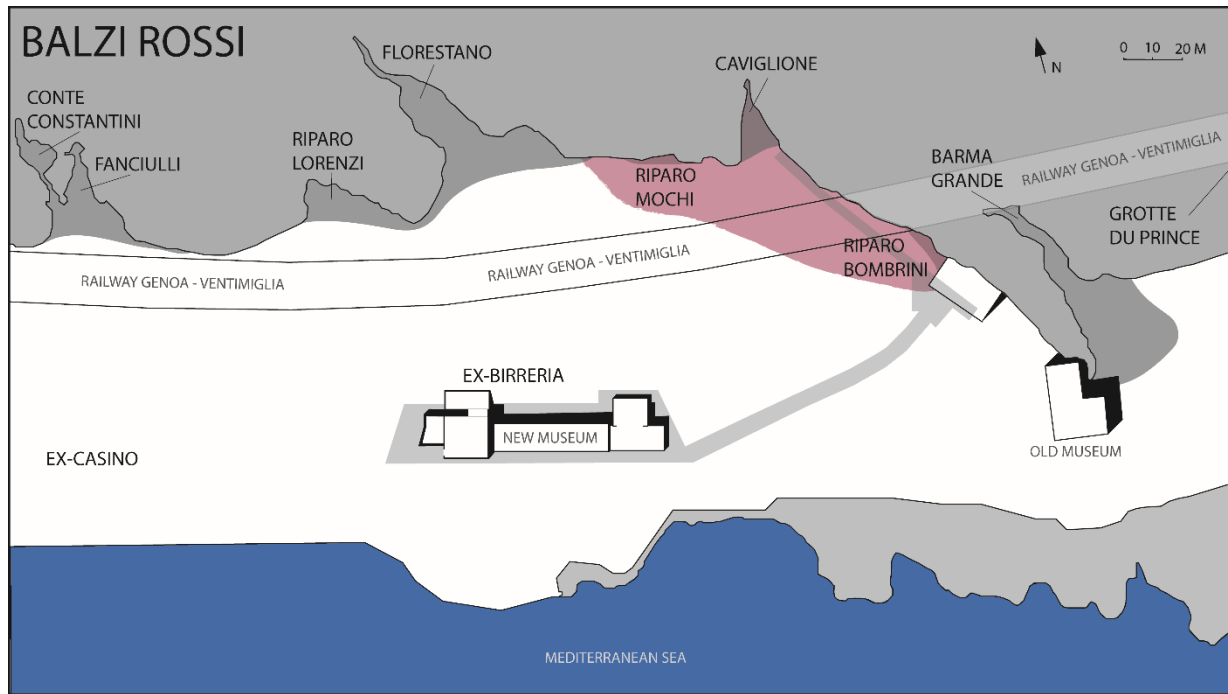
Daujeard, C., Moncel, M.-H., 2010. On Neanderthal subsistence strategies and land use: a regional focus on the Rhone Valley area in southeastern France. *J. Anthropol. Archaeol.* 29, 368–391.

Douka, K., Grimaldi, S., Boschian, G., del Lucchese, A., Higham, T.F., 2012. A new chronostratigraphic frame-

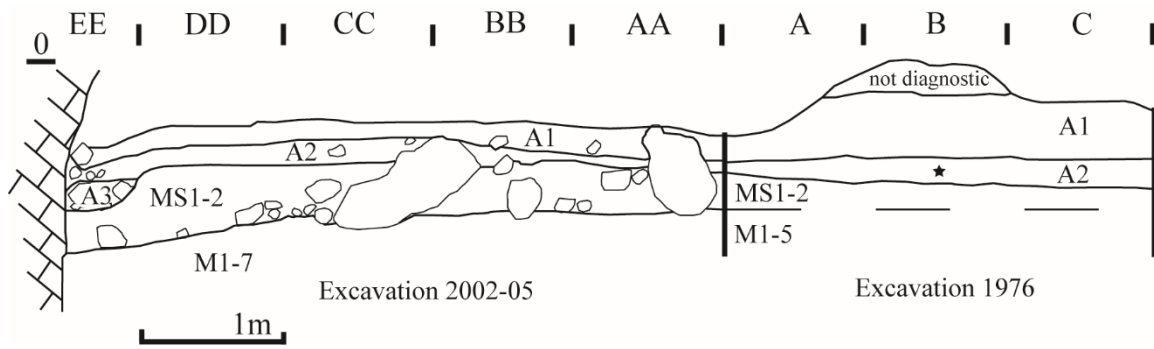
- work for the Upper Palaeolithic of Riparo Mochi (Italy). *J. Hum. Evol.* 62, 286–299.
- Formicola, V., 1989. Early Aurignacian deciduous incisor from Riparo Bombrini at Balzi Rossi (Grimaldi, Italy). *Riv. antropol.* 67, 287–292.
- Formicola, V., Holt, B.M., 2015. Tall guys and fat ladies: Grimaldi's Upper Paleolithic burials and figurines in an historical perspective. *J. Anthropol. Sci.* 93, 71–88.
- Higham, J., Thomas, Douka, K., Wood, R., Ramsey, C.B., Brock, F., Basell, L., Camps, M., Arrizabalaga, A., Bae, J., Barroso-Ruiz, C., Bergman, C., Boitard, C., Boscatto, P., Caparrós, M., Conard, N.J., Draily, C., Froment, A., Galván, B., Gambassini, P., Garcia-Moreno, A., Grimaldi, S., Haesaerts, P., Holt, B., Iriarte-Chiapusso, M.-J., Jelinek, A., Jordá Pardo, J.F., Maíllo-Fernández, J.-M., Marom, A., Maroto, J., Menéndez, M., Metz, L., Morin, E., Moroni, A., Negrino, F., Panagopoulou, E., Peresani, M., Pirson, S., de la Rasilla, M., Riel-Salvatore, J., Ronchitelli, A., Santamaria, D., Semal, P., Slimak, L., Soler, J., Soler, N., Villaluenga, A., Pinhasi, R., Jacobi, R., 2014. The timing and spatiotemporal patterning of Neanderthal disappearance. *Nature* 512, 306–309.
- Holt, B., Negrino, F., Riel-Salvatore, J., Formicola, V., Arelano, A., Arobba, D., Boschian, G., Churchill, S.E., Cristiani, E., Di Canzio, E., Vicino, G., 2019. The Middle-Upper Paleolithic transition in northwest Italy: new evidence from Riparo Bombrini (Balzi Rossi, Liguria, Italy). *Quatern. Int.* 508, 142–152.
- Kuhn, S., Stiner, M.C., 1992. New research on Riparo Mochi, Balzi Rossi (Liguria): preliminary results. *Quatern. Nova* 2, 77–90.
- Kuhn, S.L., Stiner, M.C., 1998. The earliest Aurignacian of Riparo Mochi (Liguria, Italy). *Curr. Anthropol.* 39, S175–S189.
- Marean, C.W., 1991. Measuring the post-depositional destruction of bone in archaeological assemblages. *J. Archaeol. Sci.* 18, 677–694.
- Morin, E., 2008. Evidence for declines in human population densities during the early Upper Paleolithic in western Europe. *Proc. Nat. Acad. Sci. U.S.A.* 105, 48–53.
- Morin, E., 2012. Reassessing Paleolithic Subsistence: The Neanderthal and Modern Human Foragers of Saint-Césaire. Cambridge University Press, New York.
- Morin, E., Soulier, M.-C., 2017. New criteria for the archaeological identification of bone grease processing. *Am. Antiq.* 82, 96–122.
- Negrino, F., Riel-Salvatore, J., 2018. From Neanderthals to Anatomically Modern Humans in Liguria (Italy): the current state of knowledge. In: Borgia, V., Cristiani, E. (Eds.), *Palaeolithic Italy. Advanced Studies on Early Human Adaptations in the Apennine Peninsula*. Sidestone Press Academics, Leiden, Netherlands, pp. 159–180.
- Outram, A.K., 2001. A new approach to identifying bone marrow and grease exploitation: why the indeterminate fragments should not be ignored. *J. Archaeol. Sci.* 28, 401–410.
- Perez, A., Santaniello, F., Hohenstein, U.T., Grimaldi, S., 2022. The faunal assemblage from the Riparo Mochi site (Balzi Rossi): new insights on the Mousterian-Aurignacian human-environment relationship. *Alp. Mediterr. Quatern.* 35, 135–155.
- Pike-Tay, A., Cabrera Valdés, V., Bernaldo de Quirós, F., 1999. Seasonal variations of the Middle-Upper Paleolithic transition at El Castillo, Cueva Morín and El Pendo (Cantabria, Spain). *J. Hum. Evol.* 36, 283–317.
- Pothier-Bouchard, G., Riel-Salvatore, J., Negrino, F., Buckley, M., 2020. Archaeozoological, taphonomic and ZooMS insights into The Protoaurignacian faunal record from Riparo Bombrini. *Quatern. Int.* 551, 243–263.
- Psathi, E., 2003. Les sites moustériens de la Caverna delle Fate et de l'Arma delle Manie (Liguria, Italie) : Étude paléontologique et archéozoologique des faunes des grands mammifères. Muséum national d'histoire naturelle, Paris.
- Raynal J.-P., Fernandes P., Santagata C., Guadelli J.-L., Moncel M.-H., Daujeard C., Pape J.-M.L., Bindon P., Fiore I., Beux M.L.-L., Tagliacozzo A., Seret H., Liabeuf R., Servant L., Aulanier M., 2013. Land-use strategies, related tool-kits and social organization of Lower and Middle Palaeolithic groups in the south-east of the Massif Central, France. *Quartär* 60, 29–59.
- Rendu, W., Renou, S., Soulier, M.-C., Rigaud, S., Roussel, M., Soressi, M., 2019. Subsistence strategy changes during the Middle to Upper Paleolithic transition reveals specific adaptations of human populations to their environment. *Sci. Rep.* 9, 15817.
- Riel-Salvatore, J., Ludeke, I.C., Negrino, F., Holt, B.M., 2013. A spatial analysis of the late Mousterian levels of Riparo Bombrini (Balzi Rossi, Italy). *Can. J. Archaeol.* 37, 70–92.
- Riel-Salvatore, J., Negrino, F., 2018a. Proto-Aurignacian Lithic Technology, Mobility, and Human Niche Construction: A Case Study from Riparo Bombrini, Italy. In: Robinson, E., Sellet, F. (Eds.), *Lithic Technological Organization and Paleoenvironmental Change, Studies in Human Ecology and Adaptation*. Springer, Cham, pp. 163–187.
- Riel-Salvatore, J., Negrino, F., 2018b. Human adaptations to climatic change in Liguria across the Middle-Upper Paleolithic transition. *J. Quatern. Sci.* 3, 313–322.
- Riel-Salvatore, J., Negrino, F., Pothier Bouchard, Geneviève, Vallerand, A., Costa, S., Benazzi, S., 2022. The “Semi-Sterile Mousterian” of Riparo Bombrini: Evidence of a Late-Lasting Neanderthal Refugium in Liguria? *J. Quatern. Sci.* 37, 268–282.
- Romandini, M., Crezzini, J., Bortolini, E., Boscatto, P., Boschian, F., Carrera, L., Nannini, N., Tagliacozzo, A., Terlato, G., Arrighi, S., Badino, F., Figus, C., Lugli, F., Marciani, G., Oxilia, G., Moroni, A., Negrino, F., Peresani, M., Riel-Salvatore, J., Ronchitelli, A., Spinapolice, E.E., Benazzi, S., 2020. Macromammal and bird assemblages across the late Middle to Upper Palaeolithic transition in Italy: an extended zooarchaeological review. *Quatern. Int.* 551, 188–223.
- Silvestrini, S., Lugli, F., Romandini, M., Real, C., Sommel-

- la, E., Salviati, E., Arrighi, S., Bortolini, E., Figus, C., Higgins, O.A., Marciani, G., Oxilia, G., Delpiano, D., Vazzana, A., Piperno, M., Crescenzi, C., Campiglia, P., Collina, C., Peresani, M., Spinapolice, E.E., Benazzi, S., 2022. Integrating ZooMS and zooarchaeology: new data from the Uluzzian levels of Uluzzo C Rock Shelter, Rocca San Sebastiano cave and Riparo del Broion. *PLoS One* 17, e0275614.
- Soulier, M.-C., 2013. Entre alimentaire et technique : l'exploitation animale aux débuts du paléolithique supérieur : stratégies de subsistance et chaînes opératoires de traitement du gibier à Isturitz, La Quina aval, Roc-de-Combe et Les Abeilles. Ph.D. Dissertation. Université Toulouse le Mirail - Toulouse II.
- Valensi, P., Psathi, E., 2004. Faunal Exploitation during the Middle Palaeolithic in south-eastern France and north-western Italy. *Int. J. Osteoarchaeol.* 14, 256–272.
- Valensi, P., Psathi, E., Lacombat, F., 2004. Le cerf elaphe dans les sites du paleolithique moyen du sud-est de la France et de Ligurie. Interets biostratigraphique, environnemental et taphonomique. In: Haesaerts, P., Damblon, F. (Eds.), *Acts of the XIVth UISPP Congress, 2-8 September 2001. Presented at the Section 3 Paléocologie/Paleoecology*, Archaeopress. Université de Liège, Belgique, pp. 97–106.
- Vehik, S.C., 1977. Bone Fragments and Bone Grease Manufacturing: A Review of their Archaeological Use and Potential. *Plains Anthropol.* 22, 169–182.
- Vicino, G., 1984. Lo scavo paleolitico al Riparo Bombrini (Balzi Rossi di Grimaldi, Ventimiglia). *Riv. Ing. Intem.* 39, 1–10.

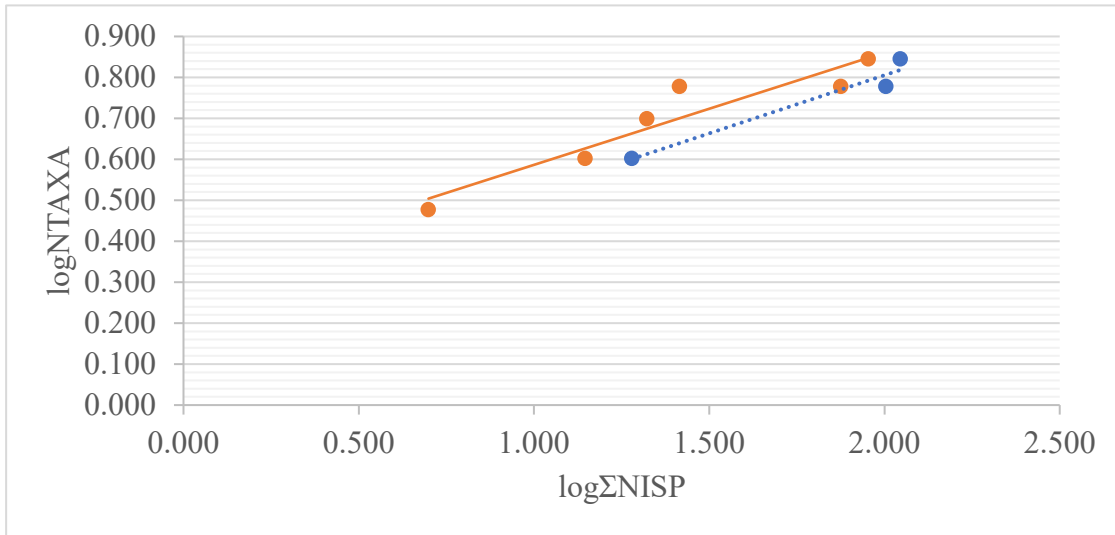
SUPPLEMENTARY FIGURES



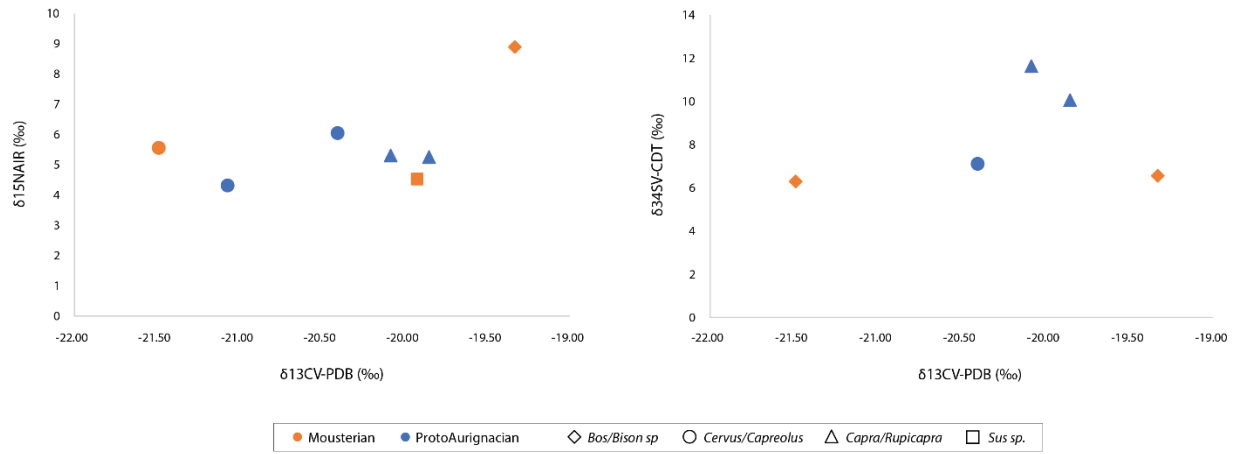
SI Figure 1. Cartographic sketch of the Balzi Rossi showing the talus connecting Riparo Mochi, Grotta del Caviglione, and Riparo Bombrini (in red).



SI Figure 2. Stratigraphic sequence of Riparo Bombrini based on the 2002–2005 and 1976 excavations. The star shows the position of the human incisor in Level A2 (modified from Benazzi et al. 2015).



SI Figure 3. Relationship between the $\log(10)$ of NTAXA and Σ NISP of ungulates per assemblages (blue, Levels A1, A2, and MS) and sub-assemblages divided by areas (orange, Levels A1, A2, and MS, inside and outside). Dashed, best-fit regression line, $r=0.96$, $p=0.14$; solid, best-fit regression line, $r=0.94$, $p=0.0048$.



SI Figure 4. Bone collagen $\delta^{13}\text{C}$ and $\delta^{15}\text{N}$ values (left) and $\delta^{13}\text{C}$ and $\delta^{34}\text{S}$ values (right) of Bos/Bison, Cervus/Capreolus, Capra/Rupicapra, and Sus sp. from different Mousterian and Proto-Aurignacian levels at Riparo Bombrini.

SUPPLEMENTARY TABLES

SI Table 1. Proto-Aurignacian and Mousterian sites with documented faunal assemblages in the Liguro-Provençal arc, along with other relevant faunal assemblages in neighboring regions.

Site	Associated technocomplex	References
Liguro-Provençal arc		
Riparo Bombrini	M, PA	Holt et al. (2019) Pothier-Bouchard et al. (2020)
Riparo Mochi	M, PA	Alhaique (2000)
Grotte de l'Observatoire	M, PA	Perez et al. (2022)
Caverna delle Fate	M	Romandini (2017)
Arma delle Manie	M	Brugal, Fourvel, and Fosse (2017)
Madonna dell'Arma	M	Valensi and Psathi (2004)
Santa Lucia Superiore	M	Valensi, Psathi, and Lacombat (2004)
Via San Francesco	M	Psathi (2003)
Comparative sites in Italy		
Rio Secco	M	<i>Ibid.</i>
Fumane	M, UL, PA	Romandini et al. (2020)
Bernardino	M	<i>Ibid.</i>
Broion	UL	<i>Ibid.</i>
Cala	M, UL, PA	<i>Ibid.</i>
Castelcivita	M, UL, PA	<i>Ibid.</i>
Cavallo	M, UL	<i>Ibid.</i>
Oscurusciuto	M	<i>Ibid.</i>
Comparative sites in France		
Les Cottés	PA	<i>Ibid.</i>
Saint-Césaire	PA	Rendu et al. (2019)
El Castillo	PA	Morin (2008; 2012)
Le Piage	PA	Pike-Tay et al. (1999)
Gatzarria	PA	Soulier (2013)
Les Abeilles	PA	Soulier (2013)
Payre	M	Soulier (2013; 2014)
Abri des Pêcheurs	M	Daujeard and Moncel (2010)
Balazuc	M	Daujeard et al. (2012)
Baume-Vallée	M	Raynal et al. (2013)
Abri du Maras	M	<i>Ibid.</i>
Sainte-Anne I	M	<i>Ibid.</i>

Baume d'Oullins	M	Daujeard and Moncel (2010) Daujeard et al. (2012)
Figuier	M	<i>Ibid.</i>
Ranc Pointu 2	M	<i>Ibid.</i>
Saint-Marcel	M	<i>Ibid.</i>
Baume Flandin	M	<i>Ibid.</i>
Baume des Peyrards	M	<i>Ibid.</i>

SI Table 2. Peptide markers used in ZooMS identifications. Buckley et al. (2009, 2010, 2011, 2017), and Brown et al. (2016).

Taxa	2t85(A)	2t43(B)	2t45(C)	2t69(D)	1t66/67	2t41/42(E)	1t55/56(F)	2t67(G)	2t76
Herbivores									
<i>Bos/Bison</i>	1208.6	1427.7	1580.8	2131.1	N/A	N/A	2853.4	3033.4	
<i>Capra</i>	1196.6	1427.7	1580.8	2131.1	N/A	N/A	2883.4	3093.4	
<i>Cervus/Dama</i>	1196.6	1427.7	1550.8	2131.1	N/A	N/A	2883.4	3033.4	
<i>Capreolus</i>	1196.6	1427.7	1550.8	2131.1	N/A	N/A	2883.4	3059.4	
<i>Coelodonta/Diceros</i>	1198.6	1453.7	1550.8	2145.1	N/A	N/A	2869.4	2999.4	
<i>Equus</i>	1198.6	1427.7	1550.8	2145.1	N/A	N/A	2883.4	2999.4	
<i>Mammuthus</i>	N/A	1453.7	1579.8	2115.1	N/A	N/A	2853.4	3015.4	
<i>Ovibos</i>	1208.6	1427.7	1580.8	2131.1	N/A	N/A	2883.4	3033.4	
<i>Rangifer</i>	1166.6	1427.7	1580.8	2131.1	N/A	N/A	2883.4	3093.4	
<i>Rupicapra/Ovis</i>	1196.6	1427.7	1580.8	2131.1	N/A	N/A	2883.4	3033.4	
<i>Sus</i>	1196.6	1453.7	1550.8	2131.1	N/A	N/A	2883.3	3033.4	
Carnivores									
<i>Alopex</i>	1226.6	1453.7	1566.8	2131.1	N/A	N/A	2853.4	2999.4	1548.8
<i>Canis</i>	1226.6	1453.7	1566.8	2131.1	N/A	N/A	2853.4	2999.4	1576.8
<i>Crocuta</i>	1207.6	1453.7	1566.8	2147.1	2246.1	2808.3	2853.4	2999.4	
<i>Gulo/Mustela/Martes</i>	1235.6	1453.7	1566.8	2147.1	N/A	N/A	2853.4	2999.4	
<i>Homo</i>	1235.6	1477.8	1580.8	2115.1	N/A	2832.4	2885.4	2957.4+ 2959.4	
<i>Lutra</i>	1235.6	1453.7	1566.8	2147.1	N/A	N/A	2853.4	2973.4	
<i>Lynx</i>	1207.6	1453.7	1566.8	2163.1	N/A	N/A	2853.4	2999.4	
<i>Meles</i>	1235.6	1453.7	1566.8	2147.1	N/A	N/A	2853.4	2957.4	
<i>Panthera</i>	1207.6	1453.7	1566.8	2147.1	2216.1	2820.3	2853.4	2999.4	
<i>Ursus</i>	1233.7	1453.7	1566.8	2163.1	N/A	N/A	2853.4	2957.4	
<i>Vulpes</i>	1226.6	1437.7	1566.8	2131.1	N/A	N/A	2853.4	2999.4	1548.8
Lagomorphs									
<i>Oryctolagus</i>	1235.6	1453.7	1566.8	2129.1	N/A	2836.3	2883.4	2957.4	
<i>Lepus</i>	1235.6	1453.7	1566.8	2129.1	N/A	2808.3	2883.4	2957.4	
Rodents									
<i>Castor</i>	1193.6	1427.7	1576.8	2129.1	N/A	N/A	2883.4	2999.4	

SI Table 3. Sample information for bone collagen samples and Carbon, Nitrogen and Sulphur results.

c	Archaeo. Level	Species	Element	Iso Code	% Collagen	Nitrogen Content (%)	$\delta^{15}\text{NAIR}$ (‰)	Carbon Content (%)	$\delta^{13}\text{CV-PDB}$ (‰)	Sulfur Content (%)	$\delta^{34}\text{SV-CDT}$ (‰)	C:N	C:S	N:S
B1734	A1	<i>Cervus-Capreolus</i>	Humerus	BOM1	10.0	0.68	---	2.24	---	---	---	3.8		
B1736	A1	<i>Cervus-Capreolus</i>	Metacarpal	BOM2	3.1	1.52	4.31	4.60	-21.07	0.05	---	3.5	261.6	74.2
B1744	A1	<i>Cervus-Capreolus</i>	Metatarsal	BOM3	3.1	0.86	---	2.74	---	---	---	3.7		
B1749	A1	<i>Capra-Rupicapra</i>	femur/humerus	BOM4	2.9	2.38	5.25	6.67	-19.85	0.06	10.05	3.3	277.0	84.6
B1771	A1	<i>Cervus</i>	femur/humerus	BOM5	?	?	?	?	?	?	?			
B1930	A1	<i>Capra-Rupicapra</i>	cranium	BOM6	4.5	1.66	5.30	5.00	-20.08	0.06	11.63	3.5	224.4	63.6
B1956	A1	<i>Cervus</i>	temporal, rocher	BOM7	3.2	0.48	---	1.62	---	---	---	4.0		
B1983	A1	<i>Cervus</i>	Mandible	BOM8	11.3	0.48	---	1.68	---	---	---	4.1		
B2158	A2	<i>Capra</i>	Humerus	BOM9	1.7	0.44	---	1.83	---	---	---	4.8		
B2159	A2	<i>Sus</i>	Humerus	BOM10	0.0	-	-	-	-	-	-			
B2192	A2	<i>Cervus-Capreolus</i>	Metapodial	BOM11	4.1	2.7	6.0	7.4	-20.4	0.08	7.10	3.2	241.2	74.8
B1608	M3	<i>Cervus</i>	Tibia	BOM12	0.8	-	-	-	-	-	-			
B1625	M3	<i>Cervus</i>	Metatarsal	BOM13	2.0	4.08	5.56	11.27	-21.49	0.16	6.29	3.2	186.5	57.9
B1791	M4	<i>Sus</i>	Metapodial	BOM14	1.1	2.20	4.53	6.34	-19.92	0.03	---	3.4	588.1	174.5
B1804	M4	<i>Cervus</i>	Tibia	BOM15	3.8	1.56	3.94	5.02	-21.36	---	---	3.8		
B1872	M5	<i>Bos/Bison</i>	Metapodial	BOM16	3.1	15.61	8.89	41.31	-19.33	0.08	6.56	3.1	1398.4	452.8

SI Table 4. General taphonomic variables. The variables in italics were excluded from this study due to insufficient data.

Taphonomic variables	Description/ specifications
General assemblage data	Relevant archaeozoological values used to calculate various taphonomic variables
NSP	The total number of specimens for each assemblage
NISP	The number of identified specimens for each assemblage
NSP.Ib	The number of specimens of long bone shaft fragments (taxonomically identifiable and unidentifiable) for each assemblage
Quarry data	
Size of studied area (m ²)	Area size for each assemblage, measured in square meters
Deposit volume (m ³)	Volume of excavated sediments, measured in cubic meters
Density of piece-plotted artifacts (N/m ³)	Density of all piece-plotted artifacts (lithic, ochre, and shell) per cubic meter
Density of piece-plotted fauna (N/m ³)	Density of piece-plotted fauna per cubic meter
Density of bone fragments (NSP/m ³)	Density of piece-plotted fauna and sieve-recovered fauna per cubic meter
<i>Spatial arrangement (random vs preferred orientation)</i>	<i>Qualitative description of faunal remains' spatial arrangement as defined by Behrensmeier (1991)</i>
<i>Spatial arrangement (high dips vs horizontal)</i>	<i>Ibid.</i>
Spatial distribution of fauna (even, uneven, highly patchy)	<i>Ibid.</i>
Bone state of preservation	Describes the extent of bone damage
%identifiable before ZooMS (NSP)	Percentage of identifiable bones (NISP divided by NSP) before ZooMS identifications to illustrate the morphological state of preservation
%bone fragments <2 cm (NSP)	Percentage of bone fragments smaller than 2 centimeters indicating the extent of fragmentation
%ZooMS success (N ZooMS samples)	Percentage of successful ZooMS identification according to the total number of ZooMS samples after initial FTIR preselection)
Long bone damage (NSP.Ib)	Describes the intensity of natural and anthropic processes affecting each faunal assemblage, expressed as percentages of the NSP of the long bone shaft
%Abrasion stage 2 <	Percentage of long bone shafts with abrasion of stage 2 or higher
%Abrasion and polish	Percentage of long bone shafts with the combined abrasion and polished surfaces
%Concretion stage 2 <	Percentage of long bone shafts with concretion of stage 2 or higher
%manganese coloration stage 2 <	Percentage of long bone shafts with manganese coloration of stage 2 or higher
%Trampling	Percentage of long bone shafts with trampling
%Etching stage 2 <	Percentage of long bone shafts with etching of stage 2 or higher
%Carnivore gnawing	Percentage of long bone shafts with carnivore gnawing

%Weathering stage 2 <	Percentage of long bone shafts with weathering of stage 2 or higher
%Modern fractures	Percentage of long bone shafts with modern fractures
Mean FFI score of long bones	Average fresh fracture index score calculated for long bone shaft fragments

Long bone damage resulting from anthropic processes (NSP.Ib)

% fresh fracture angles
%Burned (carbonized + calcined)
% anthropic percussion
% cut marks
N percussion flakes
N bone manufacture

Examines long bone shaft surface damages specific to human activity, expressed as percentages of the NSP.Ib or the absolute number of specimens

Percentage of long bone shafts with fresh fracture angles
Percentage of burned bones according to the NSP of long bone shaft fragments
Absolute number of anthropic percussion marks
Absolute number of cut marks on bone surfaces
Absolute number of percussion flakes
Absolute number of manufacture marks on bones

SI Table 5. Taphonomic variables for investigating bone completeness and fragmentation. The variables in *italics* were excluded from this study due to insufficient data.

Taphonomic variables	Description/specifications
General data	Relevant archaeozoological values used to calculate the different taphonomic variables
NISP small game	Number of identified specimens of small game for each assemblage
NISP large game	Number of identified specimens of large game for each assemblage
NISP.lb small game	Number of identified specimens of long bone shaft fragments of small game for each assemblage
NISP.lb large game	Number of identified specimens of long bone shaft fragments of large game for each assemblage
Density-mediated attrition	Investigating how density-mediated factors influence each assemblage's bone fragmentation patterns
<i>Spearman's rs: bone survivorship (%MAU) vs. Bone density (BMD)</i>	<i>The qualitative expression (significant vs insignificant) of Spearman's correlation (rs) of %MAU vs BMD</i>
Ratio NISP of small game : NISP of large game	The ratio of the NISP of the small game to the NISP of the large game
<i>Proximal: distal humeri and tibiae</i>	See Bar-Oz and Munro (2004)
Ratio N compact bones : N long bones and axial elements	The ratio of small compact bones (tarsals, carpals, sesamoids, and phalanx) to long bones and axial elements (excluding loose teeth), replacing "Proximal: distal humeri and tibiae"
Ratio N appendicular cancellous bone : N appendicular cortical bone	The ratio of the number of appendicular cancellous bones to appendicular cortical bones to assess overall survivorship of less dense cancellous bones, replacing "Proximal: distal humeri and tibiae"
Post-depositional in situ attrition	Evaluating the attritional factors affecting skeletal remains after deposition
<i>%completeness of astragalus</i>	<i>Completeness index of compact bones as defined by Marean (1991, p. 685): (Σ of the estimated fraction of each specimen of tarsal or carpal/total number of specimens) * 100</i>
<i>%completeness of central fourth tarsal</i>	<i>Ibid.</i>
%completeness of tarsals and carpals	Index of the combined tarsals and carpals ff. Bar-Oz and Dayan (2003)
%completeness of phalanx1 and phalanx2	Completeness index of the combined first and second phalanx (i.e., the most abundant small compact ones at Bombrini), replacing the %completeness of astragalus and tarsals with phalanx
Tooth: cranial elements (MNE)	The ratio of teeth to cranial bones to directly measure <i>in situ</i> attrition since teeth are expected to survive post-depositional attrition better than the cranium (Stiner 1991 in Bar-Oz and Dayan 2003)
Pre-depositional fragmentation	Evaluating the attritional factors affecting skeletal remains before deposition
Mean FFI (NISP.lb)	The mean FFI according to the NISP of bone shaft fragments

SI Table 6. Taphonomic variables for investigating bone accumulation. The variables in italics were excluded from this study due to insufficient data.

Taphonomic variables	Description/specifications
General data	The relevant general archaeozoological data is specified in the preceding multivariate tables
Carnivore action	Investigating the role of carnivores in the accumulation of the faunal remains
% carnivores (NISP)	Percentage of the combined medium and large carnivores
N Coprolites	Absolute number (N) of coprolites
Density of coprolites (g/m ³)	Density of coprolites in grams per cubic meter
% long bone shafts >1/2 circumference	Percentage of long bone shaft fragments preserving half or more of their complete circumference, more common in carnivore faunal accumulations than in human ones.
% carnivore alteration	Percentage of carnivore alteration (gnawing, teeth punctures, digestion)
% head skeletal remains	Percentage of head skeletal remains (teeth, cranium, and mandible) as carnivore accumulations in caves and rockshelters tend to be head-dominated.
Human action	Evaluating the role of humans in the accumulation of the faunal remainss
% percussion marks	Percentage of percussion marks (the most abundant anthropic bone surface alteration at Riparo Bombrini)
% burned bones	Percentage of burned bones
<i>Skeletal portion representation (dominated by a specific portion or not)</i>	<i>Qualitative expression of skeletal portion representation</i>

SI Table 7. Taphonomic variables for investigating carcass processing. The variables in italics were excluded from this study due to insufficient data.

Taphonomic variables	Description
General data	Relevant archaeozoological values used to calculate the different taphonomic variables in addition to the ones specified in the preceding multivariate tables
NISP cervid size 2/3	
NISP.lb caprine	
NISP.lb Capreolus	
NISP.lb cervid size 2/3	
NISP.lb bovine	
NISP.lb equid	
Marrow extraction	Investigating differential carcass treatment between taxa
Mean FFI (NISP.lb of different taxa)	Mean FFI of long bone shaft fragments
% bone flakes (NISP of different taxa)	Percentage of bone flakes
% percussion marks (NISP of different taxa)	Percentage of percussion marks
Grease rendering	Variables based on the ethnoarchaeological and experimental observations on grease processing and grease rendering involving crushing and boiling the cancellous parts of post-cranial bones (Vehik, 1977; Outram, 2001; Costamagno, 2013; Morin and Soulier, 2017)
% cancellous unburned bones (NSP, NISP small and large games)	Percentage of unburned epiphyseal cancellous bones
% epiphysial cancellous unburned bones (NSP, NISP of small and large games)	Percentage of unburned cancellous bones
Bone fuel (NSP)	Investigating bone fuel through the general intensity of burning (1 and 2), the differential burning among bone type categories (2,3,4,5,6,7,8), and the intentional burning of epiphyses (9,10,11,12)
% burned* bones	(1) Percentage of carbonized bones
% calcined bones	(2) Percentage of calcined bones
% cranial unburned bones	(3) Percentage of unburned cranial bones
% cranial burned* bones	(4) Percentage of burned cranial bones
% axial post-cranial unburned bones	(5) Percentage of unburned axial post-cranial bones
% axial post-cranial burned* bones	(6) Percentage of burned axial post-cranial bones
% appendicular unburned bones	(7) Percentage of unburned appendicular bones
% appendicular burned* bones	(8) Percentage of burned appendicular bones
% cancellous bones	(9) Percentage of unburned cancellous bones
% cancellous burned* bones	(10) Percentage of burned cancellous bones
% cancellous calcined bones	(11) Percentage of calcined cancellous bones
% burned* long bone diaphysis fragments	(12) Percentage of burned long bone shaft fragments

*The burned category includes carbonized and calcined bones.

SI Table 9. Data on age, sex, and seasonality in Levels A1, A2, and MS. J=juvenile, A=prime aged adult, O=old.

Taxa	Area	Element	Age estimate	J	A	O	Sex	Season
Level A1								
Teeth								
<i>Cervus elaphus</i>	outside	maxillary with M2	2-3.5 years	n/a	1	n/a	n/a	n/a
<i>Cervus elaphus</i>	outside	indeter. molar maxillary	< 3 years	n/a	n/a	n/a	n/a	n/a
<i>Cervus elaphus</i>	outside	P2 maxillary	2-3 years	n/a	1	n/a	n/a	n/a
<i>Dama dama</i>	outside	indeter. molar maxillary	< 4 years	n/a	n/a	n/a	n/a	n/a
<i>Capra ibex</i>	outside	P3 maxillary	1-3 years	n/a	1	n/a	n/a	n/a
<i>Sus scrofa</i>	inside	indeter. premolar	>3 years	n/a	n/a	1	n/a	n/a
Bovidae size 1/2	inside	indeter. molar mandibular	n/a	n/a	1	n/a	n/a	n/a
Level A2								
Teeth								
<i>Cervus sp.</i>	outside	P4 mandibular	5-6.5 years	n/a	1	n/a	n/a	n/a
Cervidae size 2/3	inside	indeter. molar	n/a	n/a	1	n/a	n/a	n/a
Cervidae size 2/3	inside	P1 mandibular	2-3 years	n/a	1	n/a	n/a	n/a
<i>Capra ibex</i>	inside	indeter. molar	<4 years	n/a	n/a	n/a	n/a	n/a
<i>Bos/Bison sp.</i>	inside	indeter. molar	n/a	n/a	1	n/a	n/a	n/a
<i>Equus sp.</i>	outside	molar/premolar maxillary	<2 years	1	n/a	n/a	n/a	n/a
<i>Equus sp.</i>	outside	premolar mandibular	>10 years	n/a	n/a	1	n/a	n/a
<i>Equus sp.</i>	outside	M3 maxillary	1-2 years	1	n/a	n/a	n/a	n/a
Artiodactyla size 3/4	inside	indeter. molar	< 2 years	1	n/a	n/a	n/a	n/a
Bones								
Cervidae size 2/3	inside	antler	n/a	n/a	n/a	n/a	male	winter/ spring
<i>Bos/Bison sp.</i>	outside	radius prox. epiphysis	>3.5-4 years	n/a	1	n/a	n/a	n/a
Artiodactyla size 3/4	outside	indeter. rib	n/a	1	n/a	n/a	n/a	n/a
Artiodactyla size 3/4	outside	stylohyoid	n/a	n/a	1	n/a	n/a	n/a
Indeterminate	inside	long bone	fetal	n/a	n/a	n/a	n/a	winter/ spring
Level MS								
Teeth								
<i>Cervus elaphus</i>	outside	canine	2-4 years	n/a	1	n/a	male	n/a
<i>Capra ibex</i>	outside	M3 maxillary	3-4 years	n/a	1	n/a	n/a	n/a
<i>Capra ibex</i>	inside	M2 mandibular	1.5-2 years	n/a	1	n/a	n/a	n/a
<i>Capra ibex</i>	inside	P2 maxillary	8-10 years	n/a	n/a	1	n/a	n/a

<i>Equus</i> sp.	outside	I1 maxillary	3-9 years	n/a	1	n/a	n/a	n/a
<i>Ursus</i> sp.	inside	M1 maxillary	n/a	1	n/a	n/a	n/a	n/a
Carnivore size 3	inside	M1 mandibular	< 1 year	1	n/a	n/a	n/a	n/a
Carnivore size 3	inside	indeter. canine	< 1 year	1	n/a	n/a	n/a	n/a
Bones								
<i>Cervus</i> sp.	outside	Femur dist. epiphysis	2-4 years	n/a	1	n/a	n/a	n/a
<i>Cervus</i> sp.	outside	Rib 3-6 prox. epiphysis	n/a	n/a	1	n/a	n/a	n/a
Cervidae size 2/3	outside	Rib 3-6 prox. epiphysis	n/a	n/a	1	n/a	n/a	n/a
Cervidae size 2/3	outside	Rib 7-10	n/a	n/a	1	n/a	n/a	n/a
<i>Cervus</i> sp.	outside	Ulna prox. epiphysis	>2-7 years	n/a	1	n/a	n/a	n/a
Artiodactyla size 1/2	inside	tibia prox. epiphysis	<2 years	1	n/a	n/a	n/a	n/a

SI Table 10. Taxonomic identifications of the 438 ZooMS samples including their original morphological identifications.

Sample Number	Archaeo. Level	Taxonomic Identification					Final Identification
		Morphology	ZooMS Acid-soluble	ZooMS Acid-insoluble	RPC Acid-soluble	RPC Acid-insoluble	
B98	A2	Indeterminate	<i>Capra</i>	<i>Capra</i>	n/a	n/a	<i>Capra</i>
B99	A2	Indeterminate	<i>Bos/Bison</i>	<i>Bos/Bison</i>	n/a	n/a	<i>Bos/Bison</i>
B114	A2	Indeterminate	Poor collagen	n/a	n/a	n/a	Indeterminate
B118	A2	Indeterminate	<i>Cervus/Capreolus</i>	n/a	Ungulate	n/a	Cervidae
B123	A2	Indeterminate	Poor collagen	n/a	n/a	n/a	Indeterminate
B124	A2	Indeterminate	Poor collagen	n/a	n/a	n/a	Indeterminate
B125	A2	Indeterminate	<i>Cervus</i>	n/a	n/a	n/a	<i>Cervus</i>
B127	A2	Indeterminate	<i>Equus</i>	n/a	n/a	n/a	<i>Equus</i>
B129	A2	Indeterminate	Poor collagen	n/a	n/a	n/a	Indeterminate
B135	A2	Indeterminate	Poor collagen	n/a	n/a	n/a	Indeterminate
B145	A2	Indeterminate	<i>Cervus</i>	n/a	n/a	n/a	<i>Cervus</i>
B147	A2	Indeterminate	<i>Bos/Bison</i>	n/a	n/a	n/a	<i>Bos/Bison</i>
B150	A2	Indeterminate	<i>Cervus</i>	n/a	n/a	n/a	<i>Cervus</i>
B153	A2	Indeterminate	<i>Cervus/Capreolus</i>	n/a	n/a	n/a	Cervidae
B154	A2	Indeterminate	<i>Capreolus</i>	n/a	<i>Cervus/Capreolus</i>	n/a	<i>Capreolus</i>
B155	A2	Indeterminate	Poor collagen	n/a	n/a	n/a	Indeterminate

B164	A2	Indeterminate	Poor collagen	n/a	n/a	n/a	Indeterminate
B165	A2	Indeterminate	Poor collagen	n/a	n/a	n/a	Indeterminate
B166	A2	Indeterminate	<i>Cervus/Capreolus</i>	n/a	<i>Cervus/Capreolus</i>	n/a	Cervidae
B181	A2	Indeterminate	Poor collagen	n/a	n/a	n/a	Indeterminate
B182	A1	Indeterminate	Poor collagen	n/a	n/a	n/a	Indeterminate
B191	A2	Indeterminate	Ungulate	n/a	n/a	n/a	Ungulate
B192	A2	Indeterminate	Poor collagen	n/a	n/a	n/a	Indeterminate
B194	A2	Indeterminate	Poor collagen	n/a	n/a	n/a	Indeterminate
B195	A2	Indeterminate	Poor collagen	n/a	n/a	n/a	Indeterminate
B198	A2	Indeterminate	Poor collagen	n/a	n/a	n/a	Indeterminate
B199	A2	Indeterminate	<i>Cervus</i>	n/a	n/a	n/a	<i>Cervus</i>
B200	A1	Indeterminate	Poor collagen	n/a	n/a	n/a	Indeterminate
B201	A1	Indeterminate	Poor collagen	n/a	n/a	n/a	Indeterminate
B204	A1	Indeterminate	Poor collagen	n/a	n/a	n/a	Indeterminate
B205	A1	Indeterminate	Poor collagen	n/a	n/a	n/a	Indeterminate
B207	A1	Indeterminate	Poor collagen	n/a	n/a	n/a	Indeterminate
B208	A1	Indeterminate	Poor collagen	n/a	n/a	n/a	Indeterminate
B211	A1	Indeterminate	Poor collagen	n/a	n/a	n/a	Indeterminate

B212	A1	Indeterminate	Poor collagen	n/a	n/a	n/a	Indeterminate
B215	A1	Indeterminate	Poor collagen	n/a	n/a	n/a	Indeterminate
B216	A1	Indeterminate	Poor collagen	n/a	n/a	n/a	Indeterminate
B217	A1	Indeterminate	Poor collagen	n/a	n/a	n/a	Indeterminate
B218	A1	Indeterminate	Poor collagen	n/a	n/a	n/a	Indeterminate
B223	A1	Indeterminate	Poor collagen	n/a	n/a	n/a	Indeterminate
B224	A1	Indeterminate	Poor collagen	n/a	n/a	n/a	Indeterminate
B225	A1	Indeterminate	Poor collagen	n/a	n/a	n/a	Indeterminate
B228	A2	Indeterminate	Poor collagen	n/a	n/a	n/a	Indeterminate
B229	A2	Indeterminate	Poor collagen	n/a	n/a	n/a	Indeterminate
B230	A2	Indeterminate	Poor collagen	n/a	n/a	n/a	Indeterminate
B231	A2	Indeterminate	Poor collagen	n/a	n/a	n/a	Indeterminate
B232	A2	Indeterminate	Poor collagen	n/a	n/a	n/a	Indeterminate
B233	A2	Indeterminate	Poor collagen	n/a	n/a	n/a	Indeterminate
B234	A2	Indeterminate	Poor collagen	n/a	n/a	n/a	Indeterminate
B235	A2	Indeterminate	Poor collagen	n/a	n/a	n/a	Indeterminate
B236	A2	Indeterminate	Poor collagen	n/a	n/a	n/a	Indeterminate

B237	A2	Indeterminate	Poor collagen	n/a	n/a	n/a	Indeterminate
B238	A2	Indeterminate	Poor collagen	n/a	n/a	n/a	Indeterminate
B239	A2	Indeterminate	<i>Cervus/Capreolus</i>	n/a	n/a	n/a	Cervidae
B264	A2	Indeterminate	Poor collagen	n/a	n/a	n/a	Indeterminate
B269	A2	Indeterminate	<i>Cervus</i>	n/a	n/a	n/a	<i>Cervus</i>
B296	A2	Indeterminate	Poor collagen	n/a	n/a	n/a	Indeterminate
B299	A2	Indeterminate	Poor collagen	n/a	n/a	n/a	Indeterminate
B304	A2	Indeterminate	<i>Cervus/Capreolus</i>	n/a	n/a	n/a	Cervidae
B306	A2	Indeterminate	Poor collagen	n/a	n/a	n/a	Indeterminate
B307	A2	Indeterminate	<i>Capra/Rangifer</i>	n/a	n/a	n/a	<i>Capra</i>
B308	A2	Indeterminate	Poor collagen	n/a	n/a	n/a	Indeterminate
B309	A2	Indeterminate	Poor collagen	n/a	n/a	n/a	Indeterminate
B310	A2	Indeterminate	Poor collagen	n/a	n/a	n/a	Indeterminate
B330	A2	Indeterminate	<i>Cervus</i>	n/a	n/a	n/a	<i>Cervus</i>
B365	A2	Indeterminate	Poor collagen	n/a	n/a	n/a	Indeterminate
B385	A1	Indeterminate	Poor collagen	n/a	n/a	n/a	Indeterminate
B386	A1	Indeterminate	Poor collagen	n/a	n/a	n/a	Indeterminate
B390	A1	Indeterminate	Poor collagen	n/a	n/a	n/a	Indeterminate

B393	A1	Indeterminate	Poor collagen	n/a	n/a	n/a	Indeterminate
B399	A2	Indeterminate	Poor collagen	n/a	n/a	n/a	Indeterminate
B407	A2	Indeterminate	Poor collagen	n/a	n/a	n/a	Indeterminate
B408	A2	Indeterminate	Poor collagen	n/a	n/a	n/a	Indeterminate
B409	A2	Indeterminate	Poor collagen	n/a	n/a	n/a	Indeterminate
B473	A2	Indeterminate	Poor collagen	n/a	n/a	n/a	Indeterminate
B474	A2	Indeterminate	Poor collagen	n/a	n/a	n/a	Indeterminate
B475	A2	Indeterminate	Poor collagen	n/a	n/a	n/a	Indeterminate
B476	A2	Indeterminate	Poor collagen	n/a	n/a	n/a	Indeterminate
B487	A2	Indeterminate	Poor collagen	n/a	n/a	n/a	Indeterminate
B489	A2	Indeterminate	Poor collagen	n/a	n/a	n/a	Indeterminate
B491	A2	Indeterminate	Poor collagen	n/a	n/a	n/a	Indeterminate
B492	A2	Indeterminate	Poor collagen	n/a	n/a	n/a	Indeterminate
B493	A2	Indeterminate	Poor collagen	n/a	n/a	n/a	Indeterminate
B500	A2	Indeterminate	Poor collagen	n/a	n/a	n/a	Indeterminate
B501	A2	Indeterminate	Poor collagen	n/a	n/a	n/a	Indeterminate
B502	A2	Indeterminate	Poor collagen	n/a	n/a	n/a	Indeterminate

B510	A2	Indeterminate	Poor collagen	n/a	n/a	n/a	Indeterminate
B511	A2	Indeterminate	Poor collagen	n/a	n/a	n/a	Indeterminate
B512	A2	Indeterminate	Poor collagen	n/a	n/a	n/a	Indeterminate
B513	A2	Indeterminate	Poor collagen	n/a	n/a	n/a	Indeterminate
B514	A2	Indeterminate	Poor collagen	n/a	n/a	n/a	Indeterminate
B515	A2	Indeterminate	Poor collagen	n/a	n/a	n/a	Indeterminate
B516	A2	Indeterminate	Poor collagen	n/a	n/a	n/a	Indeterminate
B517	A2	Indeterminate	Poor collagen	n/a	n/a	n/a	Indeterminate
B794	A2	Indeterminate	Poor collagen	n/a	n/a	n/a	Indeterminate
B795	A2	Indeterminate	Poor collagen	n/a	n/a	n/a	Indeterminate
B796	A2	Indeterminate	Ungulate	n/a	n/a	n/a	Ungulate
B797	A2	Indeterminate	Poor collagen	n/a	n/a	n/a	Indeterminate
B799	A2	Indeterminate	Poor collagen	n/a	n/a	n/a	Indeterminate
B800	A2	Indeterminate	Poor collagen	n/a	n/a	n/a	Indeterminate
B801	A2	Indeterminate	Poor collagen	n/a	n/a	n/a	Indeterminate
B804	A2	Indeterminate	<i>Bos/Bison</i>	n/a	n/a	n/a	<i>Bos/Bison</i>
B805	A2	Indeterminate	Poor collagen	n/a	n/a	n/a	Indeterminate
B808	A2	Indeterminate	Poor collagen	n/a	n/a	n/a	Indeterminate

B809	A2	Indeterminate	Poor collagen	n/a	n/a	n/a	Indeterminate
B816	A2	Indeterminate	Poor collagen	n/a	n/a	n/a	Indeterminate
B833	A2	Indeterminate	Poor collagen	n/a	n/a	n/a	Indeterminate
B840	A2	Indeterminate	Poor collagen	n/a	n/a	n/a	Indeterminate
B850	A2	Indeterminate	Poor collagen	n/a	n/a	n/a	Indeterminate
B860	A2	Indeterminate	Poor collagen	n/a	n/a	n/a	Indeterminate
B863	A2	Indeterminate	Poor collagen	n/a	n/a	n/a	Indeterminate
B867	A2	Indeterminate	Poor collagen	n/a	n/a	n/a	Indeterminate
B870	A2	Indeterminate	Poor collagen	n/a	n/a	n/a	Indeterminate
B877	A2	Indeterminate	Poor collagen	n/a	n/a	n/a	Indeterminate
B881	A2	Indeterminate	Poor collagen	n/a	n/a	n/a	Indeterminate
B889	A2	Indeterminate	Poor collagen	n/a	n/a	n/a	Indeterminate
B891	A2	Indeterminate	Poor collagen	n/a	n/a	n/a	Indeterminate
B893	A2	Indeterminate	Poor collagen	n/a	n/a	n/a	Indeterminate
B896	A2	Indeterminate	Poor collagen	n/a	n/a	n/a	Indeterminate
B897	A2	Indeterminate	Poor collagen	n/a	n/a	n/a	Indeterminate
B898	A2	Indeterminate	Poor collagen	n/a	n/a	n/a	Indeterminate

B910	A2	Indeterminate	<i>Cervus</i>	n/a	n/a	n/a	<i>Cervus</i>
B911	A2	Indeterminate	<i>Bos/Bison</i>	n/a	n/a	n/a	<i>Bos/Bison</i>
B912	A2	Indeterminate	<i>Cervus</i>	n/a	n/a	n/a	<i>Cervus</i>
B926	A2	Indeterminate	Poor collagen	n/a	n/a	n/a	Indeterminate
B928	A2	Indeterminate	Poor collagen	n/a	n/a	n/a	Indeterminate
B929	A2	Indeterminate	Poor collagen	n/a	n/a	n/a	Indeterminate
B933	A2	Indeterminate	Poor collagen	n/a	n/a	n/a	Indeterminate
B935	A2	Indeterminate	Poor collagen	n/a	n/a	n/a	Indeterminate
B936	A2	Indeterminate	<i>Cervus/Capreolus</i>	n/a	<i>Cervus/Capreolus</i>	n/a	Cervidae
B938	A2	Indeterminate	Poor collagen	n/a	n/a	n/a	Indeterminate
B951	A2	Indeterminate	Poor collagen	n/a	n/a	n/a	Indeterminate
B952	A2	Indeterminate	Poor collagen	n/a	n/a	n/a	Indeterminate
B953	A2	Indeterminate	Poor collagen	n/a	n/a	n/a	Indeterminate
B954	A2	Indeterminate	Poor collagen	n/a	n/a	n/a	Indeterminate
B955	A2	Indeterminate	Poor collagen	n/a	n/a	n/a	Indeterminate
B959	A2	Indeterminate	Poor collagen	n/a	n/a	n/a	<i>Indeterminate</i>
B960	A2	Indeterminate	Poor collagen	n/a	n/a	n/a	Indeterminate
B968	A2	Indeterminate	<i>Cervus</i>	n/a	n/a	n/a	<i>Cervus</i>

B975	A2	Indeterminate	Poor collagen	n/a	n/a	n/a	Indeterminate
B976	A2	Indeterminate	Poor collagen	n/a	n/a	n/a	Indeterminate
B977	A2	Indeterminate	Poor collagen	n/a	n/a	n/a	Indeterminate
B979	A2	Indeterminate	Poor collagen	n/a	n/a	n/a	Indeterminate
B983	A2	Ungulate	Poor collagen	n/a	n/a	n/a	Ungulate
B984	A2	Indeterminate	Poor collagen	n/a	n/a	n/a	Indeterminate
B985	A2	Indeterminate	Poor collagen	n/a	n/a	n/a	Indeterminate
B989	A2	Indeterminate	Poor collagen	n/a	n/a	n/a	Indeterminate
B990	A2	Indeterminate	Poor collagen	n/a	n/a	n/a	Indeterminate
B992	A2	Indeterminate	Poor collagen	n/a	n/a	n/a	Indeterminate
B994	A2	Indeterminate	Poor collagen	n/a	n/a	n/a	Indeterminate
B995	A2	Indeterminate	Poor collagen	n/a	n/a	n/a	Indeterminate
B1004	A1	Ungulate	Poor collagen	n/a	n/a	n/a	Ungulate
B1005	A1	Indeterminate	<i>Cervus/Capreolus</i>	n/a	<i>Cervus</i>	n/a	<i>Cervus</i>
B1006	A1	Indeterminate	Ungulate	n/a	n/a	n/a	Ungulate
B1008	A1	Indeterminate	<i>Bos/Bison</i>	n/a	n/a	n/a	<i>Bos/Bison</i>
B1010	A1	Indeterminate	<i>Bos/Bison</i>	n/a	n/a	n/a	<i>Bos/Bison</i>
B1011	A1	Indeterminate	<i>Bos/Bison</i>	n/a	n/a	n/a	<i>Bos/Bison</i>
B1012	A1	Indeterminate	<i>Capra</i>	n/a	n/a	n/a	<i>Capra</i>

B1013	A1	Indeterminate	Poor collagen	n/a	n/a	n/a	Indeterminate
B1017	A1	Indeterminate	<i>Cervus</i>	n/a	n/a	n/a	<i>Cervus</i>
B1028	A1	Indeterminate	Poor collagen	n/a	n/a	n/a	Indeterminate
B1030	A1	Indeterminate	Poor collagen	n/a	n/a	n/a	Indeterminate
B1031	A1	Indeterminate	Poor collagen	n/a	n/a	n/a	Indeterminate
B1032	A1	Indeterminate	Poor collagen	n/a	n/a	n/a	Indeterminate
B1033	A1	Indeterminate	Poor collagen	n/a	n/a	n/a	Indeterminate
B1034	A1	Indeterminate	Poor collagen	n/a	n/a	n/a	Indeterminate
B1042	A1	Indeterminate	Poor collagen	n/a	n/a	n/a	Indeterminate
B1043	A1	Indeterminate	Ungulate	n/a	n/a	n/a	Ungulate
B1044	A1	Indeterminate	Poor collagen	n/a	n/a	n/a	Indeterminate
B1045	A1	Indeterminate	Poor collagen	n/a	n/a	n/a	Indeterminate
B1046	A1	Indeterminate	<i>Cervus</i>	n/a	n/a	n/a	<i>Cervus</i>
B1048	A1	Indeterminate	<i>Bos/Bison</i>	n/a	n/a	n/a	<i>Bos/Bison</i>
B1049	A1	Indeterminate	<i>Bos/Bison</i>	n/a	n/a	n/a	<i>Bos/Bison</i>
B1050	A1	Indeterminate	<i>Bos/Bison</i>	n/a	n/a	n/a	<i>Bos/Bison</i>
B1053	A1	Indeterminate	Poor collagen	n/a	n/a	n/a	Indeterminate
B1055	A1	Indeterminate	<i>Bos/Bison</i>	n/a	n/a	n/a	<i>Bos/Bison</i>
B1056	A1	Indeterminate	<i>Equus</i>	n/a	n/a	n/a	<i>Equus</i>
B1057	A1	Indeterminate	Poor collagen	n/a	n/a	n/a	Indeterminate

B1058	A1	Indeterminate	<i>Capra</i>	n/a	n/a	n/a	<i>Capra</i>
B1059	A1	Indeterminate	<i>Cervus</i>	n/a	n/a	n/a	<i>Cervus</i>
B1060	A1	Indeterminate	<i>Bos/Bison</i>	n/a	n/a	n/a	<i>Bos/Bison</i>
B1062	A1	Indeterminate	Poor collagen	n/a	n/a	n/a	Indeterminate
B1070	A1	Indeterminate	<i>Cervus/Capreolus</i>	n/a	<i>Cervus/Capreolus</i>	n/a	Cervidae
B1075	A1	Indeterminate	Poor collagen	n/a	n/a	n/a	Indeterminate
B1076	A1	Indeterminate	<i>Cervus/Capreolus</i>	n/a	<i>Cervus/Capreolus</i>	n/a	Cervidae
B1077	A1	Indeterminate	Poor collagen	n/a	n/a	n/a	Indeterminate
B1079	A1	Indeterminate	Poor collagen	n/a	n/a	n/a	Indeterminate
B1080	A1	Indeterminate	Poor collagen	n/a	n/a	n/a	Indeterminate
B1084	A1	Indeterminate	<i>Cervus</i>	n/a	n/a	n/a	<i>Cervus</i>
B1086	A1	Indeterminate	Poor collagen	n/a	n/a	n/a	Indeterminate
B1089	A1	Indeterminate	<i>Cervus</i>	n/a	n/a	n/a	<i>Cervus</i>
B1090	A1	<i>Sus scrofa</i>	<i>Sus</i>	n/a	n/a	n/a	<i>Sus scrofa</i>
B1092	A1	Indeterminate	Poor collagen	n/a	n/a	n/a	Indeterminate
B1231	A1	Indeterminate	Poor collagen	n/a	n/a	n/a	Indeterminate
B1232	A1	Indeterminate	Poor collagen	n/a	n/a	n/a	Indeterminate
B1236	A1	Indeterminate	<i>Cervus/Capreolus</i>	n/a	Poor collagen	n/a	Cervidae
B1238	A1	Indeterminate	Poor collagen	n/a	n/a	n/a	Indeterminate

B1239	A1	Indeterminate	Poor collagen	n/a	n/a	n/a	Indeterminate
B1241	A1	Indeterminate	Poor collagen	n/a	n/a	n/a	Indeterminate
B1254	A2	Indeterminate	<i>Cervus/Capreolus</i>	n/a	<i>Cervus/Capreolus</i>	n/a	Cervidae
B1259	A2	Indeterminate	Poor collagen	n/a	n/a	n/a	Indeterminate
B1262	A2	Indeterminate	Poor collagen	n/a	n/a	n/a	Indeterminate
B1264	A2	Indeterminate	Poor collagen	n/a	n/a	n/a	Indeterminate
B1268	A2	<i>Sus scrofa</i>	Poor collagen	n/a	n/a	n/a	<i>Sus scrofa</i>
B1270	A2	Indeterminate	Poor collagen	n/a	n/a	n/a	Indeterminate
B1273	A2	Indeterminate	Poor collagen	n/a	n/a	n/a	Indeterminate
B1280	A2	Ungulate	Poor collagen	n/a	n/a	n/a	Artiodactyla
B1282	A2	Indeterminate	Poor collagen	n/a	n/a	n/a	Indeterminate
B1289	A2	Indeterminate	Poor collagen	n/a	n/a	n/a	Indeterminate
B1291	A2	Indeterminate	Poor collagen	n/a	n/a	n/a	Indeterminate
B1293	A2	Indeterminate	Poor collagen	n/a	n/a	n/a	Indeterminate
B1297	A2	Indeterminate	Mammal	n/a	n/a	n/a	Mammal
B1299	A2	Indeterminate	Poor collagen	n/a	n/a	n/a	Indeterminate
B1303	A1	Ungulate	Poor collagen	n/a	n/a	n/a	Ungulate

B1310	A1	Indeterminate	Poor collagen	n/a	n/a	n/a	Indeterminate
B1312	A1	Indeterminate	<i>Cervus/Capreolus</i>	n/a	<i>Cervus</i>	n/a	<i>Cervus</i>
B1317	A1	Indeterminate	Poor collagen	n/a	n/a	n/a	Indeterminate
B1319	A1	Indeterminate	Poor collagen	n/a	n/a	n/a	Indeterminate
B1336	A1	Indeterminate	Poor collagen	n/a	n/a	n/a	Indeterminate
B1337	A1	Indeterminate	Poor collagen	n/a	n/a	n/a	Indeterminate
B1345	A2	Indeterminate	Ungulate	n/a	n/a	n/a	Ungulate
B1346	A2	Indeterminate	Poor collagen	n/a	n/a	n/a	Indeterminate
B1348	A1	Indeterminate	Poor collagen	n/a	n/a	n/a	Indeterminate
B1352	A1	Indeterminate	Poor collagen	n/a	n/a	n/a	Indeterminate
B1353	A1	Indeterminate	Poor collagen	n/a	n/a	n/a	Indeterminate
B1355	A1	Indeterminate	Poor collagen	n/a	n/a	n/a	Indeterminate
B1356	A1	Indeterminate	Poor collagen	n/a	n/a	n/a	Indeterminate
B1357	A1	Indeterminate	Poor collagen	n/a	n/a	n/a	Indeterminate
B1358	A1	Indeterminate	Poor collagen	n/a	n/a	n/a	Indeterminate
B1362	A1	Indeterminate	<i>Cervus</i>	n/a	n/a	n/a	<i>Cervus</i>
B1364	A1	Indeterminate	Poor collagen	n/a	n/a	n/a	Indeterminate
B1366	A1	Indeterminate	<i>Cervus</i>	n/a	n/a	n/a	<i>Cervus</i>

B1370	A1	Indeterminate	Poor collagen	n/a	n/a	n/a	Indeterminate
B1379	A1	Indeterminate	Poor collagen	n/a	n/a	n/a	Indeterminate
B1441	A1	Indeterminate	Poor collagen	n/a	n/a	n/a	Indeterminate
B1442	A1	Indeterminate	Poor collagen	n/a	n/a	n/a	Indeterminate
B1468	MS	Indeterminate	Poor collagen	Poor collagen	n/a	n/a	Indeterminate
B1500	MS	Indeterminate	<i>Cervus/Capreolus</i>	n/a	<i>Cervus</i>	n/a	<i>Cervus</i>
B1591	MS	Indeterminate	Poor collagen	Poor collagen	n/a	n/a	Indeterminate
B1602	MS	Indeterminate	Poor collagen	<i>Cervus/Capreolus</i>	n/a	<i>Cervus/Capreolus</i>	Cervidae
B1699	A2	<i>Equus</i>	<i>Equus</i>	n/a	<i>Equus</i>	n/a	<i>Equus</i>
B1700	A1	<i>Capra ibex</i>	<i>Capra/Rupicapra</i>	n/a	<i>Capra/Rupicapra</i>	n/a	<i>Capra ibex</i>
B1701	MS	<i>Equus</i>	<i>Equus</i>	n/a	n/a	n/a	<i>Equus</i>
B1706	MS	Artiodactyla	Poor collagen	<i>Cervus/Capreolus</i>	n/a	n/a	Cervidae
B1707	MS	Ungulate	Ungulate	<i>Cervus</i>	n/a	<i>Cervus</i>	<i>cervus</i>
B1708	MS	Ungulate	<i>Cervus/Capreolus</i>	n/a	<i>Cervus</i>	n/a	<i>Cervus</i>
B1709	MS	Ungulate	<i>Cervus/Capreolus</i>	n/a	<i>Cervus</i>	n/a	<i>Cervus</i>
B1710	MS	Ungulate	<i>Cervus/Capreolus</i>	n/a	<i>Cervus</i>	n/a	<i>Cervus</i>
B1713	MS	Ungulate	Ungulate	<i>Cervus/Capreolus</i>	n/a	<i>Cervus</i>	<i>Cervus</i>
B1716	MS	Indeterminate	Poor collagen	<i>Sus</i>	n/a	n/a	<i>Sus</i>

B1717	A2	Indeterminate	Ungulate	<i>Bos/Bison</i>	n/a	<i>Bos/Bison</i>	<i>Bos/Bison</i>
B1718	A2	Indeterminate	Poor collagen	<i>Bos/Bison</i>	n/a	n/a	<i>Bos/Bison</i>
B1719	A2	Indeterminate	Ungulate	<i>Bos/Bison</i>	n/a	<i>Bos/Bison</i>	<i>Bos/Bison</i>
B1720	A2	Indeterminate	Ungulate	n/a	<i>Bos/Bison</i>	n/a	<i>Bos/Bison</i>
B1721	A2	Indeterminate	<i>Cervus/Capreolus</i>	n/a	<i>Cervus</i>	n/a	<i>Cervus</i>
B1722	A2	Indeterminate	<i>Bos/Bison</i>	n/a	n/a	n/a	<i>Bos/Bison</i>
B1725	A2	Artiodactyla	<i>Bos/Bison</i>	n/a	n/a	n/a	<i>Bos/Bison</i>
B1726	A1	Indeterminate	Poor collagen	n/a	n/a	n/a	Indeterminate
B1727	MS	Cervid	Ungulate	<i>Cervus</i>	n/a	<i>Cervus</i>	<i>Cervus</i>
B1728	MS	Artiodactyla	Poor collagen	<i>Cervus</i>	n/a	n/a	<i>Cervus</i>
B1729	MS	Artiodactyla	Poor collagen	Mammal	n/a	n/a	Artiodactyla
B1730	MS	Artiodactyla	Poor collagen	<i>Cervus/Capreolus</i>	n/a	n/a	Cervidae
B1731	A1	Artiodactyla	<i>Capra/Rupicapra</i>	n/a	<i>Capra/Rupicapra</i>	n/a	Caprinae
B1732	A1	Indeterminate	Poor collagen	Poor collagen	n/a	n/a	Indeterminate
B1733	MS	Artiodactyla	<i>Cervus/Capreolus</i>	n/a	<i>Cervus</i>	n/a	<i>Cervus</i>
B1734	A1	Artiodactyla	<i>Cervus/Capreolus</i>	<i>Cervus/Capreolus</i>	n/a	n/a	Cervidae
B1736	A1	Artiodactyla	<i>Cervus/Capreolus</i>	<i>Cervus</i>	<i>Cervus/Capreolus</i>	n/a	<i>Cervus</i>
B1738	A1	Indeterminate	<i>Bos/Bison</i>	n/a	n/a	n/a	<i>Bos/Bison</i>
B1741	A2	Indeterminate	<i>Bos/Bison</i>	n/a	n/a	n/a	<i>Bos/Bison</i>
B1744	A1	Artiodactyla	<i>Cervus/Capreolus</i>	n/a	<i>Cervus</i>	n/a	<i>Cervus</i>

B1745	A1	Indeterminate	Ungulate	n/a	Poor collagen	n/a	Ungulate
B1746	A1	Indeterminate	<i>Cervus/Capreolus</i>	n/a	<i>Cervus</i>	n/a	<i>Cervus</i>
B1747	A1	Artiodactyla	Poor collagen	<i>Cervus/Capreolus</i>	n/a	n/a	Cervidae
B1748	A1	Ungulate	<i>Cervus/Capreolus</i>	n/a	<i>Cervus</i>	n/a	Cervidae
B1749	A1	Artiodactyla	<i>Capra/Rupicapra</i>	n/a	<i>Capra</i>	n/a	<i>Capra</i>
B1751	A1	<i>Cervus/Dama</i>	<i>Cervus/Capreolus</i>	n/a	<i>Cervus</i>	n/a	<i>Cervus</i>
B1752	A1	Artiodactyla	Poor collagen	n/a	n/a	n/a	Artiodactyla
B1753	A1	Indeterminate	Ungulate	<i>Cervus/Capreolus</i>	n/a	<i>Cervus</i>	<i>Cervus</i>
B1755	A1	Indeterminate	<i>Cervus</i>	n/a	<i>Cervus</i>	n/a	<i>Cervus</i>
B1756	A1	Ungulate	<i>Bos/Bison</i>	n/a	n/a	n/a	<i>Bos/Bison</i>
B1758	A1	Indeterminate	<i>Bos/Bison</i>	n/a	n/a	n/a	<i>Bos/Bison</i>
B1759	A1	Indeterminate	<i>Capra/Rupicapra</i>	n/a	<i>Capra</i>	n/a	<i>Capra</i>
B1760	A1	Artiodactyla	<i>Cervus/Capreolus</i>	n/a	<i>Cervus</i>	n/a	<i>cervus</i>
B1762	A1	Indeterminate	<i>Cervus</i>	n/a	n/a	n/a	<i>Cervus</i>
B1763	A1	Indeterminate	<i>Cervus/Capreolus</i>	n/a	<i>Cervus</i>	n/a	<i>Cervus</i>
B1765	A1	Indeterminate	<i>Cervus</i>	n/a	n/a	n/a	<i>Cervus</i>
B1766	A1	Indeterminate	<i>Cervus</i>	n/a	n/a	n/a	<i>Cervus</i>
B1767	A1	Indeterminate	<i>Cervus</i>	n/a	n/a	n/a	<i>Cervus</i>
B1768	A1	Indeterminate	Poor collagen	<i>Cervus</i>	n/a	n/a	<i>Cervus</i>

B1769	A1	Indeterminate	<i>Cervus/Capreolus</i>	n/a	<i>Cervus</i>	n/a	<i>Cervus</i>
B1770	A1	Indeterminate	<i>Cervus</i>	n/a	n/a	n/a	<i>Cervus</i>
B1771	A1	Indeterminate	<i>Cervus</i>	n/a	n/a	n/a	<i>Cervus</i>
B1772	A1	Indeterminate	<i>Cervus/Capreolus</i>	<i>Cervus/Capreolus</i>	<i>Cervus</i>	n/a	<i>Cervus</i>
B1773	A1	Indeterminate	<i>Cervus</i>	n/a	n/a	n/a	<i>Cervus</i>
B1774	A1	Ungulate	<i>Cervus/Capreolus</i>	n/a	<i>Cervus</i>	n/a	<i>Cervus</i>
B1775	A1	Ungulate	Ungulate	<i>Cervus</i>	n/a	<i>Cervus</i>	<i>Cervus</i>
B1777	A1	Indeterminate	Poor collagen	<i>Equus</i>	n/a	n/a	<i>Equus</i>
B1781	MS	Artiodactyla	<i>Cervus/Capreolus</i>	n/a	<i>Cervus</i>	n/a	<i>Cervus</i>
B1923	A1	Indeterminate	Ungulate	<i>Capra</i>	<i>Capra</i>	<i>Capra</i>	<i>Capra</i>
B1924	A1	Indeterminate	<i>Capra/Rupicapra</i>	n/a	<i>Capra</i>	n/a	<i>Capra</i>
B1925	A1	Indeterminate	<i>Cervus/Capreolus</i>	n/a	<i>Cervus</i>	n/a	<i>Cervus</i>
B1927	A1	Indeterminate	Ungulate	<i>Cervus</i>	n/a	<i>Cervus</i>	<i>Cervus</i>
B1929	A1	Indeterminate	<i>Capra/Rupicapra</i>	n/a	<i>Capra</i>	n/a	Caprinae
B1930	A1	Indeterminate	<i>Capra/Rupicapra</i>	n/a	<i>Capra</i>	n/a	<i>Capra</i>
B1931	A1	Indeterminate	<i>Cervus/Capreolus</i>	n/a	<i>Cervus</i>	n/a	<i>Cervus</i>
B1933	A1	Indeterminate	<i>Capra/Rupicapra</i>	n/a	<i>Capra</i>	n/a	<i>Capra</i>
B1934	A1	Indeterminate	<i>Capra/Rupicapra</i>	n/a	<i>Capra</i>	n/a	<i>Capra</i>
B1935	A1	Indeterminate	<i>Capra/Rupicapra</i>	n/a	<i>Capra</i>	n/a	<i>Capra</i>

B1936	A1	Indeterminate	<i>Capra/Rangifer</i>	n/a	<i>Capra</i>	n/a	<i>Capra</i>
B1938	A1	Indeterminate	<i>Capra/Rangifer</i>	n/a	<i>Capra</i>	n/a	<i>Capra</i>
B1940	A1	Indeterminate	<i>Capra/Rupicapra</i>	n/a	n/a	n/a	Caprinae
B1942	A1	Indeterminate	<i>Cervus</i>	n/a	n/a	n/a	<i>Cervus</i>
B1944	A1	Indeterminate	<i>Cervus</i>	n/a	n/a	n/a	<i>Cervus</i>
B1954	A1	Indeterminate	Ungulate	<i>Capra</i>	n/a	<i>Capra</i>	<i>Capra</i>
B1956	A1	Indeterminate	<i>Cervus</i>	n/a	n/a	n/a	<i>Cervus</i>
B1957	A1	Indeterminate	Poor collagen	<i>Cervus</i>	n/a	n/a	<i>Cervus</i>
B1959	A1	Indeterminate	<i>Cervus</i>	n/a	n/a	n/a	<i>Cervus</i>
B1963	A1	Indeterminate	<i>Capra/Rupicapra</i>	n/a	<i>Capra</i>	n/a	<i>Capra</i>
B1964	A1	Indeterminate	<i>Capra/Rupicapra</i>	n/a	<i>Capra</i>	n/a	<i>Capra</i>
B1965	A1	Indeterminate	<i>Capra/Rupicapra</i>	n/a	<i>Capra</i>	n/a	<i>Capra</i>
B1966	A1	Indeterminate	<i>Cervus/Capreolus</i>	n/a	<i>Cervus</i>	n/a	<i>Cervus</i>
B1968	A1	Indeterminate	<i>Cervus</i>	n/a	n/a	n/a	<i>Cervus</i>
B1972	A1	Indeterminate	<i>Cervus</i>	n/a	n/a	n/a	<i>Cervus</i>
B1973	A1	Indeterminate	<i>Cervus</i>	n/a	n/a	n/a	<i>Cervus</i>
B1974	A1	Indeterminate	<i>Cervus/Capreolus</i>	n/a	<i>Capreolus</i>	n/a	<i>Capreolus</i>
B1976	A1	Indeterminate	<i>Cervus</i>	n/a	n/a	n/a	<i>Cervus</i>
B1977	A1	Indeterminate	<i>Capra/Rangifer</i>	n/a	<i>Capra</i>	n/a	<i>Capra</i>
B1978	A1	Indeterminate	<i>Capreolus</i>	n/a	n/a	n/a	<i>Capreolus</i>

B1979	A1	Indeterminate	<i>Capra/Rupicapra</i>	n/a	<i>Capra</i>	n/a	<i>Capra</i>
B1983	A1	Indeterminate	<i>Cervus</i>	n/a	n/a	n/a	<i>Cervus</i>
B1985	A1	Indeterminate	<i>Cervus/Capreolus</i>	n/a	<i>Capreolus</i>	n/a	<i>Capreolus</i>
B1986	A1	Indeterminate	<i>Capra/Rangifer</i>	n/a	<i>Capra</i>	n/a	<i>Capra</i>
B1988	A1	Indeterminate	<i>Cervus</i>	n/a	n/a	n/a	<i>Cervus</i>
B1989	A1	Indeterminate	<i>Capra/Rupicapra</i>	n/a	n/a	n/a	Caprinae
B1990	A1	Indeterminate	<i>Sus</i>	n/a	n/a	n/a	<i>Sus</i>
B1993	A1	Indeterminate	<i>Bos/Bison</i>	n/a	n/a	n/a	<i>Bos/Bison</i>
B1995	A1	Ungulate	<i>Cervus</i>	n/a	n/a	n/a	<i>Cervus</i>
B1998	A1	Ungulate	<i>Cervus</i>	n/a	n/a	n/a	<i>Cervus</i>
B2004	A1	Indeterminate	<i>Cervus/Capreolus</i>	n/a	<i>Capreolus</i>	n/a	<i>Capreolus</i>
B2007	A1	Indeterminate	Poor collagen	<i>Capra</i>	n/a	n/a	<i>Capra</i>
B2010	A1	Indeterminate	<i>Cervus/Capreolus</i>	n/a	<i>Cervus</i>	n/a	<i>Cervus</i>
B2011	A1	Indeterminate	<i>Cervus</i>	n/a	n/a	n/a	<i>Cervus</i>
B2018	A1	Indeterminate	<i>Cervus/Capreolus</i>	n/a	<i>Cervus</i>	n/a	<i>Cervus</i>
B2019	A1	Indeterminate	<i>Cervus</i>	n/a	n/a	n/a	<i>Cervus</i>
B2020	A1	Indeterminate	<i>Cervus</i>	n/a	n/a	n/a	<i>Cervus</i>
B2021	A1	Indeterminate	<i>Capreolus</i>	n/a	n/a	n/a	<i>Capreolus</i>
B2025	A1	Indeterminate	<i>Cervus/Capreolus</i>	n/a	<i>Cervus</i>	n/a	<i>Cervus</i>
B2026	A1	Indeterminate	<i>Cervus</i>	n/a	n/a	n/a	<i>Cervus</i>
B2027	A1	Indeterminate	<i>Bos/Bison</i>	n/a	n/a	n/a	<i>Bos/Bison</i>

B2028	A1	Indeterminate	<i>Cervus</i>	n/a	n/a	n/a	<i>Cervus</i>
B2029	A1	Indeterminate	<i>Cervus/Capreolus</i>	n/a	<i>Cervus</i>	n/a	<i>Cervus</i>
B2030	A1	Indeterminate	<i>Cervus</i>	n/a	n/a	n/a	<i>Cervus</i>
B2032	A1	Indeterminate	<i>Cervus/Capreolus</i>	n/a	<i>Cervus</i>	n/a	<i>Cervus</i>
B2033	A1	Indeterminate	<i>Cervus/Capreolus</i>	n/a	<i>Capreolus</i>	n/a	<i>Capreolus</i>
B2034	A1	Indeterminate	<i>Bos/Bison</i>	n/a	n/a	n/a	<i>Bos/Bison</i>
B2036	A1	Indeterminate	<i>Capra/Rupicapra</i>	n/a	<i>Capra</i>	n/a	<i>Capra</i>
B2037	A1	Indeterminate	<i>Cervus</i>	n/a	n/a	n/a	<i>Cervus</i>
B2038	A1	Indeterminate	<i>Capra/Rangifer</i>	n/a	<i>Capra</i>	n/a	<i>Capra</i>
B2040	A1	<i>Cervus elaphus</i>	<i>Cervus/Capreolus</i>	n/a	<i>Cervus</i>	n/a	<i>Cervus elaphus</i>
B2042	A1	<i>Dama dama</i>	<i>Cervus</i>	n/a	n/a	n/a	<i>Dama dama</i>
B2043	A1	Artiodactyla	<i>Cervus/Capreolus</i>	<i>Cervus/Capreolus</i>	n/a	<i>Cervus</i>	<i>Cervus</i>
B2046	A2	Cervid	Ungulate	<i>Cervus</i>	n/a	n/a	<i>Cervus</i>
B2048	A2	<i>Equus</i>	Poor collagen	<i>Equus</i>	n/a	n/a	<i>Equus</i>
B2049	A2	Ungulate	<i>Equus</i>	n/a	n/a	n/a	<i>Equus</i>
B2052	A2	Artiodactyla	<i>Equus</i>	n/a	n/a	n/a	<i>Equus</i>
B2053	A2	Indeterminate	<i>Capra/Rupicapra</i>	n/a	<i>Capra</i>	n/a	<i>Capra</i>
B2059	A2	Indeterminate	<i>Capra</i>	n/a	n/a	n/a	<i>Capra</i>
B2060	A2	Indeterminate	<i>Capra</i>	n/a	n/a	n/a	<i>Capra</i>
B2061	A2	Indeterminate	<i>Capra</i>	n/a	n/a	n/a	<i>Capra</i>
B2062	A2	Indeterminate	<i>Cervus</i>	n/a	n/a	n/a	<i>Cervus</i>

B2063	A2	Indeterminate	<i>Capra</i>	n/a	n/a	n/a	<i>Capra</i>
B2065	A2	Indeterminate	<i>Cervus</i>	n/a	n/a	n/a	<i>Cervus</i>
B2069	A2	Indeterminate	Poor collagen	n/a	n/a	n/a	Indeterminate
B2079	A2	Indeterminate	<i>Cervus/Capreolus</i>	n/a	<i>Cervus</i>	n/a	<i>Cervus</i>
B2082	A2	Indeterminate	<i>Cervus</i>	n/a	n/a	n/a	<i>Cervus</i>
B2084	A2	Indeterminate	<i>Bos/Bison</i>	n/a	n/a	n/a	<i>Bos/Bison</i>
B2085	A2	Indeterminate	<i>Capra</i>	n/a	n/a	n/a	<i>Capra</i>
B2086	A2	Indeterminate	<i>Cervus</i>	n/a	n/a	n/a	<i>Cervus</i>
B2088	A2	Indeterminate	<i>Bos/Bison</i>	n/a	n/a	n/a	<i>Bos/Bison</i>
B2089	A2	Indeterminate	<i>Cervus</i>	n/a	n/a	n/a	<i>Cervus</i>
B2090	A2	Indeterminate	<i>Cervus</i>	n/a	n/a	n/a	<i>Cervus</i>
B2094	A2	Indeterminate	Ungulate	Mammal	n/a	Ungulate	Ungulate
B2097	A2	Indeterminate	<i>Bos/Bison</i>	n/a	n/a	n/a	<i>Bos/Bison</i>
B2103	A2	Artiodactyla	<i>Cervus</i>	n/a	n/a	n/a	<i>Cervus</i>
B2114	A2	Indeterminate	<i>Capra</i>	n/a	n/a	n/a	<i>Capra</i>
B2121	A2	Indeterminate	<i>Bos/Bison</i>	n/a	n/a	n/a	<i>Bos/Bison</i>
B2129	A2	Indeterminate	<i>Cervus/Capreolus</i>	n/a	<i>Cervus</i>	n/a	<i>Cervus</i>
B2134	A2	Indeterminate	<i>Capra/Rupicapra</i>	n/a	<i>Capra</i>	n/a	<i>Capra</i>
B2135	A2	Indeterminate	<i>Cervus/Capreolus</i>	n/a	<i>Cervus</i>	n/a	<i>Cervus</i>
B2136	A2	Indeterminate	<i>Bos/Bison</i>	n/a	n/a	n/a	<i>Bos/Bison</i>
B2141	A2	Indeterminate	<i>Bos/Bison</i>	n/a	n/a	n/a	<i>Bos/Bison</i>
B2142	A2	Indeterminate	Ungulate	<i>Bos/Bison</i>	n/a	<i>Bos/Bison</i>	<i>Bos/Bison</i>
B2144	A2	Indeterminate	<i>Cervus</i>	n/a	n/a	n/a	<i>Cervus</i>

B2145	A2	Ungulate	<i>Equus</i>	n/a	<i>Equus</i>	n/a	<i>Equus</i>
B2148	A2	Indeterminate	Ungulate	<i>Cervus</i>	n/a	<i>Cervus</i>	<i>Cervus</i>
B2150	A2	Indeterminate	Poor collagen	n/a	n/a	n/a	Indeterminate
B2152	A2	Indeterminate	<i>Bos/Bison</i>	n/a	n/a	n/a	<i>Bos/Bison</i>
B2153	A2	Indeterminate	<i>Cervus/Capreolus</i>	n/a	<i>Capreolus</i>	n/a	<i>Capreolus</i>
B2154	A2	Indeterminate	<i>Bos/Bison</i>	n/a	n/a	n/a	<i>Bos/Bison</i>
B2158	A2	Artiodactyla	<i>Capra</i>	n/a	<i>Capra</i>	n/a	<i>Capra</i>
B2159	A2	Artiodactyla	<i>Sus</i>	n/a	<i>Sus</i>	n/a	<i>Sus</i>
B2160	A2	Indeterminate	<i>Cervus/Capreolus</i>	n/a	<i>Cervus</i>	n/a	<i>Cervus</i>
B2161	A2	Indeterminate	<i>Cervus</i>	n/a	n/a	n/a	<i>Cervus</i>
B2162	A2	Artiodactyla	<i>Cervus/Capreolus</i>	<i>Cervus/Capreolus</i>	<i>Cervus/Capreolus</i>	<i>Cervus</i>	<i>Cervus</i>
B2164	A2	Indeterminate	<i>Ursus</i>	n/a	Carnivore	n/a	<i>Ursus</i>
B2165	A2	Indeterminate	<i>Capra/Rupicapra</i>	n/a	<i>Capra</i>	n/a	<i>Capra</i>
B2168	A2	Artiodactyla	<i>Capra</i>	n/a	n/a	n/a	<i>Capra</i>
B2172	A2	Indeterminate	Poor collagen	<i>Cervus</i>	n/a	n/a	<i>Cervus</i>
B2174	A2	Indeterminate	<i>Cervus/Capreolus</i>	n/a	<i>Cervus</i>	n/a	<i>Cervus</i>
B2177	A2	Indeterminate	<i>Cervus/Capreolus</i>	n/a	<i>Cervus</i>	n/a	<i>Cervus</i>
B2178	A2	Indeterminate	<i>Cervus/Capreolus</i>	Poor collagen	<i>Cervus</i>	<i>Cervus</i>	<i>Cervus</i>
B2179	A2	Indeterminate	<i>Cervus</i>	n/a	n/a	n/a	<i>Cervus</i>
B2180	A2	Indeterminate	<i>Cervus</i>	n/a	n/a	n/a	<i>Cervus</i>
B2181	A2	Indeterminate	<i>Cervus/Capreolus</i>	n/a	<i>Cervus</i>	n/a	<i>Cervus</i>

B2182	A2	Indeterminate	<i>Capra/Rupicapra</i>	n/a	<i>Capra</i>	n/a	<i>Capra</i>
B2183	A2	Indeterminate	<i>Sus</i>	n/a	<i>Sus</i>	n/a	<i>Sus</i>
B2184	A2	Indeterminate	<i>Equus</i>	n/a	n/a	n/a	<i>Equus</i>
B2186	A2	Indeterminate	Poor collagen	Poor collagen	n/a	n/a	Indeterminate
B2188	A2	Indeterminate	<i>Cervus/Capreolus</i>	n/a	<i>Cervus</i>	n/a	<i>Cervus</i>
B2189	A2	Indeterminate	<i>Bos/Bison</i>	n/a	n/a	n/a	<i>Bos/Bison</i>
B2190	A2	Indeterminate	<i>Capra</i>	n/a	n/a	n/a	<i>Capra</i>
B2192	A2	Artiodactyla	<i>Cervus/Capreolus</i>	n/a	<i>Cervus</i>	n/a	<i>Cervus</i>
B2193	A2	Indeterminate	<i>Capra/Rupicapra</i>	n/a	<i>Capra</i>	n/a	<i>Capra</i>
B2194	A2	Indeterminate	<i>Cervus</i>	n/a	n/a	n/a	<i>Cervus</i>
B2196	A2	Indeterminate	<i>Bos/Bison</i>	n/a	<i>bos/bison</i>	n/a	<i>Bos/Bison</i>
B2197	A2	Indeterminate	<i>Cervus/Capreolus</i>	n/a	<i>Cervus/Capreolus</i>	n/a	Cervidae
B2199	A2	Indeterminate	<i>Capra</i>	n/a	n/a	n/a	<i>Capra</i>
B2211	MS	Indeterminate	Poor collagen	Poor collagen	n/a	n/a	Indeterminate
B2294	MS	Indeterminate	Poor collagen	Ungulate	n/a	n/a	Ungulate
B2299	MS	Indeterminate	Poor collagen	<i>Cervus/Capreolus</i>	n/a	n/a	Cervidae
B2304	MS	<i>Capra ibex</i>	<i>Capra/Rupicapra</i>	n/a	<i>Capra</i>	n/a	<i>Capra ibex</i>
B2308	MS	Indeterminate	Poor collagen	Poor collagen	n/a	n/a	Indeterminate
B2311	MS	Indeterminate	Poor collagen	<i>Cervus/Capreolus</i>	n/a	n/a	Indeterminate
B2330	MS	Indeterminate	<i>Cervus</i>	n/a	<i>Cervus</i>	n/a	<i>Cervus</i>

B2360	MS	Indeterminate	Poor collagen	Poor collagen	n/a	n/a	Indeterminate
B2363	MS	Indeterminate	Poor collagen	<i>Cervus/Capreolus</i>	n/a	n/a	Cervidae
B2447	A2	Indeterminate	Poor collagen	Poor collagen	n/a	n/a	Indeterminate
B2448	A2	Indeterminate	Ungulate	Poor collagen	n/a	n/a	Ungulate

SI Table 11. Skeletal representation of *Cervus* sp. in Level A1. Number of identified specimens of skeletal elements (NISPe) and minimum number of elements (MNE).

Skeletal elements	Left	Right	Left/Right	NISPe	MNE
<u>HEAD</u>					
Teeth	3	0	0	3	n/a
Antler/horn	0	0	0	0	0
Maxillary	1	0	1	2	1
Mandibule	0	0	1	1	1
Cranium	0	0	2	2	1
<u>AXIAL SKELETON</u>					
Total vertebra	0	0	0	0	0
Total rib	0	0	4	4	1
Atlas	0	0	0	0	0
Axis	0	0	0	0	0
Cervical vertebra	0	0	0	0	0
Thoracic vertebra	0	0	0	0	0
Lumbar vertebra	0	0	0	0	0
Intederminate vertebra	0	0	0	0	0
Sacrum	0	0	0	0	0
Caudal vertebra	0	0	0	0	0
Rib diaphysis	0	0	4	4	1
Rib epiphysis	0	0	0	0	0
sternum	0	0	0	0	0
hyoid	0	0	0	0	0
<u>UPPER FORELIMB</u>					
Total humerus	0	0	0	0	0
Total scapula	0	0	0	0	0
Humerus proximal	0	0	0	0	0
Humerus diaphysis	0	0	0	0	0
Humerus distal	0	0	0	0	0
Scapula proximal	0	0	0	0	0
Scapula middle	0	0	0	0	0
Scapula distal	0	0	0	0	0
<u>UPPER HINDLIMB</u>					
Total femur	0	0	0	0	0
Total Pelvis	0	0	0	0	0
Femur proximal	0	0	0	0	0
Femur diaphysis	0	0	0	0	0
Femur distal	0	0	0	0	0
Ilium	0	0	0	0	0
Acetabulum	0	0	0	0	0
Pubis	0	0	0	0	0
Ischium	0	0	0	0	0
<u>LOWER FORELIMB</u>					
Total carpal	0	0	0	0	0
Total metacarpal	0	0	2	2	1

Total Radius.Ulna	0	0	0	0	0
Metacarpal proximal	0	0	0	0	0
Metacarpal diaphysis	0	0	2	2	1
Metacarpal distal	0	0	0	0	0
Radius.Ulna proximal	0	0	0	0	0
Radius.Ulna diaphysis	0	0	0	0	0
Radius.Ulna distal	0	0	0	0	0
<u>LOWER HINDLIMB</u>					
Total tarsal	0	0	0	0	0
Talus	0	0	0	0	0
Calcaneum	0	0	0	0	0
Total Metatarsal	0	0	2	2	1
Total Tibia	0	0	0	0	0
Patella	0	0	0	0	0
Metatarsal proximal	0	0	0	0	0
Metatarsal diaphysis	0	0	2	2	1
Metatarsal distal	0	0	0	0	0
Tibia.fibula proximal	0	0	0	0	0
Tibia.fibula diaphysis	0	0	0	0	0
Tibia.fibula distal	0	0	0	0	0
<u>INDETERMINATE LIMB</u>					
Total Metapodial	0	0	1	1	1
Long bone diapysis	0	0	20	20	n/a
Long bone epiphysis	0	0	1	1	n/a
Metapodial proximal	0	0	0	0	0
Metapodial_diaph	0	0	1	1	1
Metapodial_dist	0	0	0	0	0
<u>TOES</u>					
Phalanx 1	0	0	0	0	0
Phalanx 2	0	0	0	0	0
Phalanx 3	0	0	0	0	0
Phalanx indeterminate	0	0	0	0	0
<u>OTHER</u>					
Sesamoid	0	0	0	0	0

SI Table 12. Skeletal representation of *Cervus* sp. in Level A2. Number of identified specimens of skeletal elements (NISPe) and minimum number of elements (MNE).

Skeletal elements	Left	Right	Left/Right	NISPe	MNE
<u>HEAD</u>					
Teeth	0	0	3	3	n/a
Antler/horn	0	0	0	0	0
Maxillary	0	0	0	0	0
Mandibule	0	0	0	0	0
Cranium	0	0	0	0	0
<u>AXIAL SKELETON</u>					
Total vertebra	0	0	1	1	1
Total rib	0	0	0	0	0
Atlas	0	0	0	0	0
Axis	0	0	0	0	0
Cervical vertebra	0	0	0	0	0
Thoracic vertebra	0	0	0	0	0
Lumbar vertebra	0	0	0	0	0
Intederminate vertebra	0	0	1	1	1
Sacrum	0	0	0	0	0
Caudal vertebra	0	0	0	0	0
Rib diaphysis	0	0	0	0	0
Rib epiphysis	0	0	0	0	0
sternum	0	0	0	0	0
hyoid	0	0	0	0	0
<u>UPPER FORELIMB</u>					
Total humerus	0	0	0	0	0
Total scapula	0	0	0	0	0
Humerus proximal	0	0	0	0	0
Humerus diaphysis	0	0	0	0	0
Humerus distal	0	0	0	0	0
Scapula proximal	0	0	0	0	0
Scapula middle	0	0	0	0	0
Scapula distal	0	0	0	0	0
<u>UPPER HINDLIMB</u>					
Total femur	0	0	0	0	0
Total Pelvis	0	0	0	0	0
Femur proximal	0	0	0	0	0
Femur diaphysis	0	0	0	0	0
Femur distal	0	0	0	0	0
Ilium	0	0	0	0	0
Acetabulum	0	0	0	0	0
Pubis	0	0	0	0	0
Ischium	0	0	0	0	0
<u>LOWER FORELIMB</u>					

Total carpal	0	0	0	0	0
Total metacarpal	0	0	0	0	0
Total Radius.Ulna	0	0	0	0	0
Metacarpal proximal	0	0	0	0	0
Metacarpal diaphysis	0	0	0	0	0
Metacarpal distal	0	0	0	0	0
Radius.Ulna proximal	0	0	0	0	0
Radius.Ulna diaphysis	0	0	0	0	0
Radius.Ulna distal	0	0	0	0	0
<u>LOWER HINDLIMB</u>					
Total tarsal	0	0	0	0	0
Talus	0	0	0	0	0
Calcaneum	0	0	0	0	0
Total Metatarsal	0	0	0	0	0
Total Tibia	0	0	0	0	0
Patella	0	0	0	0	0
Metatarsal proximal	0	0	0	0	0
Metatarsal diaphysis	0	0	0	0	0
Metatarsal distal	0	0	0	0	0
Tibia.fibula proximal	0	0	0	0	0
Tibia.fibula diaphysis	0	0	0	0	0
Tibia.fibula distal	0	0	0	0	0
<u>INDETERMINATE</u>					
<u>LIMB</u>	0	0	16	16	n/a
Total Metapodial	0	0	1	1	1
Long bone diaphysis	0	0	15	15	n/a
Long bone epiphysis	0	0	0	0	n/a
Metapodial proximal	0	0	0	0	0
Metapodial_diaph	0	0	1	1	1
Metapodial_dist	0	0	0	0	0
<u>TOES</u>					
Phalanx 1	0	0	0	0	0
Phalanx 2	0	0	0	0	0
Phalanx 3	0	0	0	0	0
Phalanx indeterminate	0	0	0	0	0
<u>OTHER</u>					
Sesamoid	0	0	0	0	0

SI Table 13. Skeletal representation of *Cervus* sp. in Level MS. Number of identified specimens of skeletal elements (NISPe) and minimum number of elements (MNE).

Skeletal elements	Left	Right	Left/Right	NISPe	MNE
<u>HEAD</u>					
Teeth	1	0	0	1	n/a
Antler/horn	0	0	0	0	0
Maxillary	0	0	0	0	0
Mandibule	0	0	0	0	0
Cranium	0	0	0	0	0
<u>AXIAL SKELETON</u>					
Total vertebra	0	0	1	1	1
Total rib	2	0	2	4	3
Atlas	0	0	0	0	0
Axis	0	0	0	0	0
Cervical vertebra	0	0	0	0	0
Thoracic vertebra	0	0	1	1	1
Lumbar vertebra	0	0	0	0	0
Intederminate vertebra	0	0	0	0	0
Sacrum	0	0	0	0	0
Caudal vertebra	0	0	0	0	0
Rib diaphysis	1	0	2	3	2
Rib epiphysis	1	0	0	1	1
sternum	0	0	0	0	0
hyoid	0	0	0	0	0
<u>UPPER FORELIMB</u>					
Total humerus	0	0	0	0	0
Total scapula	0	0	0	0	0
Humerus proximal	0	0	0	0	0
Humerus diaphysis	0	0	0	0	0
Humerus distal	0	0	0	0	0
Scapula proximal	0	0	0	0	0
Scapula middle	0	0	0	0	0
Scapula distal	0	0	0	0	0
<u>UPPER HINDLIMB</u>					
Total femur	2	0	0	2	1
Total Pelvis	0	0	0	0	0
Femur proximal	1	0	0	1	1
Femur diaphysis	1	0	0	1	1
Femur distal	0	0	0	0	0
Ilium	0	0	0	0	0
Acetabulum	0	0	0	0	0
Pubis	0	0	0	0	0
Ischium	0	0	0	0	0
<u>LOWER FORELIMB</u>					

Total carpal	0	0	0	0	0
Total metacarpal	0	0	0	0	0
Total Radius.Ulna	0	1	0	1	1
Metacarpal proximal	0	0	0	0	0
Metacarpal diaphysis	0	0	0	0	0
Metacarpal distal	0	0	0	0	0
Radius.Ulna proximal	0	1	0	1	1
Radius.Ulna diaphysis	0	0	0	0	0
Radius.Ulna distal	0	0	0	0	0

LOWER HINDLIMB

Total tarsal	0	0	0	0	0
Talus	0	0	0	0	0
Calcaneum	0	0	0	0	0
Total Metatarsal	0	0	0	0	0
Total Tibia	0	0	0	0	0
Patella	0	0	0	0	0
Metatarsal proximal	0	0	0	0	0
Metatarsal diaphysis	0	0	0	0	0
Metatarsal distal	0	0	0	0	0
Tibia.fibula proximal	0	0	0	0	0
Tibia.fibula diaphysis	0	0	0	0	0
Tibia.fibula distal	0	0	0	0	0

INDETERMINATE

LIMB

Total Metapodial	0	0	0	0	0
Long bone diapysis	0	0	0	0	n/a
Long bone epiphysis	0	0	0	0	n/a
Metapodial proximal	0	0	0	0	0
Metapodial_diaph	0	0	0	0	0
Metapodial_dist	0	0	0	0	0

TOES

Phalanx 1	0	0	0	0	0
Phalanx 2	0	0	0	0	0
Phalanx 3	0	0	0	0	0
Phalanx indeterminate	0	0	0	0	0

OTHER

Sesamoid	0	0	0	0	0
----------	---	---	---	---	---

SI Table 14. Skeletal representation of *Bos/Bison* sp. in Level A1. Number of identified specimens of skeletal elements (NISPe) and minimum number of elements (MNE).

Skeletal elements	Left	Right	Left/Right	NISPe	MNE
<u>HEAD</u>					
Teeth	0	0	0	0	n/a
Antler/horn	0	0	0	0	0
Maxillary	0	0	0	0	0
Mandibule	0	0	0	0	0
Cranium	0	0	0	0	0
<u>AXIAL SKELETON</u>					
Total vertebra	0	0	0	0	0
Total rib	0	0	0	0	0
Atlas	0	0	0	0	0
Axis	0	0	0	0	0
Cervical vertebra	0	0	0	0	0
Thoracic vertebra	0	0	0	0	0
Lumbar vertebra	0	0	0	0	0
Intederminate vertebra	0	0	0	0	0
Sacrum	0	0	0	0	0
Caudal vertebra	0	0	0	0	0
Rib diaphysis	0	0	0	0	0
Rib epiphysis	0	0	0	0	0
sternum	0	0	0	0	0
hyoid	0	0	0	0	0
<u>UPPER FORELIMB</u>					
Total humerus	0	0	0	0	0
Total scapula	0	0	0	0	0
Humerus proximal	0	0	0	0	0
Humerus diaphysis	0	0	0	0	0
Humerus distal	0	0	0	0	0
Scapula proximal	0	0	0	0	0
Scapula middle	0	0	0	0	0
Scapula distal	0	0	0	0	0
<u>UPPER HINDLIMB</u>					
Total femur	0	0	0	0	0
Total Pelvis	0	0	0	0	0
Femur proximal	0	0	0	0	0
Femur diaphysis	0	0	0	0	0
Femur distal	0	0	0	0	0
Ilium	0	0	0	0	0
Acetabulum	0	0	0	0	0
Pubis	0	0	0	0	0
Ischium	0	0	0	0	0
<u>LOWER FORELIMB</u>					

Total carpal	0	0	0	0	0
Total metacarpal	0	0	0	0	0
Total Radius.Ulna	0	0	0	0	0
Metacarpal proximal	0	0	0	0	0
Metacarpal diaphysis	0	0	0	0	0
Metacarpal distal	0	0	0	0	0
Radius.Ulna proximal	0	0	0	0	0
Radius.Ulna diaphysis	0	0	0	0	0
Radius.Ulna distal	0	0	0	0	0

LOWER HINDLIMB

Total tarsal	0	0	0	0	0
Talus	0	0	0	0	0
Calcaneum	0	0	0	0	0
Total Metatarsal	0	0	0	0	0
Total Tibia	0	0	0	0	0
Patella	0	0	0	0	0
Metatarsal proximal	0	0	0	0	0
Metatarsal diaphysis	0	0	0	0	0
Metatarsal distal	0	0	0	0	0
Tibia.fibula proximal	0	0	0	0	0
Tibia.fibula diaphysis	0	0	0	0	0
Tibia.fibula distal	0	0	0	0	0

INDETERMINATE

LIMB

Total Metapodial	0	0	0	0	0
Long bone diaphysis	0	0	10	10	n/a
Long bone epiphysis	0	0	0	0	n/a
Metapodial proximal	0	0	0	0	0
Metapodial_diaph	0	0	0	0	0
Metapodial_dist	0	0	0	0	0

TOES

Phalanx 1	0	0	0	0	0
Phalanx 2	0	0	0	0	0
Phalanx 3	0	0	0	0	0
Phalanx indeterminate	0	0	0	0	0

OTHER

Sesamoid	0	0	0	0	0
----------	---	---	---	---	---

SI Table 15. Skeletal representation of *Bos/Bison* sp. in Level A2. Number of identified specimens of skeletal elements (NISPe) and minimum number of elements (MNE).

Skeletal elements	Left	Right	Left/Right	NISPe	MNE
<u>HEAD</u>					
Teeth	1	0	1	2	n/a
Antler/horn	0	0	0	0	0
Maxillary	0	0	0	0	0
Mandibule	0	0	0	0	0
Cranium	0	0	0	0	0
<u>AXIAL SKELETON</u>					
Total vertebra	0	0	0	0	0
Total rib	0	0	0	0	0
Atlas	0	0	0	0	0
Axis	0	0	0	0	0
Cervical vertebra	0	0	0	0	0
Thoracic vertebra	0	0	0	0	0
Lumbar vertebra	0	0	0	0	0
Intederminate vertebra	0	0	0	0	0
Sacrum	0	0	0	0	0
Caudal vertebra	0	0	0	0	0
Rib diaphysis	0	0	0	0	0
Rib epiphysis	0	0	0	0	0
sternum	0	0	0	0	0
hyoid	0	0	0	0	0
<u>UPPER FORELIMB</u>					
Total humerus	0	0	1	1	1
Total scapula	0	0	0	0	0
Humerus proximal	0	0	1	1	1
Humerus diaphysis	0	0	0	0	0
Humerus distal	0	0	0	0	0
Scapula proximal	0	0	0	0	0
Scapula middle	0	0	0	0	0
Scapula distal	0	0	0	0	0
<u>UPPER HINDLIMB</u>					
Total femur	0	0	0	0	0
Total Pelvis	0	0	0	0	0
Femur proximal	0	0	0	0	0
Femur diaphysis	0	0	0	0	0
Femur distal	0	0	0	0	0
Ilium	0	0	0	0	0
Acetabulum	0	0	0	0	0
Pubis	0	0	0	0	0
Ischium	0	0	0	0	0
<u>LOWER FORELIMB</u>					

Total carpal	0	0	0	0	0
Total metacarpal	0	0	0	0	0
Total Radius.Ulna	0	0	1	1	1
Metacarpal proximal	0	0	0	0	0
Metacarpal diaphysis	0	0	0	0	0
Metacarpal distal	0	0	0	0	0
Radius.Ulna proximal	0	0	0	0	0
Radius.Ulna diaphysis	0	0	0	0	0
Radius.Ulna distal	0	0	1	1	1

LOWER HINDLIMB

Total tarsal	0	0	1	1	1
Talus	0	0	0	0	0
Calcaneum	0	0	0	0	0
Total Metatarsal	0	0	0	0	0
Total Tibia	0	0	0	0	0
Patella	0	0	0	0	0
Metatarsal proximal	0	0	0	0	0
Metatarsal diaphysis	0	0	0	0	0
Metatarsal distal	0	0	0	0	0
Tibia.fibula proximal	0	0	0	0	0
Tibia.fibula diaphysis	0	0	0	0	0
Tibia.fibula distal	0	0	0	0	0

INDETERMINATE

LIMB

Total Metapodial	0	0	0	0	0
Long bone diapysis	0	0	8	8	n/a
Long bone epiphysis	0	0	0	0	n/a
Metapodial proximal	0	0	0	0	0
Metapodial_diaph	0	0	0	0	0
Metapodial_dist	0	0	0	0	0

TOES

Phalanx 1	0	0	0	0	0
Phalanx 2	0	0	0	0	0
Phalanx 3	0	0	1	1	1
Phalanx indeterminate	0	0	0	0	0

OTHER

Sesamoid	0	0	0	0	0
----------	---	---	---	---	---

SI Table 16. Skeletal representation of *Bos/Bison* sp. in Level MS. Number of identified specimens of skeletal elements (NISPe) and minimum number of elements (MNE).

Skeletal elements	Left	Right	Left/Right	NISPe	MNE
<u>HEAD</u>					
Teeth	0	0	0	0	n/a
Antler/horn	0	0	0	0	0
Maxillary	0	0	0	0	0
Mandibule	0	0	0	0	0
Cranium	0	0	0	0	0
<u>AXIAL SKELETON</u>					
Total vertebra	0	0	0	0	0
Total rib	0	0	0	0	0
Atlas	0	0	0	0	0
Axis	0	0	0	0	0
Cervical vertebra	0	0	0	0	0
Thoracic vertebra	0	0	0	0	0
Lumbar vertebra	0	0	0	0	0
Intederminate vertebra	0	0	0	0	0
Sacrum	0	0	0	0	0
Caudal vertebra	0	0	0	0	0
Rib diaphysis	0	0	0	0	0
Rib epiphysis	0	0	0	0	0
sternum	0	0	0	0	0
hyoid	0	0	0	0	0
<u>UPPER FORELIMB</u>					
Total humerus	0	0	0	0	0
Total scapula	0	0	0	0	0
Humerus proximal	0	0	0	0	0
Humerus diaphysis	0	0	0	0	0
Humerus distal	0	0	0	0	0
Scapula proximal	0	0	0	0	0
Scapula middle	0	0	0	0	0
Scapula distal	0	0	0	0	0
<u>UPPER HINDLIMB</u>					
Total femur	0	0	0	0	0
Total Pelvis	0	0	0	0	0
Femur proximal	0	0	0	0	0
Femur diaphysis	0	0	0	0	0
Femur distal	0	0	0	0	0
Ilium	0	0	0	0	0
Acetabulum	0	0	0	0	0
Pubis	0	0	0	0	0
Ischium	0	0	0	0	0
<u>LOWER FORELIMB</u>					

Total carpal	0	0	0	0	0
Total metacarpal	0	0	0	0	0
Total Radius.Ulna	0	0	0	0	0
Metacarpal proximal	0	0	0	0	0
Metacarpal diaphysis	0	0	0	0	0
Metacarpal distal	0	0	0	0	0
Radius.Ulna proximal	0	0	0	0	0
Radius.Ulna diaphysis	0	0	0	0	0
Radius.Ulna distal	0	0	0	0	0

LOWER HINDLIMB

Total tarsal	0	0	0	0	0
Talus	0	0	0	0	0
Calcaneum	0	0	0	0	0
Total Metatarsal	0	0	0	0	0
Total Tibia	0	0	0	0	0
Patella	0	0	0	0	0
Metatarsal proximal	0	0	0	0	0
Metatarsal diaphysis	0	0	0	0	0
Metatarsal distal	0	0	0	0	0
Tibia.fibula proximal	0	0	0	0	0
Tibia.fibula diaphysis	0	0	0	0	0
Tibia.fibula distal	0	0	0	0	0

INDETERMINATE

LIMB

Total Metapodial	0	0	0	0	0
Long bone diaphysis	0	0	0	0	n/a
Long bone epiphysis	0	0	0	0	n/a
Metapodial proximal	0	0	0	0	0
Metapodial_diaph	0	0	0	0	0
Metapodial_dist	0	0	0	0	0

TOES

Phalanx 1	0	0	0	0	0
Phalanx 2	0	0	0	0	0
Phalanx 3	0	0	0	0	0
Phalanx indeterminate	0	0	0	0	0

OTHER

Sesamoid	0	0	0	0	0
----------	---	---	---	---	---

SI Table 17. Skeletal representation of *Capra* sp. in Level A1. Number of identified specimens of skeletal elements (NISPe) and minimum number of elements (MNE).

Skeletal elements	Left	Right	Left/Right	NISPe	MNE
<u>HEAD</u>					
Teeth	0	1	0	1	n/a
Antler/horn	0	0	0	0	0
Maxillary	0	0	0	0	0
Mandibule	0	0	0	0	0
Cranium	0	0	1	1	1
<u>AXIAL SKELETON</u>					
Total vertebra	0	0	1	1	1
Total rib	0	0	3	3	1
Atlas	0	0	0	0	0
Axis	0	0	0	0	0
Cervical vertebra	0	0	0	0	0
Thoracic vertebra	0	0	0	0	0
Lumbar vertebra	0	0	0	0	0
Intederminate vertebra	0	0	1	1	1
Sacrum	0	0	0	0	0
Caudal vertebra	0	0	0	0	0
Rib diaphysis	0	0	3	3	1
Rib epiphysis	0	0	0	0	0
sternum	0	0	0	0	0
hyoid	0	0	0	0	0
<u>UPPER FORELIMB</u>					
Total humerus	0	0	0	0	0
Total scapula	0	0	0	0	0
Humerus proximal	0	0	0	0	0
Humerus diaphysis	0	0	0	0	0
Humerus distal	0	0	0	0	0
Scapula proximal	0	0	0	0	0
Scapula middle	0	0	0	0	0
Scapula distal	0	0	0	0	0
<u>UPPER HINDLIMB</u>					
Total femur	0	0	0	0	0
Total Pelvis	0	0	0	0	0
Femur proximal	0	0	0	0	0
Femur diaphysis	0	0	0	0	0
Femur distal	0	0	0	0	0
Ilium	0	0	0	0	0
Acetabulum	0	0	0	0	0
Pubis	0	0	0	0	0
Ischium	0	0	0	0	0

LOWER FORELIMB

Total carpal	0	0	0	0	0
Total metacarpal	0	0	0	0	0
Total Radius.Ulna	0	0	0	0	0
Metacarpal proximal	0	0	0	0	0
Metacarpal diaphysis	0	0	0	0	0
Metacarpal distal	0	0	0	0	0
Radius.Ulna proximal	0	0	0	0	0
Radius.Ulna diaphysis	0	0	0	0	0
Radius.Ulna distal	0	0	0	0	0

LOWER HINDLIMB

Total tarsal	0	0	0	0	0
Talus	0	0	0	0	0
Calcaneum	0	0	0	0	0
Total Metatarsal	0	0	0	0	0
Total Tibia	0	0	0	0	0
Patella	0	0	0	0	0
Metatarsal proximal	0	0	0	0	0
Metatarsal diaphysis	0	0	0	0	0
Metatarsal distal	0	0	0	0	0
Tibia.fibula proximal	0	0	0	0	0
Tibia.fibula diaphysis	0	0	0	0	0
Tibia.fibula distal	0	0	0	0	0

INDETERMINATE

<u>LIMB</u>	0	0	12	12	n/a
Total Metapodial	0	0	0	0	0
Long bone diaphysis	0	0	12	12	n/a
Long bone epiphysis	0	0	0	0	n/a
Metapodial proximal	0	0	0	0	0
Metapodial_diaph	0	0	0	0	0
Metapodial_dist	0	0	0	0	0

TOES

Phalanx 1	0	0	0	0	0
Phalanx 2	0	0	0	0	0
Phalanx 3	0	0	0	0	0
Phalanx indeterminate	0	0	0	0	0

OTHER

Sesamoid	0	0	0	0	0
----------	---	---	---	---	---

SI Table 18. Skeletal representation of *Capra* sp. in Level A2. Number of identified specimens of skeletal elements (NISPe) and minimum number of elements (MNE).

Skeletal elements	Left	Right	Left/Right	NISPe	MNE
<u>HEAD</u>					
Teeth	0	0	3	3	n/a
Antler/horn	0	0	0	0	0
Maxillary	0	0	0	0	0
Mandibule	0	0	0	0	0
Cranium	0	0	0	0	0
<u>AXIAL SKELETON</u>					
Total vertebra	0	0	0	0	0
Total rib	0	0	0	0	0
Atlas	0	0	0	0	0
Axis	0	0	0	0	0
Cervical vertebra	0	0	0	0	0
Thoracic vertebra	0	0	0	0	0
Lumbar vertebra	0	0	0	0	0
Intederminate vertebra	0	0	0	0	0
Sacrum	0	0	0	0	0
Caudal vertebra	0	0	0	0	0
Rib diaphysis	0	0	0	0	0
Rib epiphysis	0	0	0	0	0
sternum	0	0	0	0	0
hyoid	0	0	0	0	0
<u>UPPER FORELIMB</u>					
Total humerus	0	1	0	1	1
Total scapula	0	0	0	0	0
Humerus proximal	0	0	0	0	0
Humerus diaphysis	0	1	0	1	1
Humerus distal	0	0	0	0	0
Scapula proximal	0	0	0	0	0
Scapula middle	0	0	0	0	0
Scapula distal	0	0	0	0	0
<u>UPPER HINDLIMB</u>					
Total femur	0	0	0	0	0
Total Pelvis	0	0	0	0	0
Femur proximal	0	0	0	0	0
Femur diaphysis	0	0	0	0	0
Femur distal	0	0	0	0	0
Ilium	0	0	0	0	0
Acetabulum	0	0	0	0	0
Pubis	0	0	0	0	0
Ischium	0	0	0	0	0
<u>LOWER FORELIMB</u>					

Total carpal	0	0	0	0	0
Total metacarpal	0	0	0	0	0
Total Radius.Ulna	0	0	0	0	0
Metacarpal proximal	0	0	0	0	0
Metacarpal diaphysis	0	0	0	0	0
Metacarpal distal	0	0	0	0	0
Radius.Ulna proximal	0	0	0	0	0
Radius.Ulna diaphysis	0	0	0	0	0
Radius.Ulna distal	0	0	0	0	0

LOWER HINDLIMB

Total tarsal	0	0	0	0	0
Talus	0	0	0	0	0
Calcaneum	0	0	0	0	0
Total Metatarsal	0	0	0	0	0
Total Tibia	0	0	0	0	0
Patella	0	0	0	0	0
Metatarsal proximal	0	0	0	0	0
Metatarsal diaphysis	0	0	0	0	0
Metatarsal distal	0	0	0	0	0
Tibia.fibula proximal	0	0	0	0	0
Tibia.fibula diaphysis	0	0	0	0	0
Tibia.fibula distal	0	0	0	0	0

INDETERMINATE

LIMB

Total Metapodial	0	0	0	0	0
Long bone diaphysis	0	0	10	10	n/a
Long bone epiphysis	0	0	0	0	n/a
Metapodial proximal	0	0	0	0	0
Metapodial_diaph	0	0	0	0	0
Metapodial_dist	0	0	0	0	0

TOES

Phalanx 1	0	0	0	0	0
Phalanx 2	0	0	0	0	0
Phalanx 3	0	0	0	0	0
Phalanx indeterminate	0	0	0	0	0

OTHER

Sesamoid	0	0	1	1	1
----------	---	---	---	---	---

SI Table 19. Skeletal representation of *Capra* sp. in Level MS. Number of identified specimens of skeletal elements (NISPe) and minimum number of elements (MNE).

Skeletal elements	Left	Right	Left/Right	NISPe	MNE
<u>HEAD</u>					
Teeth	1	2	0	3	n/a
Antler/horn	0	0	0	0	0
Maxillary	0	0	0	0	0
Mandibule	0	0	0	0	0
Cranium	0	0	0	0	0
<u>AXIAL SKELETON</u>					
Total vertebra	0	0	0	0	0
Total rib	0	0	0	0	0
Atlas	0	0	0	0	0
Axis	0	0	0	0	0
Cervical vertebra	0	0	0	0	0
Thoracic vertebra	0	0	0	0	0
Lumbar vertebra	0	0	0	0	0
Intederminate vertebra	0	0	0	0	0
Sacrum	0	0	0	0	0
Caudal vertebra	0	0	0	0	0
Rib diaphysis	0	0	0	0	0
Rib epiphysis	0	0	0	0	0
sternum	0	0	0	0	0
hyoid	0	0	0	0	0
<u>UPPER FORELIMB</u>					
Total humerus	0	0	0	0	0
Total scapula	0	0	0	0	0
Humerus proximal	0	0	0	0	0
Humerus diaphysis	0	0	0	0	0
Humerus distal	0	0	0	0	0
Scapula proximal	0	0	0	0	0
Scapula middle	0	0	0	0	0
Scapula distal	0	0	0	0	0
<u>UPPER HINDLIMB</u>					
Total femur	0	0	0	0	0
Total Pelvis	0	0	0	0	0
Femur proximal	0	0	0	0	0
Femur diaphysis	0	0	0	0	0
Femur distal	0	0	0	0	0
Ilium	0	0	0	0	0
Acetabulum	0	0	0	0	0
Pubis	0	0	0	0	0
Ischium	0	0	0	0	0
<u>LOWER FORELIMB</u>					

Total carpal	0	0	0	0	0
Total metacarpal	0	0	0	0	0
Total Radius.Ulna	0	0	0	0	0
Metacarpal proximal	0	0	0	0	0
Metacarpal diaphysis	0	0	0	0	0
Metacarpal distal	0	0	0	0	0
Radius.Ulna proximal	0	0	0	0	0
Radius.Ulna diaphysis	0	0	0	0	0
Radius.Ulna distal	0	0	0	0	0

LOWER HINDLIMB

Total tarsal	0	0	0	0	0
Talus	0	0	0	0	0
Calcaneum	0	0	0	0	0
Total Metatarsal	0	0	0	0	0
Total Tibia	0	0	0	0	0
Patella	0	0	0	0	0
Metatarsal proximal	0	0	0	0	0
Metatarsal diaphysis	0	0	0	0	0
Metatarsal distal	0	0	0	0	0
Tibia.fibula proximal	0	0	0	0	0
Tibia.fibula diaphysis	0	0	0	0	0
Tibia.fibula distal	0	0	0	0	0

INDETERMINATE

LIMB

Total Metapodial	0	0	0	0	0
Long bone diaphysis	0	0	0	0	n/a
Long bone epiphysis	0	0	0	0	n/a
Metapodial proximal	0	0	0	0	0
Metapodial_diaph	0	0	0	0	0
Metapodial_dist	0	0	0	0	0

TOES

Phalanx 1	0	0	0	0	0
Phalanx 2	0	0	0	0	0
Phalanx 3	0	0	0	0	0
Phalanx indeterminate	0	0	0	0	0

OTHER

Sesamoid	0	0	0	0	0
----------	---	---	---	---	---
